Division of Cardiology, Heart and Lung Center
Helsinki University Central Hospital
Helsinki, Finland

and

Faculty of Medicine, University of Helsinki
Helsinki, Finland

ASSESSMENT OF MYOCARDIAL INFARCTION INJURY BY STRAIN RATE IMAGING AND BODY SURFACE POTENTIAL MAPPING

Minna Kylmälä

ACADEMIC DISSERTATION

To be presented, with the permission of the Faculty of Medicine of the University of Helsinki,
for public examination in Auditorium 4 of Meilahti Hospital,
on September 26th, 2014, at 12 noon.

Helsinki 2014

Supervisors

Docent Lauri Toivonen, M.D., Ph.D.
Division of Cardiology, Heart and Lung Center
Helsinki University Central Hospital
University of Helsinki
Helsinki, Finland

Docent Mika Laine, M.D., Ph.D.
Division of Cardiology, Heart and Lung Center
Helsinki University Central Hospital
University of Helsinki
Helsinki, Finland

Reviewers

Docent Marja Hedman, M.D., Ph.D.
Heart Center, Kuopio Univeristy Hospital
Eastern University of Finland
Kuopio, Finland

Docent Kjell Nikus, M.D., Ph.D.
Heart Center, Tampere University Hospital
University of Tampere
Tampere, Finland

Opponent

Professor George R. Sutherland
St. George's University of London
London, UK

ISBN 978-951-51-0015-3 (Paperback)
ISBN 978-951-51-0016-0 (PDF)
https://helda.helsinki.fi

Cover design by Mikael Rehn

Unigrafia
Helsinki 2014

CONTENTS

LIST OF ORIGINAL PUBLICATIONS

This thesis is based on the following publications:

I Kylmälä MM, Antila MK, Kivistö SM, Lauerma K, Vesterinen PH, Hänninen HA, Toivonen L, Laine MK. Tissue Doppler strain-mapping in the assessment of the extent of chronic myocardial infarction: validation using magnetic resonance imaging. European Journal of Echocardiography. 2008;9(5):678-84.

II Kylmälä MM, Antila M, Kivistö SM, Lauerma K, Toivonen L, Laine MK. Can strain rate imaging predict recovery of contraction after acute myocardial infarction? European Journal of Echocardiography. 2011;12(5):364-71.

III Kylmälä MM, Konttila, T, Vesterinen P, Lindholm M, Nieminen MS, Stenroos M, Väänänen H, Hänninen H, Toivonen L. Predicting recovery of myocardial function by electrocardiography after acute infarction. Annals of Noninvasive Electrocardiology 2013;18(3):230-239.

IV Kylmälä MM, Vesterinen P, Konttila T, Kivistö SM, Lauerma K, Lindholm M, Nieminen MS, Stenroos M, Väänänen H, Hänninen H, Toivonen L. Assessment of myocardial infarction size by body surface potential mapping: Validation against contrast-enhanced cardiac magnetic resonance imaging. Annals of Noninvasive Electrocardiology, in press.

The original publications are published with the permission of the copyright holders and are referred to in the text by their Roman numerals.

ABBREVIATIONS

ACS	acute coronary syndrome
BSPM	body surface potential mapping
CABG	coronary artery bypass grafting
CK	creatine kinase
CK-MB	creatine kinase MB
CMR	cardiac magnetic resonance imaging
DE-CMR	cardiac magnetic resonance imaging with delayed contrast enhancement
DSE	dobutamine stress echocardiography
ECG	electrocardiography
EF	ejection fraction
LAD	left anterior descending coronary artery
LCX	left circumflex coronary artery
LV	left ventricle
MI	myocardial infarct / infarction
NQMI	non-Q-wave myocardial infarction
NSTEMI	non-ST-elevation myocardial infarction
PCI	percutaneous coronary intervention
PET	positron emission tomography
QMI	Q-wave myocardial infarction
RCA	right coronary artery
SMS	strain-mapping score
SPECT	single-photon emission computed tomography
SRI	strain rate imaging
STEMI	ST-elevation myocardial infarction
STR	ST-segment resolution
TnI	troponin I
TnT	troponin T
WMS	wall-motion score

ABSTRACT

Myocardial infarct size is clinically relevant, affecting heart function and patient prognosis. After myocardial infarction (MI), it is important to establish whether myocardial dysfunction is due to permanent infarct damage, or if the myocardium is viable, in which case contraction may be improved by revascularization. Established methods for assessing infarct size and viability, such as cardiac magnetic resonance imaging with delayed contrast enhancement (DE-CMR) and myocardial perfusion imaging are neither readily available nor suitable in acute MI. In contrast, electrocardiography (ECG) and echocardiography are widely available diagnostic methods at the patient's bedside at any hour. Echocardiographic strain rate imaging, based on measurement of myocardial velocities by tissue Doppler, is a sensitive and objective method for quantification of myocardial contraction. If myocardium contracts, it is viable. Body surface potential mapping (BSPM) records ECG with multiple leads covering the entire thorax, with a variety of ECG variables automatically calculated from its recordings. The aim of the studies for this thesis was to evaluate whether infarct size and myocardial viability can be assessed by strain rate imaging and BSPM.

The studies included up to 62 patients with acute coronary syndrome, most with an infarction. BSPM with 123 leads and echocardiography were performed within 48 hours after onset of chest pain, and repeated during recovery of the infarction, at 1 to 4 weeks, and after healing, at 6 to 12 months. Global infarct size and segmental extent of infarct were determined by DE-CMR after healing.

Strain rate imaging allowed assessment of viability and global infarct size in both acute and chronic MI. Strain mapping was validated, for the first time, as a semi-quantitative method for the assessment of systolic strain, and showed excellent correlation with quantitative strain values. In chronic MI, segments with systolic strain values < -6% were most probably viable, having no infarct or a non-transmural infarct. Strain mapping proved as good as quantitative strain in distinguishing transmural from non-transmural infarcts. In acute MI, strain- and strain-rate variables could distinguish viable from non-viable segments, post-systolic strain having the best accuracy at predicting recovery of severe contraction abnormality (AUC 0.78).

BSPM could estimate infarct size at all stages of the infarction, with Q- and R-wave variables, as well as the QRS integral having the strongest correlations with infarct size at all time-points. The repolarization variables were clearly inferior; only in chronic MI did the T-wave variables have nearly as strong correlations with infarct size as did QRS variables. In contrast, the repolarization variables proved good at predicting recovery of left ventricular (LV) function in acute MI, irrespective

of MI location. The 1st QRS integral was the only depolarization variable good at predicting recovery of LV dysfunction, and the only variable able to estimate infarct size in addition to viability.

In conclusion, strain rate imaging as well as computed ECG variables can predict recovery of myocardial function in acute MI and can assess infarct size in both acute and chronic MI. Strain values can be quickly and accurately estimated by the strain-mapping method, validated now for the first time in the assessment of infarct transmurality. These methods, easily performed at bedside, may help the clinician assess patient prognosis and the need for revascularization after MI.

1 INTRODUCTION

Myocardial infarction (MI) is defined as cell death due to myocardial ischemia, that is, inadequate myocardial blood flow. Classical MI results from plaque rupture in a coronary artery leading to an occluding blood clot at the site of the rupture. Heart muscle supplied by the occluded artery becomes acutely ischemic, and subsequently undergoes necrosis. Myocardial cell death appears initially in the subendocardium, the inner layer of the left ventricular (LV) wall, and from there, necrosis extends in a wave front (Thygesen et al. Third universal definition of myocardial infarction 2012). After 6 hours of total occlusion, most of the myocardium in the ischemic region is infarcted; by 12 to 24 hours, the infarct is fully evolved (Smith et al. 1974, Reimer et al. 1977, Jennings & Reimer 1983). The occlusion may, however, be partial or intermittent, causing ischemia without necrosis, corresponding to unstable angina pectoris in clinical terms. Acute coronary syndrome is the clinical picture resulting from classical MI and unstable angina (Bassand et al. Guidelines for the diagnosis and treatment of non-ST-segment elevation acute coronary syndromes 2007).

Infarct size directly relates to the occurrence of congestive heart failure, ventricular arrhythmia, and cardiac death (Roes et al. 2007, Wu et al. 2008, Kwon et al. 2009, Larose et al. 2010, Gibbons 2011). Timely reperfusion therapy for acute MI limits infarct size, and thus plays an important part in reducing MI-related mortality rates (Boersma et al. 1996, 2006). Patients who develop a large infarct need the effective medical therapy shown to improve LV function and survival. Regular follow-up is also important in these patients, who often need resynchronizing and defibrillating pace-makers for improving symptoms and prognosis; in cases of end-stage heart failure, sometimes an option is even cardiac transplantation.

Within a few seconds after acute coronary occlusion, ischemic myocardium ceases contracting. If coronary perfusion is restored, either spontaneously or by revascularization, contraction may recover, as long as the myocardium is viable. In a wider sense, viability means the presence of life. Myocardium is most often viable and recovers after reperfusion if the infarct scar is limited to the subendocardium. Myocardium with transmural infarct (50–100% of the myocardial thickness) is unlikely to recover (Choi et al. 2001). Assessment of viability is important, as patients with ischemic, viable myocardium have substantially better event-free survival after revascularization than do those receiving only medical therapy. In patients without viability, revascularization may do more harm than good (Allman et al. 2002a, Schinkel et al. 2007).

The infarct scar can be directly visualized by several imaging methods, namely contrast-enhanced cardiac magnetic resonance imaging (DE-CMR), single-photon emission computed tomography (SPECT), and positron emission tomography

(PET). All of these methods are standard for assessment of infarct size and viability. Viability may also be assessed by stress echocardiography. However, none of these methods is widely available, they cannot be performed at the bedside, and they are seldom suitable in the acute phase of MI. Electrocardiography (ECG) and echocardiography, on the other hand, are routinely used for cardiac diagnostics, and are easy to perform also in the acute phase, at any time of day. The severity and extent of wall-motion abnormalities on two-dimensional echocardiography correlate with infarct size. LV ejection fraction (EF) is a strong predictor of survival after acute MI, and is related to the magnitude of infarcted myocardium (Weir & McMurray 2006, Wu et al. 2008, Larose et al. 2010). In acute MI, however, contraction abnormalities may overestimate infarct size, because contraction may improve if the myocardium is viable. Visual ECG analysis can demonstrate the presence of an infarct by Q waves, reduced R waves, and inverted T waves, but cannot distinguish transmural from non-transmural infarcts. Infarct-size estimation is possible by the Selvester QRS score, but the score is less validated in acute MI, and has not served to assess viability (Ideker et al. 1982, Roark et al. 1983, Ward et al. 1984a, Engblom et al. 2005b, Geerse et al. 2009, Weir et al. 2010).

Strain rate imaging, introduced in the 1990's (Fleming et al. 1994), is a new echocardiographic imaging mode for the quantification of regional myocardial deformation. This technique is based on measuring myocardial velocities by tissue Doppler. Strain rate imaging has been validated in ischemia and MI diagnosis. Compared with visual wall-motion analysis, strain rate imaging is an objective method for the assessment of myocardial contraction and is more sensitive in the detection of myocardial contraction abnormalities. Body surface potential mapping (BSPM) has been in use since the 1970's for computed analysis of ECG from 32 to 264 leads covering the thoracic surface. It has proven more sensitive than traditional ECG in the diagnosis of ischemia and infarction. Computed BPSM variables detect ECG changes not visible on the standard 12-lead ECG, and some of the best recording locations are outside the standard 12 leads. This thesis will discuss the use of strain rate imaging and BSPM in assessment of infarct size and viability.

2 REVIEW OF THE LITERATURE

2.1 Natural course of myocardial infarction

2.1.1 Evolution of myocardial infarction

Total occlusion of coronary flow causes transmural ischemia. As shown in animal studies, within 30 seconds after occlusion of coronary flow, myocardial contraction completely ceases (Theroux et al. 1974). After 20 minutes of total ischemia, myocardial cell death occurs, initially in the inner half of the ventricular wall, the subendocardium. From the subendocardium, necrosis extends in a wave front: After 3 hours of occlusion, salvageable myocardium still exists, but after 6 hours, most of the myocardium in the ischemic region is infarcted. At 24 hours, the infarct is fully evolved, extending through the full thickness of the ventricular wall in most of the ischemic region (Smith et al. 1974, Reimer et al. 1977, Jennings & Reimer 1983).

Acute partial occlusion of a coronary artery, reducing endocardial flow by only 10 to 20% of the normal at rest, causes subendocardial ischemia and impaired myocardial contraction. The contraction abnormality worsens gradually with diminished flow, but contraction is not completely lost until endocardial flow is reduced by 90% (Vatner 1980). Moderate, 40%, reduction of myocardial blood flow for 24 hours leads to significant infarction, mainly in the subendocardium, but also extending to the midmyocardium. Even 5 hours of moderate ischemia may cause patchy subendocardial necrosis (Kudej et al. 1998).

One week after the acute event, the infarcted myocardium enters the healing phase, during which the necrotic myocardium is replaced by a dense collagenous scar. When scarring is complete, after 1.5 months or later, the MI is said to be healed, or chronic (Alpert et al. 2000).

2.1.2 Clinical significance of myocardial infarct size

After acute MI, MI size is the major predictor of clinical outcome. Infarcts have been classified as small (< 10% of the LV), medium (10–30% of the LV), and large (> 30% of the LV) (Alpert et al. 2000). In the era before reperfusion therapy, all acute MI patients who died of cardiogenic shock had at autopsy an infarct size > 40% of the LV. With the introduction of reperfusion therapy and modern medical treatment, patients with MI size > 40% of the LV after acute MI have been able to survive for more than a year (McCallister et al. 1993). In a recent CMR study, 80% of the patients with prior MI who died during a 5-year follow-up had an MI size >

10%; a cutoff MI size of 24% had the best accuracy at predicting mortality (hazard ratio 2.1) (Bello et al. 2011).

Both EF and LV volume reflect MI size and are strong predictors of mortality. The 6-month mortality was higher in thrombolysed patients with predischarge EF < 40% than in those with a better EF (8.6–15.2% vs. < 2.2%) (Volpi et al. 1993). LV end-systolic volume showed independent and incremental prognostic significance over EF: In patients with EF < 50%, 5-year survival was significantly greater if end-systolic volume was below the median than above (survival 80–90% vs. 50–70%) (White et al. 1987). Importantly, an even stronger predictor of mortality than EF and LV volume was total MI size as measured directly by DE-CMR (Roes et al. 2007). MI size by CMR showed good correlation with EF and LV volumes, and predicted symptomatic heart failure. In most patients with MI size < 18.5% of the LV, EF was > 40%, and heart failure rarely occurred (Wu et al. 2008).

2.2 Viability

Viability refers to ischemic, dysfunctional myocardium at least partly alive and having the potential to recover after myocardial perfusion is restored, either spontaneously or after reperfusion therapy. The term "viability" usually signifies improvement of LV function by revascularization in patients with chronic, regional ischemia caused by significant stenosis in the coronary arteries supplying the dysfunctional LV regions (Allman 2013). Observational and retrospective studies indicate that patients with viability have substantially better event-free survival after revascularization than do those receiving medical therapy only (Allman et al. 2002b, Schinkel et al. 2002). After acute MI, dysfunctional myocardium may contain a mixture of the following: myocardium without necrosis, but dysfunctional due to stunning or hibernation; partly viable myocardium with subendocardial infarct; non-viable myocardium with transmural infarct, associated with irreversible dysfunction. Stunned and hibernating myocardium, as well as myocardium with a subendocardial infarct, has the potential to recover. Myocardium with transmural MI (50–100% of the myocardial thickness) is less likely to recover. The transmural extent of LV myocardial necrosis correlated with grade of permanent LV dysfunction, and was a better predictor of functional LV recovery after reperfusion than was total MI size (Choi et al. 2001). After acute MI, recovery of contraction of reperfused viable myocardium is delayed, requiring days to weeks, even several months (Bourdillon et al. 1989, Pfisterer et al. 1991).

2.2.1 Stunning

Stunning refers to prolonged, but completely reversible, myocardial dysfunction caused by a transient ischemic episode. Importantly, stunned myocardium is hypo- or non-contractile, despite the absence of cell death and despite normal resting coronary flow. Stunning was nicely demonstrated by Heyndrickx and co-workers (1975) in an experimental study in dogs. They showed that brief periods of coronary artery occlusion caused prolonged impairment of myocardial function despite normalized coronary flow and ECG changes. After a 5-minute occlusion, myocardial contraction recovered gradually over 2 to 6 hours; after a longer, 15-minute occlusion, recovery was slower, and normalization of contraction took up to 24 hours. After a 2-hour occlusion, recovery of regional myocardial dysfunction could continue up to 4 weeks, even though most of the improvement in contraction occurred between 24 hours and one week after reperfusion (Bush et al. 1983).

In patients, stunning is observable after successful reperfusion therapy for acute MI, after episodes of unstable angina, and after exercise-induced ischemia. The recovery time for stunned myocardium varies—depending on the severity and duration of ischemia—from a few hours to a few weeks. Even dysfunctional myocardium with subendocardial infarction may improve contraction if the outer layers of the myocardial wall are stunned (Ellis et al. 1983). The exact mechanism of ischemic injury leading to stunning is unknown, but this mechanism is associated with rapid generation of oxygen-derived free radicals after reperfusion, and with alterations in calcium homeostasis. Importantly, contraction of stunned myocardium normalizes during catecholamine infusion, indicating that the contractile apparatus of the myocyte is sufficiently intact to allow full contraction (Kloner & Jennings 2001).

2.2.2 Hibernation

Hibernating myocardium involves, similarly to stunning, reversibly dysfunctional myocardium. In contrast to stunning, hibernation is due to partially reduced coronary flow distal to a coronary artery stenosis. In hibernation, myocardial metabolism is reduced to equal hypoperfusion, with the demand for energy in balance with supply in the resting state. Acutely reduced myocardial perfusion leads to proportionally decreased contraction. Over the first few hours, myocardial metabolism is also improved, with reduced lactate production and recovery of creatine phosphate values. Thus, moderately ischemic myocardium with reduced contraction may remain viable for several hours, a phenomenon called short-term hibernation (Vatner 1980, Ross 1991, Heusch et al. 2005). Short-term hibernation was demonstrated in dogs by Matsuzaki et al. (1983). Reduction of myocardial blood flow through partial coronary artery stenosis immediately caused reduction

in systolic wall thickening. When, after 5 hours of ischemia, complete reperfusion had been established, wall thickening partially improved during the first 3 days, and completely normalized after 7 days (Matsuzaki et al. 1983). However, moderate ischemia lasting > 5 to 24 hours does lead to subendocardial, and possibly also to midmyocardial infarcts (Kudej et al. 1998).

In chronic hibernation, ischemia persists for days to months. In chronic hibernation, myocardial hypoperfusion, a consequence of, rather than the reason for myocardial dysfunction, is initiated by a reduced coronary flow reserve in the presence of normal resting perfusion. Most often, chronic hibernation is preceded by repetitive episodes of stunning. Subsequently, prolonged ischemia initiates adaptive metabolic changes in the myocytes, and structural changes also occur, including apoptosis. Because of these events, dysfunctional myocardium, after long periods of hypoperfusion, may remain viable and recover. Recovery of myocardial function after revascularization may, however, take more than a year, and due to structural changes, myocardium may recover incompletely (Bax et al. 2001, Canty & Fallavollita 2005).

2.3 Infarct size by histopathologic examination

All established non-invasive imaging methods for assessment of MI size have undergone validation against histologically determined MI size in experimental, or in anatomic pathologic clinical studies.

Standard microscopic post-mortem examination can identify myocardial necrosis 6 to 12 hours after MI onset; gross anatomic changes in the myocardium appear after 12 to 24 hours (Cotran et al. 2010). Histochemical stains can delineate necrotic myocardium and facilitate macroscopic recognition of the infarct area only 2 to 3 hours after MI onset. Staining of tissue slices with the tetrazolium salts nitro blue tetrazolium and triphenyltetrazolium chloride is the gold standard in assessment of infarct size acutely. Tetrazolium compounds are reduced by lactate dehydrogenase enzymes to a red formazan precipitate in normal myocardium, whereas the necrotic myocardium depleted of enzymes remains pale (Vargas et al. 1999). In chronic MI, the extent of infarct scar can be directly evaluated from tissue slices without any need of staining.

2.4 Biomarkers reflecting myocardial injury

Cardiac biomarkers have shown a good correlation with MI size, and thus serve as a semi-quantitative measure of MI size. In patients with acute MI, since the 1970's, cardiac enzymes have been one means of indirect MI size-assessment. CK-MB, an isoenzyme of creatine kinase (CK) found predominantly in heart muscle, is the

most specific enzymatic marker of myocardial necrosis, and therefore became the preferred marker over aspartate aminotransferase, lactate dehydrogenase, and CK; all three of these were the first available diagnostic markers of acute MI. Nowadays, for detection of myocardial injury, cardiac troponin is the standard biomarker, because of its being an extremely sensitive, and 100% specific, marker of myocardial damage (Thygesen et al. Third universal definition of myocardial infarction 2012).

2.4.1 CK and CK-MB

The most accurate methods for evaluation of enzymatic MI size in patients hospitalized for acute MI, are based on frequent sampling of total CK or CK-MB for several days. MI size calculated from such complete enzyme activity curves in non-reperfused patients has shown a strong correlation with post-mortem MI size ($r = 0.87$). The more simple measure of peak CK or peak CK-MB also showed a very good correlation with anatomic MI size ($r = 0.79$) (Hackel et al. 1984). After reperfusion, peak CK- and CK-MB values are higher and appear more rapidly, because of the wash-out phenomenon of these cytosolic enzymes that accumulate in the myocardial interstitium following coronary vessel occlusion. At similar peak CK and CK-MB levels, reperfused patients had smaller MI damage than did patients without reperfusion. Rapid appearance of peak CK and CK-MB predicted better recovery of myocardial function (Ong et al. 1983, Tamaki et al. 1983, Choi et al. 2001). In reperfused patients, the correlation between peak CK-MB and MI size on CMR or SPECT was $r = 0.65–0.83$. The peak values performed almost as well as did cumulative enzyme release (Choi et al. 2001, Hedstrom et al. 2007, Chia et al. 2008, Di Chiara et al. 2010).

2.4.2 Cardiac troponins

Cardiac troponin T (TnT) and I (TnI) prove to be contractile proteins of the myofibril, and cardiac troponins in the blood are very sensitive markers of myocardial necrosis. In patients treated with percutaneous coronary intervention (PCI) for ST-elevation MI (STEMI), peak values of troponin as well as of CK-MB appeared 3 to 12 hours after PCI. Peak troponin values correlated with MI size as well as, or better than did peak values of CK-MB. The correlation of peak TnT and TnI with MI size on CMR was $r = 0.76–0.82$, (Hedstrom et al. 2007, Di Chiara et al. 2010); the correlation was $r = 0.45–0.74$ with technetium-99m SPECT used for measurement of MI size (Chia et al. 2008, Byrne et al. 2010). Troponin values measured as early as 2 hours after PCI showed good correlation with MI size ($r > 0.6$). Prespecified time-points had comparable correlations with MI size to those of peak values: The best correlations

were obtained at 4 hours post PCI for CK-MB (r = 0.63), 24 hours for TnT (r = 0.66), and 72 hours for TnI (r = 0.73) (Chia et al. 2008).

2.5 Imaging of infarct size and viability – established methods

2.5.1 Cardiac magnetic resonance imaging

Cardiac magnetic resonance imaging (CMR) with delayed contrast enhancement is regarded as the modern golden standard for non-invasive assessment of MI size, because it has shown almost perfect agreement with the histopathologically determined shape and size of the infarct scar. Since the first studies in explanted canine hearts in the early 1980's (Goldman et al. 1982), DE-CMR has received extensive validation in experimental and clinical studies, for both acute and chronic MI (Kim et al. 2009b, Perazzolo Marra et al. 2011). With its extremely high spatial resolution, DE-CMR can detect infarcts as small as 1 gram of myocardium, and allows determination of the transmural extent of MI (Wu et al. 2001a). In a recent multicenter trial, its sensitivity in MI detection was as high as 99% in acute, and 94% in chronic cases. In 97% of the trial's patients, location of hyperenhancement and region perfused by the infarct-related artery matched (Kim et al. 2008). In the acute phase, however, hyperenhancement overestimates final infarct size by about a third (Hombach et al. 2005, Baks et al. 2006, Larose et al. 2010). MI-size measurements from DE-CMR images have shown low intra- and interobserver variability, and high reproducibility (Mahrholdt et al. 2002).

2.5.1.1 Main principles of the CMR technique

CMR relies on special software programs, called pulse sequences, to differentiate myocardium from other biological tissues, and to assess myocardial perfusion and infarct scar. Cine imaging is the CMR technique used to evaluate cardiac volume, mass, and contractile function. T2-weighted imaging reveals myocardial edema and is useful in the diagnosis of acute MI. DE-CMR, however, is the best technique for assessment of infarct scar and viability. DE-CMR uses an extracellular contrast agent, most commonly gadolinium, to visualize irreversibly injured myocardium. In DE-CMR images, normal myocardium appears black because of rapid gadolinium washout, but infarcted regions appear bright or hyperenhanced because of the higher concentration and slower washout of gadolinium associated with the greater distribution area: In acute MI, membrane rupture occurs and then gadolinium diffuses into myocytes; in chronic MI, myocytes are replaced by scar. The amount of hyperenhancement is usually assessed from short-axis images of the heart, either

visually, or by planimetry. Infarct size as a percentage of the LV is calculated by adding the percentage of hyperenhancement in each of 17 segments, and dividing by 17 (Kim et al. 2009a).

2.5.1.2 Infarct size by CMR and prognosis

Infarct size determined by DE-CMR has been a strong predictor of clinical outcome, independent from LV EF and volume. Infarct size also predicts LV function and adverse remodeling of the LV. (Roes et al. 2007, Wu et al. 2008, Kwon et al. 2009, Larose et al. 2010). In patients with acute MI, a cutoff MI size of 18.5% had a sensitivity of 88% and a negative predictive value of 96% at predicting mortality, re-infarction, or heart failure. Infarct size in subacute MI had a good correlation with EF and LV volumes measured 3 months later: r = -0.76 for EF, 0.74 for LV end-systolic volume index, and 0.64 for LV end-distolic volume index. Patients with an infarct size > 14% had reduced EF < 50% at follow-up; patients with adverse remodeling had significantly larger MI size than had those without (mean MI size 30% vs. 19%) (Wu et al. 2008). Findings indicative of microvascular damage predict adverse LV remodeling and poor clinical outcome, independently of infarct size (Hombach et al. 2005, Wu et al. 2008).

2.5.1.3 Transmurality of infarct by DE-CMR and segmental viability

Improvement of regional myocardial contraction after reperfusion is related to transmurality of infarct scar. In acute MI, myocardial function is very likely to recover, if < 25% of the LV wall thickness is hyperenhanced. Some recovery is possible with an infarct transmurality of 25 to 75%. If microvascular obstruction is evident, recovery is highly unlikely (Choi et al. 2001, Gerber et al. 2002). In chronic MI, dysfunctional myocardial segments with a transmural extent of scar ≤ 50% are likely to recover after revascularization. If the transmural extent of infarct is 51 to 75%, only about 10% of segments recover, and if > 75%, recovery is unlikely. The more dysfunctional but viable the segments, the more EF improves during follow-up (Kim et al. 2000, Selvanayagam et al. 2004, Kuhl et al. 2006). Figure 1 shows an example of an infarct scar including both transmural and non-transmural infarct.

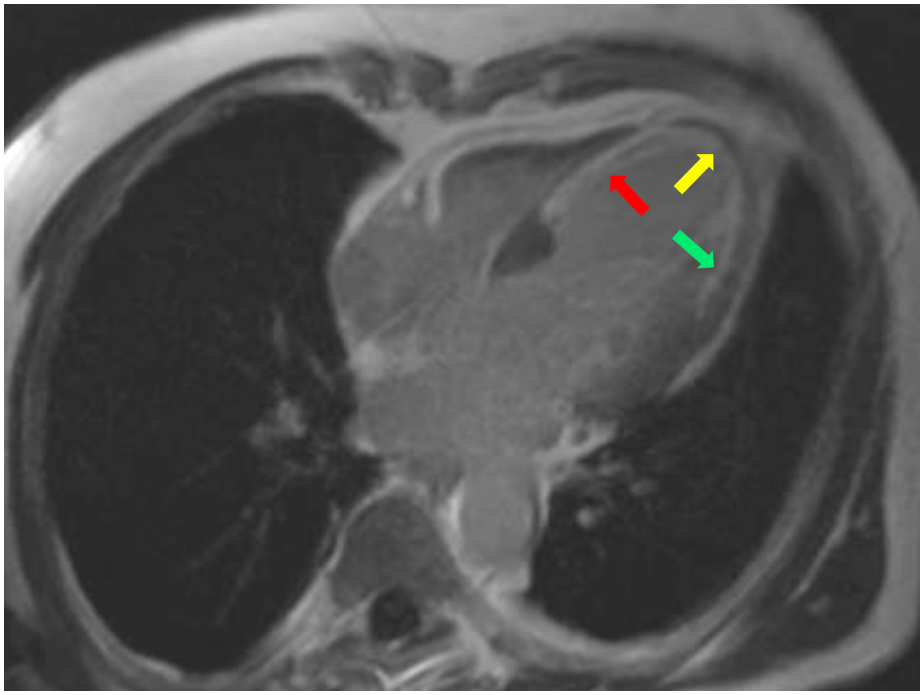

Figure 1. *This DE-CMR image shows a heart 6 months after an ST-elevation MI caused by occlusion of the proximal LAD which was treated successfully by primary PCI 2 hours after onset of chest pain. The infarct appears white, and the viable myocardium, black. Nearly 100% transmural infarction of the mid- and apical septum (red arrow). At the apex (yellow arrow), infarct transmurality is 50%, and in the mid-lateral wall the infarct is non-transmural, <50% of the wall thickness (green arrow). LAD = left anterior descending coronary artery, MI = myocardial infarct, PCI = percutaneous coronary intervention.*

2.5.2 Nuclear imaging methods

Single-photon emission computed tomography (SPECT) and positron emission tomography (PET) are nuclear imaging methods used for diagnosis of coronary artery disease and assessment of viability in patients with LV dysfunction. SPECT and PET both show good sensitivity (80–90%) for detection of viability, but specificity is lower (50–60% for SPECT, 60–70% for PET) (Schinkel et al. 2007). In ischemic cardiomyopathy, recovery of viable but dysfunctional myocardial segments after revascularization has been associated with less adverse remodeling of the LV, improved exercise capacity and symptoms, and better survival. An increase in EF after revascularization is probable if ≥ 25% (4 segments) of the LV is dysfunctional but viable (Bax et al. 2005). Studies suggest that viability on imaging predicts improved survival after revascularization of patients with ischemic cardiomyopathy (Allman et al. 2002b, Beanlands et al. 2007).

2.5.2.1 SPECT

SPECT uses radioactive tracers, namely thallium-201 and technetium-99m-labeled agents, for assessment of myocardial perfusion and viability. Tomographic images of the heart come from a gamma camera that detects the uptake of the radioactive tracer in myocardium. The activity of the tracer in the LV is then displayed in images. Myocardial uptake of the tracer relies on the presence of perfusion, as well as cell membrane- and mitochondrial integrity. In areas of myocardial infarct tracer activity at rest will be reduced, because uptake of the tracer is dependent on cellular viability. If the uptake is ≥ 50% of that in normal myocardium, the dysfunctional myocardium is considered viable; if 30 to 50%, the finding is equivocal; and if < 30%, the myocardium is considered non-viable. Use of technetium-99m-labeled agents also permits assessment of LV function, which may aid in viability detection. SPECT after stress permits detection of inducible ischemia, revealing the hemodynamic significance of coronary artery stenosis. Inducible ischemia is also a marker of viability (Beller et al. 1977, Beller 2000, Holly et al. 2010, Beller & Heede 2011).

MI size by SPECT closely reflects histologic MI size, and shows excellent correlation with MI size by DE-CMR. In acute MI, technetium-99m sestamibi SPECT can assess the size of myocardium at risk, and final MI size measured at discharge from hospital predicts mortality: Patients with < 14% MI size on SPECT have a low mortality, ≤ 2%, during 6 to 12 months of follow-up (Prigent et al. 1986, Wagner et al. 2003, Fieno et al. 2007, Gibbons 2011). Because the spatial resolution of SPECT is lower than that of CMR (10 mm vs. 1–2 mm), SPECT may fail to identify subendocardial infarcts < 50% of the wall thickness. Other disadvantages of SPECT are radiation burden and attenuation artefacts from the diaphragm and from women's breasts (Wagner et al. 2003, Holly et al. 2010).

2.5.2.2 PET

PET differs from SPECT in that, in addition to myocardial perfusion, it assesses myocardial metabolism. Radioactive perfusion tracers used for PET include N-13-ammonia, Rb-82, and O-15-water; the most usual tracer of metabolism is F-18-fluorodeoxyglucose (Ghosh et al. 2010). PET can quantify myocardial blood flow and, as compared with coronary angiography, PET has high diagnostic accuracy in coronary artery disease diagnosis (Di Carli & Hachamovitch 2007). Detection of viability is based on active glucose metabolism in myocardium with normal or reduced perfusion. Myocardium without metabolism and with severely reduced or absent perfusion is non-viable (Ghosh et al. 2010).

MI size by PET correlates strongly with MI size by CMR, and both methods are accurate in predicting recovery from myocardial dysfunction (Klein et al. 2002, Kuhl et al. 2006). The advantage of PET, as compared with SPECT, is its shorter

acquisition time, and its better diagnostic accuracy due to the lack of attenuation artefacts and better resolution. PET, however, is an expensive, time-consuming, and complex method, and therefore is rare in clinical practice (Bengel et al. 2009).

2.5.3 Echocardiography

2.5.3.1 Basic principles of echocardiography

Echocardiography, or heart ultrasound, is based on transmitting ultrasound with a transducer. Sound with a wave-frequency > 20 kHz is inaudible, and is therefore termed ultrasound. The transmitted ultrasound waves propagate through the body, and are reflected back by the heart and other structures. The transducer that transmitted the ultrasound also receives these reflected echoes. The intensity of reflected ultrasound depends on the properties of the tissue, which makes it possible to differentiate between different structures, such as between myocardium and blood. Reflections from structures further away return later than reflections closer to the transducer. Based on the intensity of reflected ultrasound and the time from transmission to reflection, a two-dimensional image of the heart can be produced by the ultrasound machine, and also be visualized on a screen in real time. Echocardiography is completely safe for the patient, and can be performed at the patient's bedside because ultrasound machines are easily movable (Otto 2004).

2.5.3.2 Assessment of infarct size by two-dimensional echocardiography

In patients with acute coronary syndrome, ischemia causes myocardial contraction abnormalities in the region distal to the occluded coronary artery. These contraction abnormalities are, on two-dimensional echocardiography, visible as regionally impaired LV wall motion or wall thickening (Schiller et al. 1989a, Lang et al. Recommendations for chamber quantification 2006). The contraction abnormality is proportional to the severity of ischemia, and accordingly, LV contraction may be reduced (hypokinetic) or absent (akinetic or dyskinetic) (Kerber et al. 1975).

Regional contraction abnormality is very sensitive (94%) for diagnosis of acute coronary syndrome, and absence of contraction abnormalities is of excellent negative predictive value (98%) (Cheitlin et al. 2003). Pioneer studies by Nieminen and Heikkilä (1975) showed echocardiography to be a valuable imaging tool for non-invasive assessment of MI location and extent in acute MI patients, a finding supported subsequently by others (Wyatt et al. 1981, Cheitlin et al. 2003). After acute MI, myocardial dysfunction may be reversible because of stunning or hibernation, and therefore the extent of myocardial dysfunction may not correlate with MI size. If the transmural extent of MI

damage is < 50%, myocardial contraction may recover completely. Thus, in the chronic phase of MI, subendocardial infarcts may cause no visible contraction abnormalities, and the infarct scar may go unnoticed (Mahrholdt et al. 2003).

Experimental studies

Studies in dogs reveal that early after coronary artery occlusion, correlation between the echocardiographic extent of myocardial dysfunction and histological MI size is poor; but at 48 hours after occlusion it becomes significant (r = 0.72–0.89) (Wyatt et al. 1981, Nieminen et al. 1982). Contraction abnormalities on echocardiography tend to overestimate MI, which may be due to myocardial stunning, tethering of normal segments adjacent to those infarcted, or transient ischemia of myocardium adjacent to the infarcted region. Indeed, after 48 hours of coronary occlusion in dogs, the transmural extent of infarct in dyskinetic segments has ranged from 21 to 100%, which is why some dyskinetic segments may show functional recovery later (Lieberman et al. 1981).

Clinical studies

Studies have shown that wall-motion abnormalities on two-dimensional echocardiography are associated with MI size in patients with recent and with old MI. In autopsy studies, the severity of segmental and global LV dysfunction on echocardiography, performed within weeks before death, shows a significant relationship with segmental and global MI size, with all segments having a transmural extent of MI > 75% as being a- or dyskinetic. Importantly, all hypokinetic segments have been viable, having no, or subendocardial infarction (Weiss et al. 1981, Shen et al. 1991). In the acute phase, within a few days after admission, the echocardiographic extent of myocardial dysfunction has shown a significant correlation with MI size on thallium-201 and technetium-99m stannous pyrophosphate scintigraphy (r = 0.87 and 0.74, respectively) (Nixon et al. 1980).

In patients with NSTEMI, a wall-motion score (WMS) index > 1.3 could differentiate among patients with substantial MI damage, ≥ 12% of the LV by DE-CMR, with good accuracy (Eek et al. 2010). In patients with STEMI, WMS could differentiate among segments with no, non-transmural, or transmural (> 50% of segment thickness on DE-CMR) MI early after thrombolysis, as well as in the healing phase 1 to 2 weeks later. A significant correlation existed between EF and global MI size by DE-CMR, increasing from the early acute phase (r = -0.51) to the healing phase (r = -0.74) (Sjoli et al. 2009). After healing of MI, the EF and WMS index has shown significant correlations with global MI size (r = 0.55–0.71 and r = 0.67–0.76, respectively), and WMS with segmental MI size (r = 0.53) by DE-CMR. EF and WMS index could distinguish large MIs from medium-size MIs, but could not differentiate between medium and small MIs. WMS could separate segments with infarct transmurality > 50% from those with a lesser extent of MI (Gjesdal et al. 2008, Thorstensen et al. 2012).

2.5.3.3 Viability assessment by echocardiography

Myocardial wall thickness

In chronic MI, akinetic, thinned, and hyperechogenic myocardium indicates an infarct scar. Myocardial wall-thickness ≤ 5 to 6 mm indicates transmural MI and, in patients with chronic MI, virtually excludes viability. Dysfunctional segments with a wall thickness > 6 mm may recover after revascularization (Cwajg et al. 2000, La Canna et al. 2000, Schinkel et al. 2002). Acute, severe ischemia causes thinning of the myocardial wall; without reperfusion, necrotic myocardium will remain thin. Thickened, edematous myocardium in the ischemic region after reperfusion therapy performed 3 to 6 hours after onset of ischemia indicates transmurally infarcted myocardium. If reperfusion is performed earlier, wall thickness remains normal, indicating myocardium that is stunned or non-transmurally infarcted (Bijnens & Sutherland 2008, Merli et al. 2008).

Dobutamine stress echocardiography

If the myocardium contracts, it is at least partly viable, but akinetic and dyskinetic myocardium may also be viable, in acute MI as well as in the chronic phase. Improved contraction of dysfunctional myocardium on echocardiography during exercise or pharmacologic stress is proof of viability. In clinical assessment of viability, the stress echo method most widely used is dobutamine stress echocardiography (DSE) (Schinkel et al. 2007, Sicari et al. 2008).

In pigs, both acutely ischemic and hibernating dysfunctional myocardium have shown a biphasic response to dobutamine: After an initial low dose, an initial improvement occurred in myocardial contraction; higher doses, however, caused a mismatch between blood supply and myocardial demand because of flow-limiting coronary artery stenosis. Consequently, contraction deteriorated together with increased myocardial lactate production and acidosis (Chen et al. 1995). Such a biphasic response in patients with chronic ischemic LV dysfunction predicted segmental recovery after coronary artery bypass surgery (CABG) in 63% of segments at 3 months, and in 75% of segments at 14 months. In patients with a biphasic response in ≥ 4 segments, global LV function was likely to improve (sensitivity 89%, specificity 81%) (Cornel et al. 1998). In stunned myocardium after acute MI, contraction has improved to normal during inotropic stimulation, without a biphasic response (Mercier et al. 1982).

The value of DSE in predicting functional recovery after CABG in patients with chronic LV dysfunction was studied in one pooled analysis including all studies available from 1980 to 2007: In predicting recovery of regional myocardial function after revascularization in patients with chronic ischemic LV dysfunction, DSE had a weighted mean sensitivity of 80%, specificity of 78%, positive predictive value of 75%, and negative predictive value of 83%. The presence of several viable but dysfunctional segments (≥ 2–4) predicted recovery of global function. Viability by

DSE also seemed to indicate better survival in revascularized patients than in those not revascularized, or in those revascularized but without viability. In comparison with SPECT, PET, and CMR, DSE showed a lower sensitivity but a higher specificity in predicting recovery of regional and global LV function (Schinkel et al. 2007).

2.5.3.4 Evaluation of prognosis in MI patients by echocardiography

Echocardiography is a useful tool in assessment of prognosis. In patients with acute MI, the presence, as well as the extent and severity of LV regional dysfunction predict clinical outcome. In general, patients with only mild and localized wall-motion abnormalities show a low risk for complications. In comparison, patients with a larger extent and severity of wall-motion abnormality by echocardiography (e.g. WMS index > 2 and EF < 45%) are at increased risk for in-hospital pump failure, malignant ventricular arrhythmia, and death (Nishimura et al. 1984, Cheitlin et al. 2003, Dokainish et al. 2014). EF during healing of MI is a strong predictor of 6-month mortality, compared with an EF ≥ 40%, an EF < 40% being associated with up to seven-fold mortality (Volpi et al. 1993).

2.6 Strain rate imaging in assessment of myocardial infarction

2.6.1 Definition of strain and strain rate

Strain is a measure of myocardial deformation, and is calculated as the percentage change in length or thickness of a myocardial segment relative to its initial value. By definition, myocardial expansion yields positive strain values, and compression, negative values. When the heart contracts, the myocardium shortens in the longitudinal direction and thickens radially. Thus, longitudinal shortening yields negative strain values, and radial thickening, positive strain values. Longitudinal lengthening and radial thinning, appearing during diastole and in the case of systolic dyskinesia, yield opposite strain values. Strain rate is the velocity of deformation, expressed as s^{-1} (D'hooge et al. 2000b).

2.6.2 The technique of tissue Doppler strain rate imaging

Strain rate imaging (SRI) is based on measurement of myocardial velocities by the tissue Doppler technique. Doppler echocardiography was initially developed for measurement of blood flow velocities, but the tissue Doppler technique is basically the same: Ultrasound waves reflected from a moving surface will have a frequency

different from frequencies transmitted by the transducer, lower if the reflector is moving away from the transducer, and higher if moving towards the transducer. This difference in frequency, termed the Doppler shift, allows determination of the velocity of the moving object. Myocardial velocities can be sampled simultaneously at multiple sites and displayed in real-time as color-coded two-dimensional images, superimposed on gray-scale images. This is termed color Doppler myocardial imaging, or tissue Doppler imaging, and the technique is basically the same as color flow-mapping of blood-flow velocities. For visualization of myocardial velocities, however, filter settings are adjusted to allow detection of the low-velocity- and high-amplitude ultrasound signals typical for myocardium; high-velocity and low-amplitude signals from normal blood flow are filtered out (McDicken et al. 1992, Miyatake et al. 1995).

Longitudinally, myocardial velocities are normally highest in the basal parts of the LV, and decrease towards the apex. Radially, myocardial velocities increase from the epicardium towards the endocardium. Subsequently, a velocity gradient exists in the myocardial wall. This gradient is the same as strain rate, calculated as the difference of local velocities between two points divided by the distance between the points (spatial derivation of velocities). Myocardial strains are then extrapolated from the strain-rate data by temporal integration of strain-rate values. Strain and strain rate are better measures of regional myocardial contraction than is velocity, because myocardial velocities are affected by the overall translational motion of the heart as well as by the tethering and traction caused by neighboring segments (Fleming et al. 1994, Heimdal et al. 1998, D'hooge et al. 2000a, Derumeaux et al. 2000, Urheim et al. 2000).

Practical issues concerning strain rate imaging

While strain and especially strain rate closely correlate with regional myocardial contractility, their values are affected by loading conditions, strains more so than strain rates: An increased preload causes an increase, and an increased afterload a decrease in these values. At high heart rates, strain values decrease, whereas strain rates are unaffected (Urheim et al. 2000, Jamal et al. 2001a, Weidemann et al. 2002b).

In the tissue Doppler technique, careful alignment of the ultrasound beam as closely parallel as possible to the direction of myocardial movement is important to avoid underestimating velocities. Consequently, only longitudinal myocardial velocities can be measured from the entire LV by use of apical views; radial velocity measurements are limited to the posterior and anteroseptal walls by use of parasternal views. In addition to Doppler angle, myocardial velocity signals may be affected by aliasing and reverberations, a fact which should be recognized (Marwick 2006).

Similar to tissue velocities, strains and strain rates can be displayed as color-coded two-dimensional images in real time. Positive strain values indicating expansion

(lengthening/thickening) of the myocardium appear in shades of blue; negative strain values indicating compression (shortening/thinning) appear in shades of yellow or red. For exact quantification, regional myocardial strain rate- and strain curves can be extracted from these color-coded maps. Image optimization allows high temporal resolution of systolic and diastolic strain and strain rates; even isovolumic pre- and post ejection strain rates are discernable.

2.6.3 Development of strain rate imaging

Tissue Doppler strain- and strain rate imaging was made possible by the advent of a technique for measuring myocardial velocities. The idea that the velocity of myocardial movement reflects myocardial function led in the early 1990's to the development of color Doppler myocardial imaging, also called tissue Doppler imaging (McDicken et al. 1992). Quantification of myocardial velocities by this technique revealed higher velocities in the endocardium than in the epicardium. Use of M-mode color Doppler myocardial imaging allowed calculation of these myocardial velocity gradients across the myocardial wall thickness, in effect, identical to radial strain rates (Fleming et al. 1994). Software for color Doppler myocardial imaging was included in standard ultrasound machines, allowing measurement of longitudinal as well as radial myocardial velocities (Wilkenshoff et al. 1998). As an extension of the processing of tissue Doppler data by this software, the first real-time application for the measurement of strain rates was proposed by Heimdal et al. (1998). Based on this SRI method, Urheim et al. measured longitudinal myocardial strain as the time integral of regional strain rates, and validated these strain measurements against sonomicrometry in dogs subjected to myocardial ischemia (Urheim et al. 2000).

2.6.4 Strain rate imaging in healthy individuals

Edvardsen et al. (2002) found that in healthy individuals, longitudinal strain- and strain-rate values in the LV were homogenous, in contrast to myocardial velocities that decreased from base to apex. In validating SRI against CMR tissue tagging, they showed that radial and longitudinal strain values, when measured by both methods, agreed very closely (Edvardsen et al. 2002). In healthy adults aged 18 to 76, normal systolic longitudinal average strain rate values have ranged from -0.9 to -1.9 1/s. Normal end-systolic longitudinal average strain values have ranged from -14% to -24%. Radial strain-rate and strain values are higher than longitudinal values, normal systolic radial strain rates > 3.0 1/s and strain > 45%. Normal diastolic strain rate values are also higher radially than longitudinally. In children

and teenagers, strain and strain rate values are higher than in adults (Kowalski et al. 2001, Weidemann et al. 2002a, Sun et al. 2004, Herbots 2006).

The effect of aging and gender on longitudinal strains and strain rates has been reported in two studies of healthy adults. No significant changes in peak systolic strains or strain rates were evident with aging. Both studies found an age-dependent increase in late diastolic strain rates, but only one found an age-dependent decrease in early diastolic strain rates. Neither study found a difference in strain rates by gender, but one study found strain values to be higher in women (Sun et al. 2004, Herbots 2006).

Feasibility of longitudinal SRI has been > 90%, apical segments, especially in the anterior and lateral walls, being more often unsuitable for analysis than mid- or basal segments because of difficulties in parallel alignment of the ultrasound beam in apical segments (Kowalski et al. 2001, Sun et al. 2004). Intra- and inter-observer variability has been 12 to 15% for longitudinal systolic strains and strain rates, the variability being higher for diastolic values (Kowalski et al. 2001, Weidemann et al. 2002a, Herbots 2006).

2.6.5 Strain rate imaging in assessment of myocardial ischemic injury

SRI was developed for evaluation of regional myocardial function, SRI allowing quantification of regional myocardial contraction and diastolic function, as well as timing of mechanical events. One of the major applications of SRI is diagnosis of myocardial ischemia, because ischemia is the most common cause of LV regional contraction abnormalities. Ischemia affects first the endocardium, the myocardial layer most vulnerable to ischemic damage. Because myocardial fibers in the endocardium are oriented longitudinally, the longitudinal strains and strain rates are especially suitable for assessment of ischemia. Studies using tissue Doppler show that absolute systolic strain- and strain-rate values decrease, or become inverted, in ischemic myocardium, while the values in adjacent, non-ischemic myocardium remain unaffected.

2.6.5.1 Experimental studies

Consequences of acute ischemia for myocardial strains and strain rates

Experimental validation studies in animals have compared systolic tissue Doppler strain- and strain-rate values to myocardial contraction measured by ultrasonic crystals implanted in the myocardial wall. LAD occlusion for two minutes in dogs causes longitudinal lengthening of ischemic segments, as revealed by positive longitudinal systolic strain- and strain-rate values. The same values remain negative in non-ischemic segments that retain normal contraction (Urheim et al. 2000).

Moderate hypoperfusion (50% reduction of myocardial blood flow) results in reduced longitudinal systolic shortening and strain values, whereas total occlusion causes systolic lengthening and inverted, positive systolic strain values. Both grades of acute ischemia cause post-systolic shortening and strain (Skulstad et al. 2006a). In response to LAD occlusion, radial thickening ceases, and radial strain rates decrease nearly to zero, while non-ischemic, normally contracting segments retain normal positive radial strain rates (Derumeaux et al. 2000).

In closed-chest pigs subjected to acute ischemia, typical changes in radial strains and strain rates occur. Brief LCX occlusion for 20 seconds has led to a marked decrease in radial end-systolic strain values in the ischemic myocardium. Onset of myocardial thickening, as defined by the appearance of a positive strain value during systole, was significantly delayed, and thickening continued after aortic valve closure (post-systolic thickening). In early diastole, acute total ischemia made peak negative strain- and strain rate values fall, but left late diastolic values during atrial contraction unaffected. Severe hypoperfusion (≤ 20 ml/min) of the LCX resulted in reduced end-systolic and early diastolic strain and strain rates, but the values remained greater than during total occlusion of coronary flow. Hypoperfusion needed to be less severe (≤ 40 ml/min) to produce post-systolic strain (Jamal et al. 2001).

Strain rate imaging distinguishing viable from non-viable myocardium

In animal studies, SRI has been able to distinguish hypoperfused from stunned myocardium, as well as stunning and non-transmural infarction from transmural infarction. In acute as well as in chronic MI, a significant correlation appears between radial systolic strain- and strain-rate values with infarct transmurality, lower values being associated with a higher transmural extent of the infarct (Derumeaux et al. 2001, Weidemann et al. 2003).

In chronic MI, response to dobutamine stress echocardiography could distinguish segments with non-transmural from those with transmural MI; radial strain rates increased with low-dose dobutamine in non-transmural MI, but failed to do so in transmural MI. Further, the amount of post-systolic strain increased with dobutamine in non-transmurally infarcted segments, whereas systolic strain values in non-transmurally as well as in transmurally infarcted segments remained reduced (Weidemann et al. 2003).

Early after reperfusion in pigs, stunned segments without infarct have shown significantly greater radial strain-rate values in both systole and diastole than did segments with transmural infarct. Systolic strain values were equally low in stunned and in transmurally infarcted segments, but post-systolic strain was greater in stunned segments and was a sign of viability. Further, end-diastolic strain (coinciding with atrial contraction) was higher in stunned segments, indicating preserved compliance, whereas the lower values in infarcted segments indicated increased stiffness (Pislaru et al. 2004b). In stunned segments, following reperfusion of total occlusion, longitudinal post-systolic strain values increased (became more

negative), whereas inverted, positive systolic strain values decreased, both being signs of active contraction; in transmurally infarcted segments, no post-systolic shortening was evident (Lyseggen et al. 2005). Post-ischemic stunned segments could also be identified by their response to dobutamine stress; radial systolic strain- and strain-rate values increased significantly, and post-systolic strain disappeared (Jamal et al. 2001b). In contrast, with dobutamine challenge, in persistently ischemic dysfunctional myocardium, radial systolic strain values decreased, and post-systolic strain values increased. Systolic strain rates remained lower than normal without any significant response to dobutamine (Jamal et al. 2001a).

2.6.5.2 Clinical studies

Strain rate imaging in diagnosis of ischemia and infarction

Early clinical studies validated SRI against standard visual two-dimensional gray-scale wall-motion analysis. In patients with chronic MI, systolic longitudinal strain- and strain-rate values have deteriorated with worsening wall-motion abnormality. Values of normokinetic segments in MI patients did not differ from those in healthy controls (Voigt et al. 2000). Moreover, in patients with recent acute MI, longitudinal strain- and strain-rate values were reduced according to degree of wall-motion abnormality. Values of normokinetic segments did not differ from those of controls, except in the presence of significant coronary artery stenosis, in which case the values were reduced (Jamal et al. 2002). When SRI was validated against CMR tissue tagging in patients with recent acute MI, agreement was good between the methods, and both showed reduced or inverted longitudinal strain values in infarcted segments, while remote uninjured segments showed strain values similar to those in healthy controls (Edvardsen et al. 2001).

In patients with stable angina pectoris undergoing angioplasty, acute ischemia during coronary artery occlusion causes a reduction in both longitudinal and radial strain values, and this occurs, according to baseline visual wall-motion analysis, in normokinetic segments as well as in those with hypo- or akinesia. The amount of post-systolic strain increased during ischemia, and was even more accurate in the detection of acute ischemia than was end-systolic strain (sensitivity 95% vs. 86% and specificity 89% vs. 83%). Strain values returned to baseline immediately after occlusion. Strain analysis appeared more sensitive than visual wall-motion analysis in detection of ischemia-related contraction abnormality, especially of dyskinesia (Edvardsen et al. 2001, Kukulski et al. 2003).

Validation of strain rate imaging in MI patients against DE-CMR

SRI in the longitudinal direction has been validated against DE-CMR for assessment of the presence, segmental transmurality, and total size of MI. In all phases of MI, systolic strains and strain rates were significantly less negative in segments with

infarct than in those without, in acute MI patients even before revascularization. After PCI for acute MI, systolic strain and strain rates remained significantly lower in segments with transmural MI than in others at all time-points (Zhang et al. 2005, Weidemann et al. 2006a, Vartdal et al. 2007). In the subacute phase, peak systolic SR > -0.6 1/s could distinguish transmural MI with a sensitivity of 95% and a specificity of 91%, whereas visual wall-motion scoring could not. At 5 months after the acute event, systolic strains and strain rates were significantly less negative in segments with transmural than in those with non-transmural MI, as well as less negative in segments with non-transmural vs. those without infarct (Weidemann et al. 2006a). In other studies, this distinction was already possible with good accuracy in subacute MI and early after PCI in acute MI (Zhang et al. 2005, Vartdal et al. 2007). Early after PCI for acute MI, the correlation between segmental infarct size and peak systolic strain was r = 0.67; the correlation between total infarct size and averaged systolic strain rates in the infarct region was r = 0.81. It was, in the entire LV (global strain) r = 0.77 (Vartdal et al. 2007). The correlation between total infarct size and global strain was similar in chronic MI: r = 0.75 (Sachdev et al. 2006).

2.7 Standard 12-lead ECG in the estimation of myocardial infarct

2.7.1 Pathologic Q waves

Extent of MI according to Q-wave status

Q waves have long served as indicators of permanent MI damage. The clinical value of classifying MIs according to Q waves has intrigued many researchers for years. Historically, pathologic Q waves have been regarded as indicators of a transmural infarct. This conception has, however, been rejected. Several anatomic-pathologic studies have consistently reported that both subendocardial and transmural infarcts may develop with or without a Q wave. Q wave was, however, more probable in infarcts with a transmural extent of 50 to 100% than in subendocardial infarcts (Cook et al. 1958a, Cook et al. 1958b, Savage et al. 1977, Raunio et al. 1979).

Clinical studies using CMR have shown that Q waves are associated more with total size and subendocardial extent of the infarct than with transmurality. One-third or more of patients with subendocardial infarction show Q waves. On the other hand, the absence of Q waves does not exclude transmural infarction. Subendocardial and transmural MIs frequently co-exist, one possible explanation for the limited advantage of Q waves in evaluation of transmurality. As the subendocardial portion of the myocardium is depolarized during the early parts of the QRS complex, Q waves are more likely in a subendocardial infarct of large endocardial extent than in a transmural MI of limited endocardial extent (Wu et al. 2001a, Moon et al. 2004, Kaandorp et al. 2005, Engblom et al. 2007). In accordance with these findings,

several studies have shown greater enzymatic MI size in STEMI with Q waves than in STEMI without Q waves, irrespective of reperfusion therapy (Bar et al. 1987, Huey et al. 1987, Isselbacher et al. 1996, Armstrong et al. 2009). The number of Q waves was associated with greater enzymatic MI size in post-procedural ECG after primary PCI for STEMI (van der Vleuten et al. 2009); in patients with NSTEMI, as well, the development of new Q waves was associated with greater enzymatic MI size (Alexander et al. 2003).

LV function and viability according to Q-wave status

Q-wave MI (QMI) in patients with STEMI has been associated with greater impairment of LV function than that from non-Q-wave MI (NQMI) (Huey et al. 1987, Isselbacher et al. 1996, Nijveldt et al. 2009). In virtually all patients with QMI in the acute phase after thrombolysis LV dysfunction was detectable, but in only 69% of patients with NQMI; moreover, NQMI was associated with a smaller extent of wall-motion abnormality than was QMI (Isselbacher et al. 1996). In patients with subacute or chronic MI, EF was lower in QMIs (47%) than in NQMIs (55%); however, when infarct location was considered, the difference was significant only in anterior MIs, not in inferior MIs (Moon et al. 2004). Studies using metabolic imaging have shown that the majority of patients with LV dysfunction associated with chronic QMI have viable myocardium, even though viability is more common in LV regions without Q waves, and more abundant in patients after NQMI (Schinkel et al. 2002, Yang et al. 2004). Importantly, Q waves in the acute phase did not exclude the presence of salvageable myocardium, even though patients presenting with STEMI without Q waves had smaller enzymatic MI size (Bar et al. 1987). In accordance, recovery of LV dysfunction after thrombolysis for STEMI was greater in NQMI than in QMI, despite a similar extent of LV dysfunction acutely (Isselbacher et al. 1996).

Prognosis according to Q-wave status

Baseline Q waves in the ischemic region predict worse clinical outcome in patients that undergo reperfusion for STEMI. Such patients with QMI had a greater incidence of in-hospital congestive heart failure, and higher 30- and 90-day mortality rates than did those with NQMI; however, their one-year mortalities did not differ (Aguirre et al. 1995, Wong et al. 2006, Armstrong et al. 2009). Number of Q waves has predicted late survival: STEMI patients with > 4 Q waves after primary PCI in the leads with ST elevation on admission had clearly the highest one-year mortality (van der Vleuten et al. 2009). Similarly, in patients with NSTEMI, development of new Q waves was associated with a higher 30-day and 6-month mortality (Alexander et al. 2003).

2.7.2 R- and S waves

It has generally been accepted that a decrease in the R wave together with the development of a Q wave reflects myocardial necrosis. Mid- and late QRS abnormalities would be expected in MIs affecting the lateral and basal parts of the LV, as these locations of the heart are the last activated. The criteria for R waves, R to S ratio, and S waves in the Selvester score, have proven of significant value for estimating posterolateral MI size (Ward et al. 1984b, Sevilla et al. 1990, Pahlm et al. 1998). Evidence is that 8 to 10% of MIs involve only the base of the LV and produce no initial QRS changes (Selvester et al. 2011a).

After experimental LAD occlusion, the sum of R- and S waves in ischemia-related leads decreases gradually for up to 6 hours after occlusion, more rapidly during the first few hours (Smith et al. 1974). In patients with first-time urgently reperfused STEMI, the amount of increase in the sum of R waves in the infarct-related leads from 1 week to 4 weeks after the acute event correlated with the increase in EF and with the amount of salvageable myocardium as assessed by scintigraphy (Isobe et al. 2006).

In patients with STEMI, ST elevation, together with terminal distortion of the QRS complex, indicates severe, grade III ischemia and predicts larger final MI size. Grade III ischemia causes the disappearance of S waves in leads that usually have an rS configuration (V1-V3), and causes a J point/R wave ratio ≥ 0.5 in leads usually having a qR configuration (Birnbaum, Drew 2003).

2.7.3 Selvester QRS score

The Selvester QRS score method for assessment of MI size and location

Of all scores for electrocardiographic estimation of MI size, the most validated, and also the best performing, is the Selvester QRS score (Pahlm et al. 1998). This score was developed by means of a computer model simulating heart activation that showed, in each of the 12 standard ECG leads, the extent of QRS change to be proportional to the extent of simulated MI. Based on the observations in the computer simulation, a 54-criteria, 32-point scoring system was developed for estimation of MI size; the greater the score, the larger the infarct. In this scoring system, each criteria has a specificity of 95% or greater in normal subjects, and each point represents 3% of total LV mass. The score is thus capable of indicating MI in 96% of the LV. A simplified 37-criterion, 29-point scoring system with equal specificity can indicate MI in only 87% of the LV, with relative under-representation of posterolateral and basal regions (Wagner et al. 1982, Hindman et al. 1985, Selvester et al. 1985a). For 10 of the 12 standard ECG leads (excluding leads III and aVR), the QRS score considers Q- and R-wave amplitudes and durations, and

S-wave amplitudes, as well as R/Q- and R/S ratios (Selvester et al. 1985b, Selvester et al. 2011b).

Histopathologic studies validating the Selvester QRS score

Originally in the pre-reperfusion era, the QRS score was validated in postmortem anatomic studies (Ideker et al. 1982, Roark et al. 1983, Ward et al. 1984a). Correlations between the simplified 37-criteria, 29-point QRS score and histopathologically determined MI size at different locations was r = 0.80 for anterior, r = 0.74 for inferior, and r = 0.72 for posterolateral MIs. Use of the complete 54-criteria, 32-point QRS score improved the correlation for anterior MIs (r = 0.89), but for inferior and posterolateral MIs, the correlations were similar. The QRS score showed only a weak correlation with MI size if the infarct involved multiple locations (r = 0.36). (Pahlm et al. 1998).

Clinical studies validating the Selvester QRS score

Estimating LV function and enzymatic MI size after acute MI by the Selvester QRS score

The earliest clinical validation studies compared the QRS score with LV EF and enzyme release after acute MI, in nonreperfused as well as in reperfused patients. In nonreperfused patients, the QRS score measured in the subacute phase showed good correlation with early EF (r = -0.71), extent of LV dyssynergy (r = 0.60), and enzymatic MI size (r = 0.65–0.72). In the late acute phase, within 3 days after the acute event, these correlations were clearly weaker (Seino et al. 1983, Hindman et al. 1986, Grande et al. 1987). Correlations after reperfusion among studies have varied widely. At best, the correlation between QRS score at 1 to 4 weeks and enzymatic MI size has been r = 0.57 to 0.75, and between QRS score and EF, r = -0.58 to -0.76 (Juergens et al. 1996, Tateishi et al. 1997, De Sutter et al. 1999). In other studies, correlations after reperfusion have been weaker (Timmis 1987, Christian et al. 1991). In many studies, correlations of the QRS scores with EF and enzymatic MI size have been stronger in anterior than in inferior MI.

Association between Selvester QRS score and MI size by myocardial perfusion imaging

Perfusion imaging studies using 201-thallium or 99m-technetium sestamibi have shown significant correlations between Selvester QRS score and MI size. In the subacute phase after thrombolysis for STEMI, the correlation was r = 0.58 to 0.79 (Juergens et al. 1996, Barbagelata et al. 2005). In patients with residual ST elevation after anterior MI, QRS score has shown no correlation with MI size (Adler et al. 2000). In the healing phase of MI, the correlation between QRS score and MI size was r = 0.70 (De Sutter et al. 1999). In the chronic phase, the correlation between QRS score and MI size was r = 0.55, unaffected by thrombolytic therapy (Marcassa et al. 2001).

Association between Selvester QRS score and MI size by DE-CMR

Studies in which DE-CMR imaging was performed simultaneously with the recording of 12-lead ECG at various phases of infarction have found significant correlations between Selvester QRS score and MI size, and good agreement for MI localization; in the subacute phase after primary PCI for STEMI, correlations were r = 0.56 to 0.79 (Engblom et al. 2005a, Geerse et al. 2009, Weir et al. 2010); after healing of the MI, at 3 to 6 months, they were = 0.41 to 0.78, being slightly higher or the same in serial measurements (Bang et al. 2008, Geerse et al. 2009, Weir et al. 2010, Carlsen et al. 2012). In one study, the late acute-phase (1–2 days) correlation was also measured, which was r = 0.39 (Bang et al. 2008). The local QRS score (at one week) correlated with MI transmurality, and the global QRS score was significantly higher in transmural than in non-transmural MIs, whereas the presence of Q waves was not indicative of transmural MI (Engblom et al. 2005b).

Estimation of prognosis by Selvester QRS score

MI size estimated by Selvester QRS score has correlated with clinical outcomes. Two large studies assessed the prognostic value of pre-discharge QRS score in patients after reperfusion for STEMI. In one study including 4,000 patients treated with primary PCI, 90-day mortality and rate of the composite outcome including congestive heart failure, shock, or death increased with increasing QRS scores, being lowest in patients with QRS score ≤ 3, and highest in patients with QRS score ≥ 8 (mortality 1.9% vs. 4.9%, and composite outcome 4.5% vs. 12.1%) (Tjandrawidjaja et al. 2010). In a study including 1,800 patients treated with thrombolysis, both 30-day and 1-year mortality were lower in patients with a QRS score < 10 than in those with a QRS score ≥ 10 (1-year mortality 5.4% vs. 12.6%) (Barbagelata et al. 2004). In 1,900 medically treated patients with angiographically confirmed significant coronary artery disease, 1-year and 5-year mortality increased with increasing QRS scores. At the extremes, QRS score 0 vs. QRS score ≥ 10, 1-year mortality was 5% vs. 9%, and 5-year mortality was 12% vs. 48% (Bounous et al. 1988).

2.7.4 ST segment and T waves

In patients with acute coronary syndrome (ACS), different changes in the repolarization phase in the 12-lead ECG on admission confer different prognoses. Patients with a negative T wave only, show the lowest incidence of adverse clinical outcomes (Savonitto et al. 1999 and 2005). Patients presenting with ST-segment depression alone have lower early mortality than do those presenting with ST-segment elevation. By 30 days, however, the rate of mortality in NSTEMI and STEMI equalizes, and by 6 months, adverse events are even more frequent in patients with NSTEMI than in patients with STEMI (Savonitto et al. 1999, Chan et al. 2009).

2.7.4.1 ST segment and T wave in STEMI

Assessment of MI size and prognosis by ST-segment- and T-wave changes before reperfusion in STEMI

Persistent ST-elevations in patients with ACS indicate transmural myocardial ischemia caused by total thrombotic occlusion of the culprit coronary artery. In order to limit MI size, such patients are treated with immediate reperfusion therapy, either by thrombolysis or primary PCI. Final MI size depends on extent and duration of ischemia before reperfusion.

Time from onset of occlusion can be approximated from the initial 12-lead ECG. High T waves (> 98th percentile) in leads with ST elevation in the presenting ECG indicate earlier time to treatment, and are associated with better clinical outcome after thrombolysis. Maximum T-wave amplitude has been a stronger predictor of 30-day and 1-year mortality than other ECG-related variables at presentation (Hochrein et al. 1998). Early presentation at thrombolysis by the Anderson-Wilkins score—which, in the presence of ST elevation, considers the number of leads with positive T waves with and without Q waves—predicts smaller final MI size as estimated by the Selvester QRS score (Johanson et al. 2005).

Extent of ischemia as assessed by the number of leads with ST elevation has been associated with short- and long-term mortality. Patients with small myocardial injury, having ST elevations in only 2 to 3 leads, had the best prognosis, a prognosis unaffected by thrombolysis. Patients with large myocardial injury, with ST elevations in ≥ 6 leads, had the worst in-hospital and 10-year prognosis; this was significantly reduced if they had received thrombolysis (Mauri et al. 2002). A higher sum of ST elevation predicted higher in-hospital mortality, higher release of α-hydroxybutyrate dehydrogenase, and lower EF, indicating greater MI damage in patients with a larger extent of ischemia (Willems et al. 1990). In these studies, anterior ST depressions associated with inferior STEMI were considered to be posterior ST elevations, and inferior ST depressions associated with anterior STEMI were considered to be superior ST elevations. One angiographic study revealed that reciprocal inferior ST depressions in patients with anterior ST elevations indicate LAD as the culprit artery, and predict higher peak CK level and lower EF than is the case when anterior ST elevations are associated with inferior ST elevations; in the latter case the culprit artery is most often RCA (Sadanandan et al. 2003).

Assessment of MI size and prognosis by ST-segment and T-wave changes after reperfusion in STEMI

Incomplete ST-segment normalization and residual ST-segment elevation after reperfusion therapy is associated with more extensive myocardial damage and higher mortality, and are better in predicting adverse prognosis than is the initial extent of ST elevation before reperfusion.

After thrombolysis, complete (≥ 70%) ST-segment resolution (STR) of the summed ST elevation at baseline has predicted the lowest short-term mortality, and was associated with the smallest MI size by peak CK and the Selvester QRS score; patients with partial (30–70%) STR had greater MI size than did those with complete STR, and clinical outcome was worst in patients with no (< 30%) STR. Analysis of the ST segment at 3 hours vs. 1 hour after thrombolysis has yielded similar results (Schroder et al. 1995, Johanson et al. 2009).

STR extent showed similar prognostic value also after successful primary PCI. As compared to no STR, partial or complete STR within 4 hours after successful primary PCI predicted smaller enzymatic MI size and better LV function. Short- and long-term survival was the best in patients with complete STR, and somewhat better in those with partial vs. no STR (van 't Hof et al. 1997, Brodie et al. 2005, De Luca et al. 2008). The relationship between MI size and extent of STR was also evident in one CMR study (Hallen et al. 2010). Measurement of ST resolution may be done from maximal single-lead ST elevation or the sum of ST elevation pre-PCI. Use of maximal residual ST-segment elevation after PCI is easier, and showed a strong prognostic value similar to that of STR, and it correlated even better with MI size. Maximal residual ST-segment elevation > 2 mm predicted larger MI size and higher in-hospital, 30-day, and late mortality than those of patients with lower residual ST-segment elevation; patients with ≤ 1 mm residual ST-segment elevation had the smallest MI size and the lowest mortality (McLaughlin et al. 2004, Brodie et al. 2005, De Luca et al. 2008, Hallen et al. 2010). Deferring the ECG assessment to 24 hours after primary PCI strengthened the correlations between residual ST elevation and MI size by CMR (Weaver et al. 2011). Evaluation of ST depression in addition to ST elevation after primary PCI gives incremental prognostic information (De Luca et al. 2008, Tjandrawidjaja et al. 2010). Maximal residual single-lead ST deviation at 3 hours post primary PCI (either ST elevation or -depression) was the best predictor of enzymatic MI size and EF, as well as of cumulative mortality up to one year (De Luca et al. 2008).

In STEMI patients treated with successful primary PCI, changes in the ST segment after reperfusion therapy reflect myocardial flow rather than epicardial flow, since almost half the patients failed to show complete STR despite restoration of flow in the culprit artery (van 't Hof et al. 1997). Residual ST-segment elevation has been an independent predictor of microvascular injury, as determined by evidence of microvascular obstruction on CMR. Residual ST elevation ≥ 1.5 mm has been

associated with evidence of microvascular obstruction on CMR (Nijveldt et al. 2009, Weaver et al. 2011).

Negative T waves after reperfusion are associated with better clinical outcome. In infarct-related leads, 24 hours after thrombolysis for STEMI, prominent negative T waves (≤ -1 mm) indicate viability: CK release was lower, recovery of LV dysfunction was better, and subsequently EF was higher at discharge and at 1 month than in patients without early prominent negative T waves. Negative T waves also showed themselves to be markers of patency of the infarct-related artery. Patients without early T-wave inversion more often had in-hospital re-infarction and higher in-hospital mortality (Matetzky et al. 1994, Corbalan et al. 1999). After thrombolysis for STEMI, prominent negative T waves (≤ -1.5 mm) at hospital discharge have predicted lower 30-day mortality. In that study, the association between negative T waves and patency of the culprit artery was not very strong, which could indicate that inverted T waves a few days after the acute event are a reflection of better microvascular perfusion (Sgarbossa et al. 2000). However, T-wave inversions before reperfusion in STEMI patients have been associated with worse coronary flow and clinical outcome (Huang et al. 2013).

2.7.4.2 ST segment and T wave in Non-ST-segment elevation ACS

In patients with ACS without STEMI, an ST deviation ≥ 0.5 mm (depression, or ST elevation < 1 mm) in at least 2 contiguous leads in the acute 12-lead ECG is an independent indicator of worse short- and long-term prognosis. Patients with isolated T-wave inversions, or no ECG changes, have clearly a more favorable outcome. The first studies demonstrating the prognostic utility of ST deviations in ACS without persistent ST elevations were conducted in the mid 1980's (Schechtman et al. 1989). Later, when ACS treatment included more aggressive anti-thrombotic medications and invasive management, several large studies still showed similar results (Cannon et al. 1997, Kaul et al. 2001, Savonitto et al. 2005, Yan et al. 2010).

The presence, degree, and extent of ST depression at admission have been associated with clinical outcome. Compared with patients showing T-wave inversions only, patients with ST depression 1 to 2 mm vs. ≥ 2 mm had a 4-fold vs. a 6-fold higher one-year mortality. Mortality was even higher, if deep ST depressions occurred in multiple ECG regions. The sum of ST depression in 11 leads (excluding aVR) showed a continuous and an incremental correlation with 30-day mortality, and a composite outcome of 30-day mortality and MI (Kaul et al. 2001, Savonitto et al 2005). Risk assessment may improve by the recording of a follow-up ECG 12 to 24 hours after admission. Persistent or de-novo ST depression on such a follow-up ECG have shown an elevated risk for MI and and a two-fold risk of early as well as late mortality.

Several clinical factors associated with adverse prognosis were more prevalent in NSTE ACS patients with persistent ST deviations than in those without, including older age, prior congestive heart failure, hypertension, and diabetes (Yan et al. 2010). Irrespective of these clinical factors, ST deviations are independent predictors of prognosis. Importantly, the presence, extent, and degree of ST deviations are associated with a higher prevalence of three-vessel disease and left main coronary disease (Cannon et al. 1997, Savonitto et al. 2005, Yan et al. 2010). The magnitude of ST depression was also related to the amount of CK release (Savonitto et al. 2005).

2.7.4.3 ST segment and T wave in chronic MI

After acute MI, evolving changes in ST segments and T waves are associated with viability and clinical outcome. Persistent ST elevations after anterior MI have been associated with clinically more severe infarction (Mills et al. 1975). In one autopsy series, ≥ 1 year after anterior MI, persistently negative T waves in leads with Q waves indicated transmural MI, and positive T waves non-transmural MI, suggesting that in chronic MI, negative T waves are associated with less non-viable myocardium (Maeda et al. 1996). In subsequent clinical studies, positive inversion of negative T waves from the acute to chronic phase of MI was, as compared to persistently negative T waves, associated with smaller enzymatic MI size, significantly better recovery from LV dysfunction, higher EF, less unfavorable remodeling of the LV, fewer adverse events, and lower mortality (Bosimini et al. 2000, Sakata et al. 2001, Lancellotti et al. 2002).

A few CMR studies have reported on the relationship between MI size and the ST segment and the T wave. The sum of T-wave amplitude at 3 months after STEMI in two adjacent leads with the greatest ST elevation on admission showed a positive correlation with EF, irrespective of MI location, and showed a negative correlation with MI size by CMR in inferior MI (Meijs et al. 2011). Patients with ST elevation > 1 mm in any of leads V2 to V5 after prior anterior MI had a significantly larger MI scar on CMR than did those with ST elevation ≤ 1 mm (Tibrewala et al. 2007).

2.8 Body surface potential mapping in assessment of myocardial infarction

Patients may develop a large MI even in the absence of changes in the acute 12-lead ECG (Kontos et al. 2001). As the standard chest leads do not directly overlie the right ventricle or the posterolateral region of the LV, ECG diagnostic sensitivity may be enhanced by extended right and posterior leads (Schmitt et al. 2001), and further by the use of BSPM.

2.8.1 The BSPM method

BSPM is a method of measuring the direction and amplitude of electrical potentials at different points in the heart cycle on the entire thoracic surface. BSPM measurements may involve different numbers of ECG leads and layouts. Complete sampling systems comprise 64 to 242 leads covering both the front and back of the thorax. BSPM data require computed analysis (Lux 2011). The main advantage of BSPM in comparison with 12-lead ECG is its spatial resolution. BSPM is a more accurate method for diagnosing and localizing the site of both acute and chronic MI, having better sensitivity than and similar specificity as the 12-lead ECG (Mirvis 1987, Kornreich et al. 1993, Murray, Alpert 1994, Vesterinen 2007, Ornato et al. 2009, Daly et al. 2012). Further, computed analysis of BSPM offers the possibility to quantify regional electrical function and to measure complicated ECG variables such as time-voltage integrals from different de- and repolarization intervals.

2.8.2 BSPM in localizing region of myocardial ischemic injury

In dogs, MI size after occlusion of the LAD could be estimated by epicardial potentials: Development of Q waves and loss of R waves correlated with MI size, and was predicted by amount of ST elevation (Hillis et al. 1976). These changes in epicardial potentials are closely reflected in potentials on the body surface, as demonstrated in one experimental study (Muller et al. 1975). Localized ST changes on the BSP map indicate the anatomic region of acute ischemia better than does the 12-lead ECG (Spekhorst et al. 1990, Shenasa et al. 1993, Kornreich 1998, Horacek &Wagner 2002). Location of Q waves on the body surface can localize an LV infarct scar in its chronic phase (Hayashi et al. 1980, Ohta et al. 1981 and 1982, Toyama et al. 1982).

2.8.3 Precordial mapping in assessment of MI size

The first clinical studies attempting to estimate MI size used precordial electrocardiographic mapping, with leads covering the region of the heart on the chest. These studies were done in patients with non-reperfused, acute anterior MI. In precordial mapping, the number of leads with ST elevation > 1.5 mm predicted the perfusion defect on scintigraphy ($r = 0.56$) in the early as well as late acute phase of anterior MI (Murray et al. 1979). The sum of ST elevation was found to correlate with enzymatic MI size ($r = 0.55$) (Herlitz et al. 1984). At 24 hours after admission, the sum of Q-wave voltages showed a strong correlation with enzymatic MI size ($r = 0.92$), unlike the number of leads with Q waves (Vachova et al. 1979); in the subacute phase, however, the number of leads with pathologic Q waves (≥ 0.04s)

showed a strong correlation with EF (r = -0.87), with segmental dyssynergy in LV cineangiograms, with stroke work index (r = -0.79), and with cardiac index (r = -0.66). Patients having the highest number of Q waves had the poorest prognosis; 60% died shortly after the MI (Awan et al. 1977). This finding was confirmed by Herliz et al. (1984), who showed in 179 patients, at 4 days after the acute event, a strong correlation between number of Q waves and enzymatically determined MI size (r = 0.66). The sum of Q-wave and of R-wave voltages both showed a significant correlation as well, albeit slightly lower.

2.8.4 Complete BSPM in assessment of MI size

As precordial mapping is suitable mainly for assessment of anterior MI, BSPM with more leads covering both the front and back of the thorax is useful in assessment of MI also involving locations other than the anterior.

Sum of Q- and R waves

The size of old anterior and inferior MI has been assessed by BSPM of Q- and R waves. The number of leads with a Q wave was greater with more extensive and severe LV dyssynergy, and it correlated inversely with EF by ventriculography in both anterior (r = -0.47) and inferoposterior (r = -0.63) MI, and correlated with amount of viable myocardium on thallium-201 scintigraphy in anterior MI (r = -0.69). The sum of R-wave voltages showed a positive correlation with EF (r = 0.51) and with amount of viable myocardium (r = 0.50) in anterior MI, but not in inferoposterior MI (Hayashi et al. 1980). A recent study found that a larger number of Q waves was associated with a greater extent of infarct scar on CMR. However, number of Q waves in anterior and inferior MIs was not comparable; because—independent of MI size—anterior MIs caused fewer Q waves in a small localized precordial area, whereas Q waves in inferior MIs covered a larger area confined to the inferior part of the front and back of the thorax (Bodi et al. 2006). In anterior MI, the sum of R-wave amplitudes correlated positively with EF and viability (Hayashi et al. 1980). The sum of R-wave amplitudes as well as R-wave areas correlated negatively with LV dyssynergy (De Ambroggi et al. 1982).

Departure maps

In MI patients, departure maps display the thoracic area of amplitudes and integrals differing more than 2 SD from those of healthy controls: This is called the departure area. Departure maps determine the location and size of MI. In patients with anterior MI not treated with reperfusion therapy, the departure area (of amplitudes yielding the largest departure area at a time-point 30–60 ms after onset of QRS) showed a significant correlation with enzymatic MI size (r = 0.57) and EF (-0.47) at 1 week. At 1 month, correlation with EF was strong (r=-0.72), and also with the perfusion-

defect area in Thallium-201 SPECT (r = 0.69) (Cahyadi et al. 1989). In patients with prior MI, Tonooka et al. (1983a) found a strong correlation between departure areas of negative QRS isointegral values and defect score on Thallium-201 SPECT in both anterior (r = 0.88) and inferior (r = 0.79) MI; this performed better than the number of leads with Q waves. Similar findings emerged in correlation of QRS isointegral departure areas with LV asynergy and EF in ventriculography (Kubota et al. 1985). In patients with prior anterior MI, in addition to QRS isointegral departure area, the QRST isointegral departure area also showed a similar strong correlation with EF (r = -0.90 and -0.84 respectively). The departure area of the QRS amplitude at 30 ms, and the number of leads with Q waves showed significant, but weaker correlations (r = -0.73 and -0.72) (Hayashi et al. 1993). Departure maps of QRS integrals were able to distinguish among MI locations, whereas isopotential maps of QRS integrals were consistent only in anterior MIs (Tonooka et al. 1983a).

3 AIMS OF THE STUDY

The aim of this thesis was to evaluate the use of strain rate imaging and computed single-lead BSPM variables in the assessment of infarct size and viability in patients with MI. These echocardiographic and electrocardiographic methods are practical, and are easily performed even at the bedside, unlike methods such as DE-CMR and SPECT. The specific aims of the studies for this thesis were the following:

1. Validation of strain mapping, a semi-quantitative method for estimation of systolic strain values, in assessment of the extent of infarct.

2. Evaluation of systolic strain in assessment of the transmural extent of an infarct and global infarct size in chronic MI with DE-CMR as the reference.

3. Evaluation of strain- and strain-rate variables in assessment of viability and in predicting recovery from severe contraction abnormality in acute MI.

4. Discovery of the best BSPM variables and the best recording sites on the thorax for predicting recovery of LV function with respect to the region of contraction abnormality in patients with acute MI.

5. Examination of which BSPM variables correlate with infarct size at different stages of MI, from acute to chronic, and which sites on the thorax yield the strongest correlations.

4 MATERIALS AND METHODS

4.1 Patients

4.1.1 Recruitment of patients

During 2003 to 2005, patients admitted to the Coronary Care Unit of Helsinki University Central Hospital for suspected acute coronary syndrome were screened during office hours. Study inclusion criteria were prolonged chest pain ≥ 20 minutes within 48 hours of recruitment, associated with evidence of acute ischemia: Either ischemic changes in the initial 12-lead ECG (ST-segment elevation, -depression, or T-wave inversions in ≥ 2 contiguous leads), or elevated cardiac biomarkers indicating myocardial infarction (CK-MBm > 7 μg/l or TnT > 0.03 μg/l), or both. Exclusion criteria were bundle branch block, atrial fibrillation, pacemaker, or need for ventilatory support. In all, 79 patients fulfilled these criteria, and agreed to participate in the study. Baseline characteristics of the patients are shown in Table 1. Study III utilized previously recorded BSPM data from 73 healthy controls. The controls were matched by age, sex, and body size.

Table 1. *Baseline characteristics.*

Baseline characteristics	Study I	Study II	Study III	Study IV
Patients, *n (male)*	26 (21)	23 (18)	62 (48)	57 (45)
Age, years	61 ± 10	60 ± 10	60 ± 11	60 ± 10
Body mass index, kg/m^2	27 ± 5	28 ± 5	27 ± 4	27 ± 4
Previous MI in clinical history, *n*	5	3	10	8
Hypertension, *n*	11	10	23	23
Peak CK-MBm (μg/L)	170 ± 144	148 ± 145	147 ± 160	137 ± 163
STEMI, *n*	19	16	48	41
QMI, *n*	16	13	24	20
PCI	17	16	46	51
CABG	5	4	9	5
Thrombolysis only	4	3	6	2
Culprit artery, *n*				
LAD	15	12	34	33
LCX	2	4	12	8
RCA	9	7	16	16

Data presented as number (n) or mean ± SD. CABG, coronary artery by-pass grafting; LAD, left anterior descending coronary artery; LCX, left circumflex coronary artery; MI, myocardial infarction; PCI, percutaneous coronary intervention; QMI, Q-wave MI; RCA, right coronary artery; STEMI, ST-elevation MI.

4.1.2 Ethical aspects

All patients gave their written informed consent. The study was approved by the ethics committee of the Helsinki University Central Hospital and complies with the Declaration of Helsinki.

4.1.3 Study protocol

The patients were examined at three time-points: in the acute phase at inclusion; during the healing phase, 7 to 30 days later; and finally after complete healing of the infarct, ≥ 6 months from inclusion. None of the patients suffered from new ischemic events between examinations. Standard two-dimensional echocardiography—with or without color tissue Doppler imaging—and in addition, BSPM were performed at all three time-points. Patients were imaged with DE-CMR close to the time of their last follow-up. The studies presented in this thesis were based on the following data:

Study I: SRI- and DE-CMR data from the final follow-up (8 ± 1 months after the acute event).

Study II: SRI data from the acute phase (17 ± 14 hours after onset of chest pain); SRI data from the final follow-up (8 ± 2 months after the acute event).

Study III: BSPM- and echocardiographic data from the acute phase (11 ± 11 hours after the acute event); echocardiographic data from the final follow-up (11 ± 4 months after the acute event).

Study IV: BSPM data from the acute phase (10.7 ± 14.4 hours after onset of chest pain), during recovery (at 16 ± 14 days), and from the final follow-up (11 ± 4 months after the acute event), and DE-CMR data from the final follow-up.

4.2 Echocardiography

4.2.1 Standard two-dimensional echocardiography

Echocardiographic images were acquired by a Vivid 5 or Vivid 7 ultrasound scanner (GE Medical Systems) by using a 1.5 to 4.0 MHz phased array transducer (M3S). We analyzed LV contraction real-time from two-dimensional B-mode images, in all standard parasternal short axis views (basal, mid-, and apical), and long axis views (2-, 3-, and 4-chamber views). The 16-segment model of the LV defined by the American Society of Echocardiography and the American Heart Association served for analysis of regional myocardial function (Schiller et al. 1989b, Cerqueira et al. 2002). Segmental wall motion and wall thickening was assessed visually as normal or abnormal. For Studies I and II, each segment was assigned a wall-motion score (WMS) from 1 to 4 according to recommendations (1, normokinesia, 2, hypokinesia, 3, akinesia, 4, dyskinesia). Global LV systolic function was quantified by ejection

fraction calculated by the Simpson rule from apical two- and four-chamber views (Lang et al. Recommendations for chamber quantification 2006).

4.2.2 Tissue Doppler strain- and strain rate imaging

Acquisition and analysis of color tissue Doppler data

For Studies I and II, color tissue Doppler loops were recorded by the Vivid 7 ultrasound scanner (GE Medical Systems), and analyzed off-line on a personal computer that used EchoPAC software provided by GE. Tissue Doppler images came from standard apical views (2-, 3-, and 4-chamber views) by limiting the imaging sector (sector angle 30°) to one LV wall at a time. The tissue-velocity scale was adjusted to avoid aliasing (pulse repetition frequency 1.0–1.5 kHz). The frame rate was 209 ± 17 frames per second. Patients were asked to hold their breath if that was necessary in order to position the myocardial wall at the center of the imaging sector during three consecutive heartbeats. Care was taken to align the ultrasound beam to be as parallel as possible to the myocardial wall. Segments in which the angle between the beam and the myocardial wall exceeded 30° were excluded from analysis, as were segments with artefacts or bad image quality.

For analysis, the LV was divided into 16 segments according to the model defined by the American Heart Association, modified by the addition of apical anteroseptal and inferolateral segments in Study II (Cerqueira et al. 2002). Strain- and strain rate curves came from color tissue Doppler data by placing the sample volume (strain length 12 mm) in the middle of each segment. Manual adjustments, if necessary, assured that sample volume was continuously retained within the myocardium. The curves of three consecutive heartbeats were averaged for analysis. End-systole definition was aortic valve closure (timed at the end of systolic flow through the aortic valve by continuous-wave Doppler).

Strain- and strain rate measurements

Of the strain-curve values obtained, end-systolic strain (S_{ES}) and post-systolic strain (S_{PSS}), S_{PSS} was defined as the peak negative strain value occurring after aortic-valve closure. The strain rate curves provided the peak negative strain rate value in systole (SR_S), and the peak positive values during early diastole (SR_E) and late diastole (SR_A). Global S_{ES}, SR_S, $SR_{E,}$ and SR_A values were calculated as the average of each patient's segmental values from the 16 LV segments as defined by the American Heart Association (Cerqueira et al. 2002).

Studies I and II measured S_{ES} from the final recording (6–12 months from the acute event). In addition, for Study II, all strain- and strain-rate analyses came from the acute recording.

Strain mapping

With tissue Doppler loops, myocardial strain values can be displayed as two-dimensional color-coded images which we call strain maps. In these strain maps, longitudinal shortening is coded in red, and lengthening in blue. Reduced or absent shortening is coded in gray (Figure 2). The transition from red to gray can be adjusted by means of various strain scales. In Study I, we analyzed the strain maps by two different strain scales: Strain values > -7% or > -12% were coded in gray on the scales ±15% and ±30%, respectively (Figure 3). These two strain scales allowed estimation of segmental strain, and each LV segment was accorded a strain-mapping score (SMS) from 1 to 4 (Table 2).

Global SMS calculation meant averaging each patient's segmental SMS by total number of LV segments analyzed, based on the 16-segment model defined by AHA/ASE (Cerqueira et al. 2002).

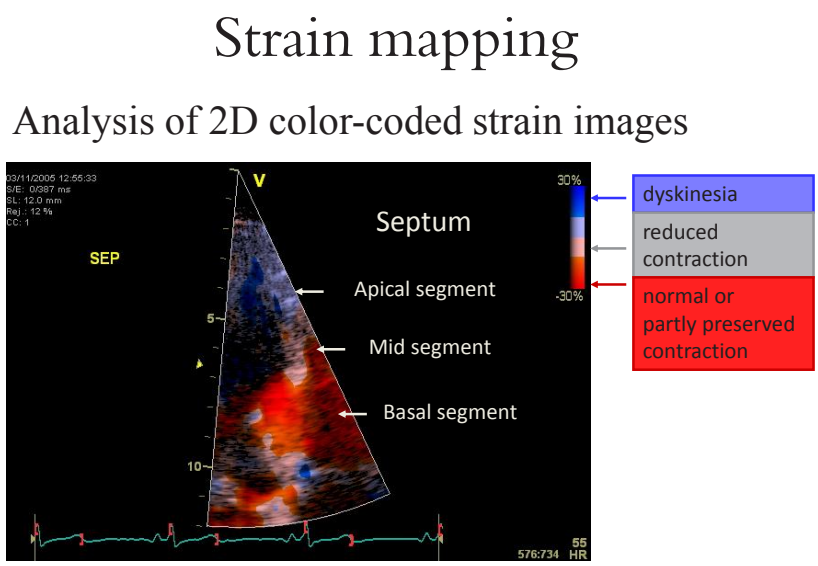

Figure 2. *Strain map of the septum. Longitudinal systolic strain is coded in color: Blue represents dyskinesia (positive strain values); gray, absent or reduced contraction; red, normal or partly preserved contraction.*

Systolic strain values by strain mapping

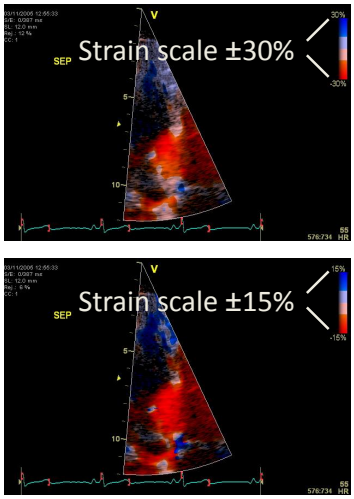

Range of strain values defined by the strain scale

	± 30%	± 15%
	> 0%	> 0%
	0 to -12%	0 to -6%
	< -12%	< -6%

Figure 3. *Strain mapping of longitudinal systolic strain values. Blue represents positive strain (myocardial lengthening, dyskinesia). The range of strain values represented by gray and red depend on the strain scale used; red always means better, or more negative strain, than does gray. Here, the range of strain values represented by gray and red are shown for strain scales ± 30% and ± 15%. In the upper image, using the strain scale ± 30%, red in the basal segment means normal contraction (strain < -12%); gray in the mid-segment means reduced contraction (strain values 0 to - 12%). Using the strain scale ± 15%, we can further determine whether contraction in the mid-segment is mildly (strain < -6%) or severely (strain > -6%) reduced. In the lower image, changing the scale to ± 15% shows red in the mid-segment (strain < -6%). Hence, the contraction there is only mildly reduced (strain values -6 to -12%).*

Table 2. *Strain-mapping (SM) scores and corresponding range of longitudinal systolic strain values.*

SM score	Strain values	Myocardial contraction
1	**< - 12 %**	Normal
2	**- 6 to -12 %**	Hypokinetic
3	**0 to - 6 %**	Akinetic/ severely hypokinetic
4	**> 0 %**	Dyskinetic

Estimation of segmental systolic strain is by the strain-mapping method in Figure 3. SM score 1 indicates normal, or near-normal segmental contraction. Higher SM scores mean increasingly reduced segmental contraction.

4.3 Cardiac magnetic resonance imaging

Cardiac magnetic resonance imaging performed in a 1.5 T scanner (Sonata, Siemens Medical Solutions) served as the reference technique for determining MI size and location (Fieno et al. 2000, Wu et al. 2001b, Kuhl et al. 2003).

DE-CMR was performed 10 to 15 min after a bolus injection of 0.2 mmol/kg of contrast agent (gadodiamide, Omniscan TM, GE Healthcare). A stack of LV short-axis images was scanned using a breath-hold T1-weighted segmented inversion-recovery turbo-FLASH sequence with the following settings: Inversion time to null the signal from normal myocardium 250 to 300 ms, repetition time 8.6 ms, echo time 4.3 ms, matrix 256 x 256, section thickness 8 mm, and intersection gap 20%. Cine magnetic resonance image series came through retrospectively ECG-gated segmented steady-state free precession imaging with the following settings: echo time 1.51 ms, repetition time 3.0 ms, flip angle 52°, matrix 256 x 256, field of view 240 x 340 mm, section thickness 6 mm, and temporal resolution 44 to 47 ms.

We analyzed the images using the same 16-segment model as for echocardiography (Cerqueira et al. 2002). Each segment we assigned a WMS from 1 to 4, as in the echocardiographic analysis (Lang et al. Recommendations for chamber quantification 2006). The presence of gadolinium delayed enhancement (DE) in a segment was considered indicative of an MI scar. In each segment, the transmural scar extent we assessed as the percentage of DE of the wall thickness (Studies I and II). Non-transmural infarcts we defined as segments with DE 1 to 50% showing normo- or hypokinesia by wall-motion analysis, and transmural infarcts as segments with DE > 50% showing hypo-, a-, or dyskinesia. In addition, the area of scar in each segment we determined by manual tracing (Study IV). Global LV infarct size we calculated by slightly differing methods: In Study I, transmural scar extent in all the LV segments was averaged; in Study II, the transmural scar extent was averaged only in those segments used for global tissue Doppler strain- and strain-rate values; and in Study IV, by dividing the sum of segmental scar areas by the total area of all segments.

Repeatability of DE-CMR analyses

In Study I, we analyzed a total of 384 segments for the presence of infarct by two independent observers. The results of the two observers were concordant for 366 (95%) of the segments ($\kappa = 0.86$).

4.4 Body surface potential mapping

Recording and analysis of BSPM

Resting BSPM for 5 minutes was recorded with 120 unipolar leads covering the whole thorax. The electrodes were 5 cm apart on 18 disposable adhesive strips, attached vertically on the thorax, with horizontal spacing according to anatomic

landmarks (Figure 4). In addition, placement of three electrodes in the standard limb lead positions provided data for the Wilson central terminal that served as the reference potential for the thoracic leads. The BSPM data were recorded with either a Mark6 or an ActiveTwo biopotential amplifier (Biosemi, Amsterdam).

BSPM data were analyzed with CAnalyze software (Department of Biomedical Engineering and Computational Science, Aalto University, Espoo, Finland). After visual inspection for validity of the recording, the data were signal-averaged according to criteria of ≥ 0.9 correlation of the QRS complex to a selected template, and noise < 30 μV. The T wave had to fit in an envelope of 110 to 150 μV around the template (Vaananen et al. 2000). The baseline was estimated by the third-order spline function fitted to consecutive PQ segments. Invalid leads were replaced by interpolating data from surrounding leads based on the method of Oostendorp et al. (1989). The QRS start and end were determined automatically from the vector magnitude of a representative precordial set of high-pass filtered leads, following the guidelines given by Simson (1981). The J point was determined for each lead

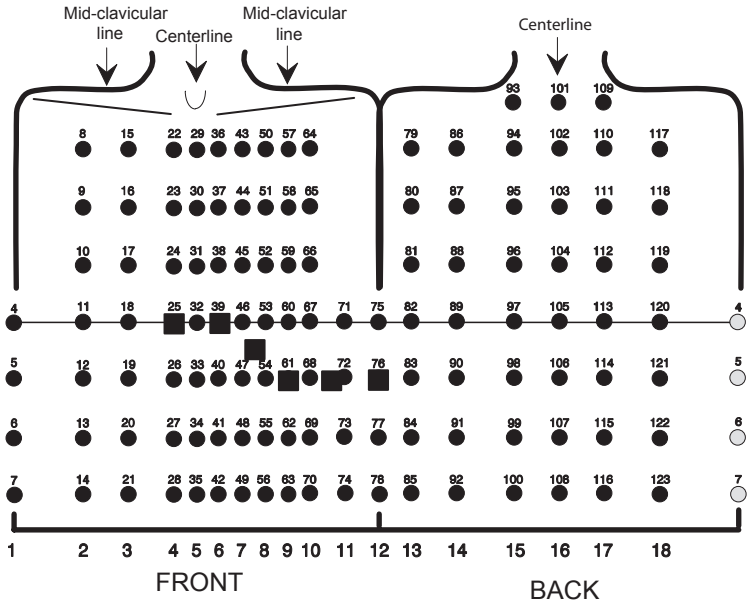

Figure 4. A) *Patient with BSPM leads on the front of thorax.* **B)** *Layout of the 120 BSPM leads on the front and back of the thorax. The horizontal line indicates the fourth intercostal space. Squares indicate standard ECG leads V1 to V6, shown here as a reference.*

separately as the time instant of the maximum curvature of the signal returning to the ST level around the QRS end. The time-points of the apex and end of the T wave we determined automatically as described elsewhere (Oikarinen et al. 1998).

ECG variables calculated from BSPM

ECG variables were calculated from the QRS complex, representing ventricular depolarization, as well as from the ST segment and the T wave, representing repolarization. Computed ECG variables included amplitudes, slopes, time-intervals, time-voltage integrals, and time-voltage areas. The time-voltage integral is the sum of areas above and below the baseline, whereas the time-voltage area is the sum of absolute values of areas above and below baseline. The ECG variables used in the study are shown and defined in Table 3.

Table 3. *Computed BSPM variables in the studies.*

Computed BSPM variables	
Q width	Time interval from QRS start to first positive peak, if initial deflection is negative.
R width	Time interval from QRS start to first negative peak, if initial deflection is positive.
Ramp	Peak (positive or negative) amplitude during the first 15-44.75% of the QRS.
Samp	Amplitude of the first opposite-sign peak after the Ramp.
1st QRSint	Integral of first quartile of QRS. Describes the Q wave.
2nd QRSint	Integral of second quartile of QRS. Describes the R wave.
3rd QRSint	Integral of third quartile of QRS. Describes the R- and the S wave.
4th QRSint	Integral of fourth quartile of QRS. Describes the S wave.
QRSint	Integral of entire QRS complex.
QRSSTTint	Integral from onset of QRS to end of T wave.
QRSTTarea	Area from onset of QRS to end of T wave.
Jamp	Amplitude at J point.
ST60amp = STamp	Average amplitude at 58 ms to 62 ms from QRS end. Describes the magnitude of ST elevation or ST depression.
ST80amp	Average amplitude at 78 ms to 82 ms from QRS end. Describes the magnitude of ST elevation or ST depression.
ST60slope	Slope from QRS end to 60 ms from QRS end.
ST80slope	Slope from QRS end to 80 ms from QRS end.
ST60int	Integral between QRS end and 60 ms from the QRS end.
ST80int	Integral between QRS end and 80 ms from the QRS end.
STint	Integral of first half of interval from QRS end to median T-wave end. Describes mainly the ST segment.
STTint	Integral from QRS end to T-wave end. Describes ST segment and T wave.
STT area	Integral of absolute values from QRS end to median T-wave end. Describes ST segment and T wave.
Tamp	T-apex amplitude.
T80int = Tint	Integral from 80 ms before to 80 ms after T-wave apex. Describes T wave.
TPEint	Integral from T-wave apex to T-wave end. Describes second half of T wave.

4.5 Statistical analyses

Expression of continuous variables is as mean ± SD. In addition, medians and inter-quartile range are reported (Studies II and III). Inter-quartile range equals the range of values falling between the 25th and the 75th percentiles. In all analyses, a p-value of < 0.05 was considered statistically significant.

Comparison of groups

Continuous variables were tested for normal distribution, and compared by analysis of variance, one-way ANOVA (Studies I and IV), or by the Mann-Whitney U-test (Studies II and III). Ordinal variables were compared by the Kruskall-Wallis H-test (Study I) and Mann-Whitney U-test (Studies I and III). The Bonferroni procedure was applied in multiple comparisons.

Correlation of continuous variables

Two-tailed Pearson's correlation analysis served to assess correlations in Studies I and IV.

Receiver operating curve (ROC) analysis

In Studies II and III, areas under the curve (AUC) were calculated by ROC analysis to evaluate the sensitivity and specificity of echo- and ECG variables to predict recovery of myocardial function. The variable value yielding the largest sum of sensitivity and specificity became the cutoff value. Values better than the cutoff were defined as positive. Positive predictive value was calculated as the number of true positives (= segments or patients with recovery) divided by the sum of true and false positives. The negative predictive value was the number of true negatives (= segments or patients without recovery) divided by the sum of true and false negatives.

In Study III, AUC values we first calculated for each ECG variable and each lead, and displayed on a color-coded map. From these AUC maps, regions were identified with the highest AUC values. Then, for each patient, values of the ECG variables in these best-discriminating regions we averaged from five to nine contiguous leads. These average values were used to calculate AUC values in order to reduce chance effect.

Reproducibility

The coefficient of agreement 'kappa' served to test repeatability of ordinal variables. A kappa-value < 0.19 means poor agreement; 0.20–0.39, fair agreement; 0.40–0.59, moderate agreement; 0.60–0.79, substantial agreement; and > 0.8, almost perfect agreement. In Study I, interobserver agreement for strain mapping was calculated by kappa-statistics over the segments of 10 randomly chosen patients analyzed independently by two observers. In Study II, intraobserver variability was calculated

from 100 randomly chosen segments. Kappa statistics served for strain-groups, and the intra-class correlation coefficient (ANOVA, two-way mixed model, single measures) for all strain- and strain-rate variables.

Statistical software

Statistical calculations were by SPSS 14.0 (Studies I and II), and PASW 18 (Studies III and IV).

5 RESULTS

5.1 Strain- and strain rate imaging of myocardial ischemic injury (I, II)

5.1.1 Validation of strain mapping for myocardial function assessment (I)

Strain mapping proved a useful method for estimating segmental and global myocardial contraction (see Figures 2 and 3 and Table 2 in Methods for a definition of strain mapping, pages 46–47). In patients with chronic infarction, segmental systolic strain assessed by strain mapping corresponded well with quantitative, end-systolic strain (S_{ES}) values. S_{ES} values significantly differed among groups of segments as defined by strain-mapping score (SMS), S_{ES} values being less negative with increasing SMS (Figure 5 A). Global SMS showed a significant linear correlation with global S_{ES} score (Figure 5 B).

Segmental SMS was associated with wall-motion score (WMS) assessed visually by B-mode echocardiography and CMR: WMS increased with increasing SMS. However, echocardiographic WMS did not differ significantly in patients with SMS 1 compared with those with SMS 2, which may indicate that echocardiographic WMS is less sensitive than SMS in detection of reduced contraction. In contrast, WMS assessed by CMR significantly differed between patients with SMS 1 and those with SMS 2. Further, WMS by echocardiography or CMR did not significantly differ between patients with SMS 3 and those with SMS 4, which indicates that dyskinesia is not so easily detected by the eye (Figures 5 C and D).

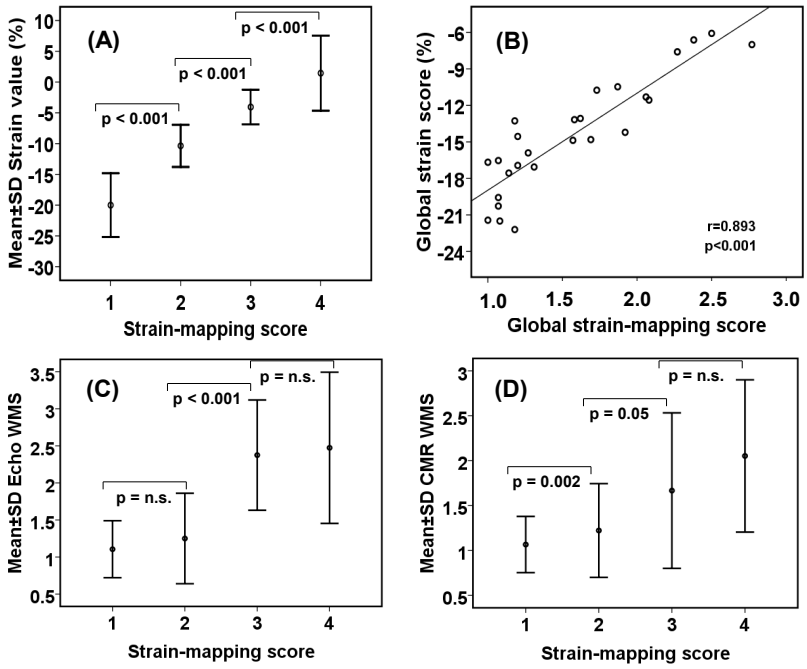

Figure 5. A) *Segments grouped according to strain-mapping score, with their respective quantitative systolic strain values.* **B)** *Correlation of global strain-mapping scores and global strain scores.* **C)** *Segments grouped according to strain-mapping score, and their respective wall-motion score by echocardiography.* **D)** *Segments grouped according to strain-mapping score, and their respective wall-motion score by CMR.*

5.1.2 Strain imaging in assessment of chronic MI injury (I)

Systolic strain and extent of MI

Strain imaging was able to provide an estimate of transmural extent of MI and global infarct size. Segmental SMS and end-systolic strain values (S_{ES}) both reflected transmural extent of chronic MI: The SMS was higher, and the S_{ES} less negative, the higher was the transmural extent of MI (Table 4). The SMS and S_{ES} significantly differed in segments with no or non-transmural infarction than in those with transmural infarction (Figures 6 A and B). Global SMS and S_{ES} each showed significant positive correlation with DE-CMR measured global LV infarction size (Figures 6 C and D).

Table 4. *Segmental strain-mapping scores and end-systolic strain values according to transmural infarction extent.*

Extent of DE, %	n	Strain-mapping score	Strain value, %
0	262	1.3±0.6	-13.6±9.2
1–25	11	1.6±1.0	-14.6±8.7
26-50	21	1.8±1.1	-12.4±10.0
51–75	13	2.3±1.2*	-7.1±10.2*
76–100	19	3.1±1.0*	-4.3±6.3*

Data presented as mean ± SD. Values differing significantly (p < 0.036) from values in segments without DE marked with an asterisk. CMR = cardiac magnetic resonance imaging; DE = delayed contrast enhancement.

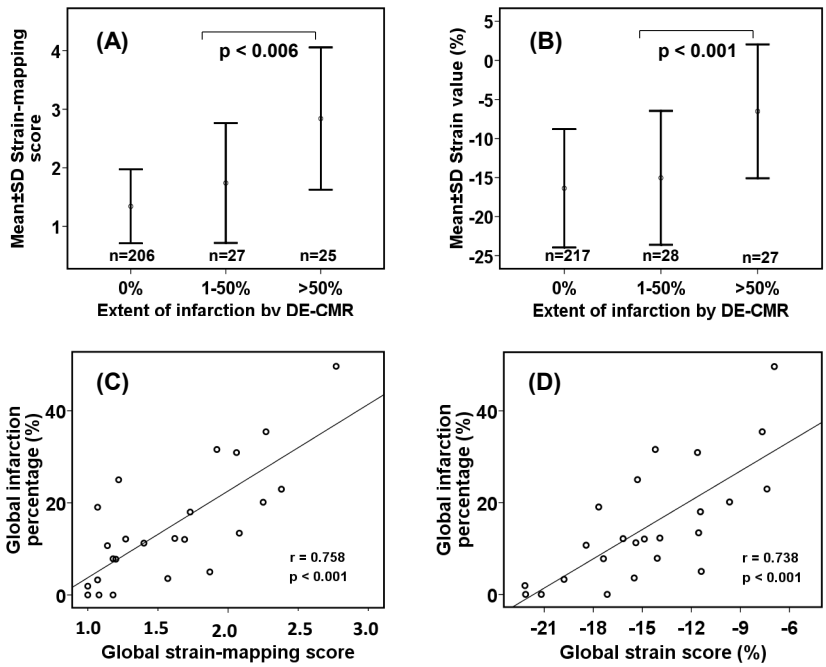

Figure 6. A) *and* **B)** *Strain-mapping scores and end-systolic strain values according to infarct transmurality by DE-CMR.* **C)** *and* **D)** *Correlation of global strain-mapping scores and global strain scores with global infarction percentage by DE-CMR.*

Strain-mapping score vs. echocardiographic WMS in estimation of MI scar

Most segments showed normal contraction on echocardiography, with strain mapping as well as with B-mode wall-motion analysis. However, a smaller proportion of segments had SMS 1 (65%) than had WMS 1 (81%), which may indicate that strain mapping is more sensitive in detecting reduced contraction than is visual wall-motion analysis. Indeed, of the segments with infarction, 62% had SMS ≥ 2; only 53% had WMS ≥ 2. Furthermore, strain mapping seemed clearly

better at detecting dyskinesia than did wall-motion analysis: The proportion of segments with SMS 4 was higher than with WMS 4 (Table 5).

Transmural MI extent was significantly higher in segments with contraction abnormalities than in segments with normal contraction. MI transmurality was also significantly higher in segments with severely reduced contraction than in segments with slightly reduced contraction. MI transmurality did not differ significantly among segments with SMS 3 or SMS 4, or among segments with WMS 3 or WMS 4 (Table 5).

Table 5. *Strain-mapping scores and echocardiographic wall-motion scores with corresponding transmural infarct extent by DE-CMR.*

Strain-mapping score	n (%)/258	Extent of DE, %	WMS by echo	n (%)/285	Extent of DE, %
1	167 (65)	4.7±15.5	1	230 (81)	5.8 ±18.2
2	63 (24)	10.5±24.6	2	30 (11)	21.1± 33.0*
3	9 (3)	44.9±41.1*	3	21 (7)	62.2 ±37.1*
4	19 (7)	57.4±42.1*	4	4 (1)	50.0± 57.7*

Data presented as mean ± SD. Values differing significantly ($p < 0.01$) from values in segments with strain-mapping score 1 or WMS 1 are marked with an asterisk. CMR = cardiac magnetic resonance imaging; DE = Delayed contrast enhancement; WMS = wall-motion score by B-mode echocardiography.

Accuracy of SMS vs. echocardiographic WMS in detection of transmural infarction

Positive predictive value

Segments with SMS 3 or 4 (representing end-systolic strain values > - 6%) as well as segments with WMS 3 or 4 have severely reduced or absent contraction; these segments were assumed to be severely damaged. Of the segments with SMS ≥ 3, 54% had transmural infarction; of the segments with WMS ≥ 3, 64% had transmural infarction. Of the segments with SMS 4 and WMS 4, indicating dyskinesia, a respective 58% and 50% had transmural infarction.

Negative predictive value

Segments with SMS 1 or 2 (representing end-systolic strain values < - 6%) as well as segments with WMS 1 or 2 have normal or slightly impaired contraction. Of the segments with SMS ≤ 2, 96% had no transmural infarct; 86% had no infarct, and 10% had a non-transmural infarct. Of the segments with WMS ≤ 2, 94% had no transmural infarct; 85% had no infarct, and 9% had a non-transmural infarct.

Sensitivity

Of the segments with transmural infarct, 60% had SMS ≥ 3, and 50% had WMS ≥ 3. Of those with a transmural extent of MI >75%, 73% had SMS ≥ 3, and 67% had WMS ≥ 3; 61% had SMS 4, and 11% had WMS 4 indicating dyskinesia.

Specificity

Of the segments with no, or non-transmural infarct, 95% had SMS ≤ 2, and 96% had WMS ≤ 2.

Estimation of global MI size in chronic MI by SMS vs. echocardiographic WMS

Global SMS, as well as global echocardiographic WMS, reflected global MI size: The higher the score, the larger the infarct. Correlation between global SMS and LV infarction percentage was r = 0.758 (p < 0.001); correlation between global WMS and LV infarction percentage was r = 0.612 (p = 0.002).

5.1.3 Strain rate imaging in assessment of acute MI injury (II)

Estimation of segmental viability by strain rate imaging

Acutely measured segmental strain- and strain-rate values showed a significant correlation with final end-systolic strain values after recovery, 8 months later. S_{ES} and S_{PSS} showed the best correlations (Figures 7 A and B). Of the segments with severely reduced or absent contraction (strain > -7%) in the acute phase, 60% (34 of 57) recovered partly (final strain -7% to -12%), or completely (final strain ≤ -13%). These viable segments showed significantly better strain and strain rate acutely than did non-viable segments (Figures 7 C and D). Accuracy of acute-phase strain- and strain-rate variables in predicting recovery of non-contractile segments is shown in Table 6. S_{ES} and S_{PSS} performed the best. Figure 8 shows an example of strain curves in a patient with MI acutely, and 8 months later, as well as a corresponding DE-CMR image.

Transmurality of infarction in viable segments was significantly smaller than in non-viable segments: 15% vs. 60%, p = 0.006. The best correlation between final segmental infarction transmurality and acute-phase measurement was for S_{ES} (r = 0.439, p < 0.001), S_{PSS} (r = 0.362, p < 0.001), and SR_S (r = 0.318, p < 001).

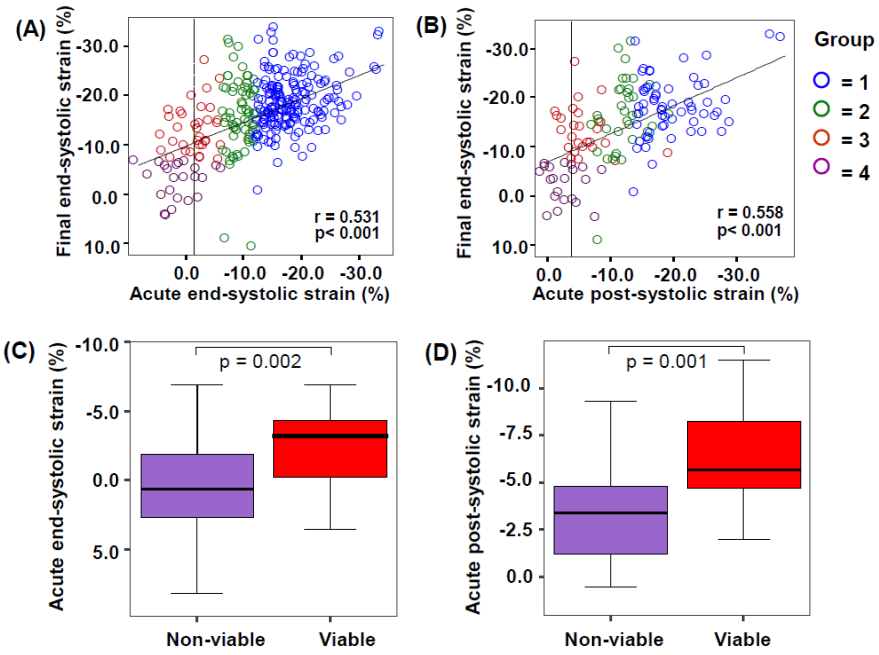

Figure 7. A) *and* **B)** *Correlation between acute end-systolic and post-systolic strain with final end-systolic strain after recovery from acute coronary syndrome. Left ventricular segments are grouped according to their contraction in the acute phase; segments with a severe contraction abnormality are further divided according to recovery: group 1 = normocontractile segments, group 2 = hypocontractile segments, group 3 = viable segments with a severe contraction abnormality, and group 4 = non-viable segments with a severe contraction abnormality. The vertical line indicates the cutoff value with the best accuracy in prediction of recovery of segments with a severe contraction abnormality.* **C)** *and* **D)** *Box-plots of acute end-systolic strain and post-systolic strain in non-viable vs. viable segments, each with a severe contraction abnormality (strain > -7 %), in patients with acute coronary syndrome. Segments grouped according to recovery of contraction 7 to 12 months after acute coronary syndrome: non-viable segments that do not recover, and viable segments that do recover. End-systolic- and post-systolic strain values are more negative in the viable segments. Each box shows the median and inter-quartile range, and whiskers show extreme values.*

Table 6. *Accuracy of acute-phase strain- and strain- rate parameters in predicting recovery of non-contractile segments after acute myocardial infarction.*

Parameter	Cut-off value	Sens, %	Spec, %	PPV, %	NPV, %	AUC	p Value
S_{ES}, %	-1.5	68	74	79	61	0.741	0.002
S_{PSS}, %	-3.8	85	62	74	76	0.783	0.001
SR_S, s^{-1}	-0.26	68	70	77	59	0.699	0.011
SR_E, s^{-1}	0.34	79	52	71	63	0.670	0.031
SR_A, s^{-1}	0.25	88	50	72	67	0.724	0.005

Cutoff values represent the point on the receiver operating characteristic curves yielding the best accuracy (= highest sum of sensitivity and specificity). Sens = sensitivity; spec = specificity; PPV = positive predictive value; NPV = negative predictive value; AUC = area under the curve; S_{ES} = end-systolic strain; S_{PSS} = post-systolic strain; SR_S = systolic strain rate; SR_E = early diastolic strain rate; SR_A = late systolic strain rate.

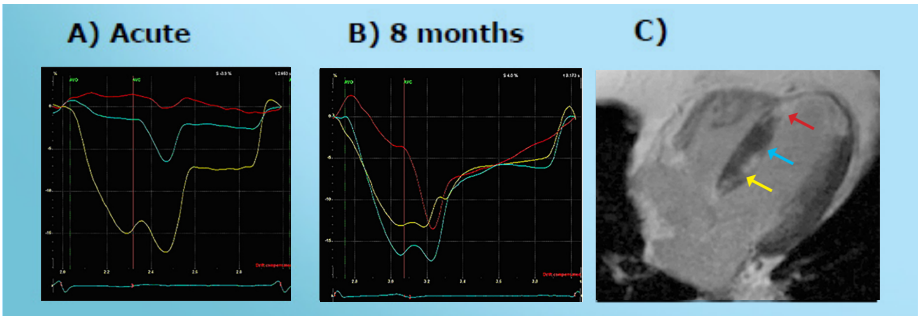

Figure 8. A) *and* **B)** *Strain curves from a patient with MI in the acute phase, and after 8 months.* **A)** *In the acute phase, end-systolic strain value is positive in the apical segment (red curve), indicating dyskinesia, and is severely reduced in the mid-segment (blue,) indicating akinesia. The basal segment (yellow) shows normal contraction. The mid-segment shows marked post-systolic strain, suggesting viability.* **B)** *After 8 months, the mid-segment has recovered, but the apical segment has not.* **C)** *DE-CMR image showing transmural infarction of the apical septum (red arrow), and subendocardial infarction in the mid- (blue), and basal (yellow) segments.*

Predicting recovery of global left ventricular function

Global S_{ES} and SR_S in the acute phase showed good correlation with global S_{ES} values after recovery ($r = 0.760$, $p < 0.001$ and $r = 0.732$, $p < 0.001$). Global S_{ES} and SR_S also correlated with global infarction percentage ($r = 0.539$, $p = 0.012$ and $r = 0.440$, $p = 0.046$). Acutely measured global SR_E had a significant correlation with final global S_{ES} value ($r = -0.523$, $p = 0.01$), but not with infarction percentage. Global SR_A did not predict recovery or MI size.

5.1.4 Feasibility of strain rate imaging (I, II)

In the chronic stage of MI, strain mapping was performed in 26 patients, yielding a total of 416 segments (16 segments per patient). Of all segments, 333 (80%) were of sufficiently good image quality for strain-mapping analysis: Of 156 basal, 134 (86%), of 156 mid-, 129 (83%), and of 104 apical segments, 70 (67%). S_{ES} could be measured in 99% of these segments.

In the acute phase, strain rate imaging was performed in 23 patients, yielding a total of 414 segments (18 segments per patient). The feasibility of strain and strain rate values were as follows: S_{ES} 78%, SR_S 73%, SR_E 73%, and SR_A 69%.

5.1.5 Reproducibility of strain rate imaging (I, II)

In order to assess reproducibility, strain mapping was performed in 10 randomly selected patients independently by two investigators (Minna Kylmälä and Mika

Laine). Inter-observer agreement of SMS was substantial: the coefficient of agreement "kappa" was 0.63 between the two observers.

Intra-observer variability of acute-phase strain- and strain-rate values was tested in 10 randomly chosen patients. The intra-class correlation coefficients were as follows: S_{ES} 0.87, S_{PSS} 0.93, SR_S 0.77, SR_E 0.67, and SR_A 0.53.

5.2 Body surface potential mapping of myocardial ischemic injury (III, IV)

5.2.1 BSPM in assessment of chronic MI injury (IV)

5.2.1.1 Correlation of BSPM variables with infarct size in chronic MI

BSPM variables are explained in Table 3 in the Methods section, page 50. The best correlations of BSPM variables and their corresponding leads are shown in Table 7 and Figure 9.

Depolarization variables

Variables from the first half of the QRS, comprising the Q- and R waves, showed strong correlations with infarct percentage by DE-CMR, their best correlations being on the left side of the chest, and reciprocally on the right upper back, with inverse correlations at these two sites. On the upper back, the QRS is a mirror image of the QRS on the left side: The "reciprocal Q wave" is represented by an initial positive deflection, and the "reciprocal R wave" a negative deflection; the "reciprocal S wave" a positive deflection.

The initial QRS variables, 1st QRSint and R width, had their strongest correlations reciprocally on the right upper back (r = 0.57 and r = 0.71). On the upper back, R width was measured as the time from QRS onset to the first negative deflection, hereafter called "reciprocal Q width." On the left side, Q width was measured as time from QRS onset to the first positive deflection. However, on the left side, the correlation of the Q width (r = 0.51) was clearly lower than that of the reciprocal Q width on the upper back. Also the 1st QRSint had a clearly weaker correlation on the left side (r = -0.38).

The 2nd QRSint and Ramp, describing the R wave, had their strongest correlations on the left side (r = -0.56 and r = -0.57). The inverse correlations of the reciprocal R-wave variables on the right upper back were almost as good (r = 0.53 and r = 0.55). The QRSint had a strong correlation on the left side (r = -0.58), and a weak inverse correlation on the upper back (r = 0.34).

Variables from the second half of the QRS, comprising the S wave and the final part of the R wave, showed significant, but weak correlations. The Samp performed the best on the central upper back (r = -0.42), with a weaker correlation on the left

side (0.39). The 3rd and 4th QRSint showed significant correlations on the left side only (r = -0.39 and r = 0.33, respectively).

Repolarization variables

Repolarization variables performed best on the left side around lead V5, with significant inverse correlations with infarct size reciprocally on the right upper back as well. The T-wave variables had slightly stronger correlations than the variables including the ST segment in addition to the T wave. The correlations of Tamp, T80int, and TPEint were negative on the left side (r = -0.55, r = -0.57, and r = -0.56). The STTint and QRSSTTint also showed negative correlations on the left side (r = -0.52 and r = -0.54). Reciprocally, the correlations for all these variables were weaker (r = 0.43–0.49). Diverging from the other repolarization variables, the QRSSTT area showed a strong negative correlation on right upper back (r = -0.50), and a weaker inverse correlation on the left shoulder (r = 0.42).

ST-segment amplitudes, slopes, and integrals had weak, or non-significant, correlations. ST60amp, STint, ST80amp, and ST80 slope performed the best on the left upper back (r = -0.3 to -0.36); the ST60 slope had a weak correlation on the left side (r = 0.27). Jamp showed a weak correlation on the right upper back (r = 0.28) and on the left side (r = -0.27); the other ST-segment variables showed no significant reciprocal correlations. The ST60int and ST80int showed no significant correlations at all.

5.2.1.2 BSPM variables differentiating large from small infarcts in chronic MI

The best-performing depolarization and repolarization variables could distinguish patients with large infarcts (LV infarct percentage by DE-CMR > 11%, the median) from those with a small or with no infarct (Figure 9). In large infarcts, the reciprocal Q width was wider, and the 1st QRSint was positive or less negative on the right upper back. On the left side, close to V3 and V4, the Ramp and the 2nd QRSint were negative, or were positive but less positive, indicating a smaller, or an absent R wave in large infarcts. At the same site, the QRSint was negative, or less positive, in large infarcts. Also on the left side, the Tamp, T80int, STTint, and QRSSTTint were negative, or less positive, due to negative, or lower T waves in large infarcts. Figure 10 shows QRSSTT examples demonstrating differences in depolarization- and repolarization variables between patients with large infarcts and patients with no infarct scar.

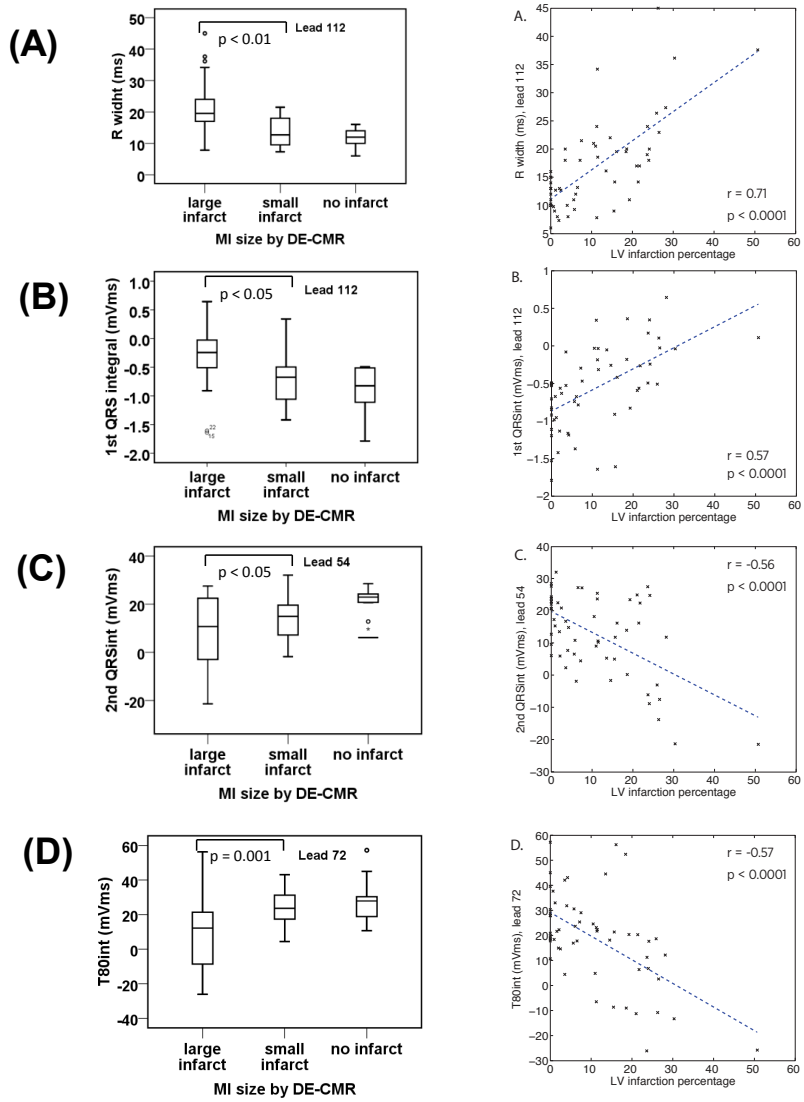

Figure 9. A) *to* **D)** *Computed BSPM variables in the chronic phase at the lead yielding the highest correlation with MI size, in patients with large, small, or no infarct.* **On the left:** *Boxes indicate medians, first and third quartiles; whiskers indicate minimum and maximum values falling within 1.5 x the interquartile range from the upper or lower edge of the box; extreme values are indicated by points falling outside 1.5 x the interquartile range. Large and small infarcts are separated by the median infarction percentage, 11%, by DE-CMR.* **On the right:** *Scatterplots showing correlations between BSPM variables and infarction percentages. For definition of BSPM variables, see Table 3.*

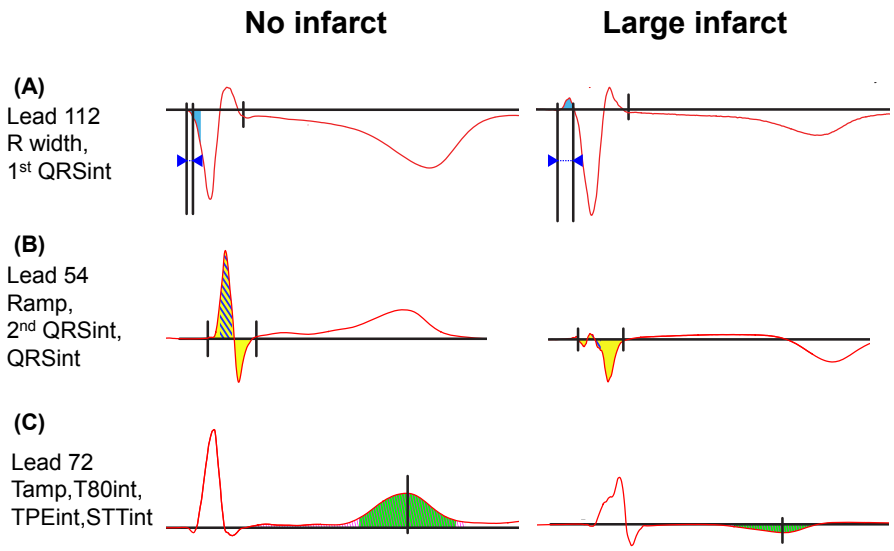

Figure 10. *Representative QRSSTT complexes demonstrating differences in BSPM variables between patients with a large infarct scar* **(right)** *or with no infarct scar* **(left)**. **A)** *R width (time-interval marked on the initial QRS) and 1st QRSint (blue area) on the upper back (lead 112).* **B)** *Ramp (peak of positive deflection), 2nd QRSint (hatched area), and QRSint (integral of the yellow area) on the left side (lead 54).* **C)** *Tamp (T-apex amplitude, marked by a line), T80int (green area), TPEint (time from T-apex to T-end), and STTint (hatched area) on the left side (lead 72). QRSSTT complexes are recorded in the chronic phase; examples shown are from leads yielding the highest correlations with MI size.*

5.2.2 BSPM in assessment of acute MI injury (III, IV)

5.2.2.1 Correlation of BSPM variables with infarct size in acute MI and during recovery (IV)

BSPM variables are explained in Table 3 in the Methods section, page 50. The best correlations of BSPM variables with infarct size by DE-CMR—along with their corresponding leads—are shown in Table 7.

BSPM in the acute phase vs. infarction percentage

The same **depolarization variables** that correlated best with infarction percentage in the chronic phase also showed strong correlations acutely with final MI size. In the acute phase, the best recording locations were the same as in the chronic phase. The Q-wave variables had slightly lower correlations, and R-wave variables had slightly higher correlations in the acute than in the chronic phase. The 1st QRSint and reciprocal Q width showed their strongest correlations on the upper back ($r = 0.56$ and $r = 0.64$). Q width had a strong correlation on the left side ($r = 0.59$) whereas that of the 1st QRSint was weak ($r = -0.39$). The 2nd QRS, Ramp,

and QRSint showed their strongest correlations on the left side (r = -0.59, r = -0.60 and r = -0.62). The 2nd QRS and Ramp also showed strong inverse correlations reciprocally on the right upper back (r = 0.50 and 0.52), whereas the QRSint had only a weak correlation reciprocally (r = 0.28). Samp had a good correlation on the central upper back (r = -0.51), and a weaker correlation on the left side (r = 0.40). The 3rd and 4th QRSint had significant correlations on the left side only (r = -0.43 and r = 0.32).

Repolarization variables showed clearly weaker correlations with infarction percentage acutely than they did in the chronic phase, but the best recording locations were the same. The QRSSTTint and the Tamp performed best, with negative correlations on the left side (r = -0.42 and r = -0.40). Moreover, the T80int and TPEint had significant correlations on the left side (r = -0.36 for both). The QRSSTT area showed a moderate correlation on the upper back (r = -0.35). These repolarization variables showed no significant reciprocal correlations. ST-segment variables had weak correlations of similar magnitude as in the chronic phase. ST-segment amplitudes and -integrals performed best on the right side (r = -0.29 to -0.33), ST60- and ST80 slopes on the left lower back (r = -0.28 for both). Only the STTint lacked significant correlations acutely.

BSPM during recovery vs. infarction percentage

At (a mean) 2 weeks (1–4 weeks) after the acute event, during healing of the infarct, recording locations providing the best data were the same as in the acute and chronic phases. **Depolarization variables** from the first half of the QRS performed best, their correlations being as strong as in the acute and chronic phases. Q-wave variables had slightly higher, and R-wave variables slightly lower correlations during recovery than in the acute phase. Reciprocal Q width and the 1st QRSint showed strong correlations on the right upper back (r = 0.65 and r = 0.56). On the left side, Q width and 1st QRSint showed significant, albeit weaker, correlations (r = 0.47 and r = -0.48). The 2nd QRSint, Ramp, and QRSint showed strong correlations on the left side, below V3 and V4 (r = -0.59, r = -0.59, and r = -0.58). The 2nd QRSint and Ramp also had strong inverse correlations reciprocally on the upper back (r = 0.56 and r = 0.57), whereas the inverse correlation for QRSint was clearly weaker (r = 0.34). Of the variables from the second part of the QRS, Samp performed the best on the right upper back (r = -0.53), slightly better than in the acute or chronic phases. The 3rd QRSint had a significant correlation on the left side only (r = -0.41); the 4th QRSint showed no significant correlations during recovery.

Repolarization variables performed clearly better during recovery than they did acutely, and almost as well as in the chronic phase. The T-wave variables Tamp, T80int, and TPEint performed the best, with strong correlations on the left side (r = -0.54, r = -0.52, and r = -0.54). The STTint and the QRSSTTint also had significant correlations on the left side (r = -0.38 and r = -0.50). All these repolarization variables had significant, albeit weaker, correlations reciprocally on the right upper back (r

= 0.33–0.39). The QRSSTT area had a strong correlation on the right upper back (r = -0.51), without any significant reciprocal correlation. ST-segment variables showed the weakest correlations of all, similar to those in the acute and chronic phases, at best r = 0.28 to 0.36 on the left shoulder. ST60- and ST80 slopes had their best correlations on the lower right back (r = -0.3 and -0.32, respectively).

Correlation of BSPM variables with CK-MBm in acute MI (IV)

In the acute phase, **depolarization variables** correlated better with peak CK-MBm than did repolarization variables, as they also did with infarction percentage, and at the same locations. The 2nd QRSint and Ramp performed the best, with strong correlations on the left side (r = -0.56 and r = -0.59), and even stronger inverse correlations reciprocally on the right upper back (r = 0.63 and r = 0.64). Q width showed strong correlations on the left side (r = 0.57), and reciprocally on the right upper back (r = 0.57). However, the 1st QRSint showed only a moderate correlation on the central upper back (r = 0.42), and an even weaker inverse correlation on the left side. As for the correlations with infarction percentage, the second part of the QRS performed worse than the first part. Again, Samp had moderate correlations on the left side (r = 0.46), and the central upper back (r = -0.47), whereas the 3rd and 4th QRSint had weaker correlations.

Of the **repolarization variables**, those confined to the ST segment performed best, with the best recording location on the left side. ST60- and ST80 amplitudes and -slopes showed good correlations with CK-MBm on the left side (r = 0.51–0.56), and ST60int, ST80int, STint, and Jamp had moderate correlations on the left side (r = 0.43–0.47). All ST-segment variables had significant inverse correlations reciprocally on the right side, or right upper back (r = -0.41 to -0.49). However, the variables including the T wave showed no significant correlations at any locations, except for QRSSTTint, with its borderline significant correlation on the right upper back (r = -0.28).

Peak CK-MBm had a good correlation with infarction percentage by DE-CMR (r = 0.65), thus reflecting final MI size. In the chronic phase, depolarization variables showed correlations as good as in the acute phase, again performing better than the repolarization variables did. With infarction recovery, correlations of T-wave variables grew stronger, and those of ST-segment variables diminished. In the chronic phase, the leads on the upper back yielded stronger correlations for the best depolarization as well as repolarization variables.

Table 7. *Best correlations of BSPM variables with LV infarct percentage at various time-points of myocardial infarction.*

	Acute phase			Recovery phase			Chronic phase		
	r max	*p*-value	Lead	r max	*p*-value	Lead	r max	*p*-value	Lead
1st QRSint	**0.56**	< 0.0001	112	**0.56**	< 0.0001	112	**0.57**	< 0.0001	112
2nd QRSint	**-0.59**	< 0.0001	61	**-0.59**	< 0.0001	55	**-0.56**	< 0.0001	54
QRSint	**-0.62**	< 0.0001	54	**-0.58**	< 0.0001	55	**-0.58**	< 0.0001	54
Ramp	**-0.60**	< 0.0001	67	**-0.59**	< 0.0001	62	**-0.57**	< 0.0001	61
Samp	**-0.51**	< 0.0001	104	**-0.53**	< 0.0001	113	-0.42	0.001	105
R width*	**0.64**	< 0.0001	112	**0.65**	< 0.0001	112	**0.71**	< 0.0001	112
Q width	**0.59**	< 0.0001	71	0.47	0.0003	61	**0.51**	< 0.0001	60
ST60	-0.30	0.02	5	0.36	0.008	63	-0.30	0.02	88
ST80	-0.33	0.01	5	0.29	0.04	63	-0.35	0.008	80
STint	-0.30	0.03	5	0.28	0.04	63	-0.31	0.02	81
ST60 slope	0.32	0.01	55	-0.30	0.03	115	0.27	0.04	70
ST80 slope	0.28	0.04	47	-0.32	0.02	115	-0.36	0.006	88
Tamp	-0.40	0.002	75	**-0.54**	< 0.0001	72	**-0.55**	< 0.0001	72
T80int	-0.36	0.006	75	**-0.52**	< 0.0001	72	**-0.57**	< 0.0001	72
TPEint	-0.36	0.006	71	**-0.54**	< 0.0001	72	**-0.56**	< 0.0001	72
STTint		n.s.		-0.38	0.004	72	**-0.52**	< 0.0001	72
QRSSTTint	-0.42	0.001	71	**-0.50**	0.0001	69	**-0.54**	< 0.0001	69
QRSSTT area	-0.35	0.007	119	**-0.51**	< 0.0001	111	**-0.50**	< 0.0001	111

**R width = "reciprocal Q width."*

For definition of BSPM variables, see Table 3.

5.2.2.2 Predicting recovery of LV function with BSPM in acute MI (III)

BSPM variables could assess myocardial viability in patients with acute MI. Viability was determined by comparing the proportion of dyssynergic LV by echocardiography in the acute phase and after healing of the infarct, on average 11 months after the acute event. If, between measurements, the number of dysfunctional segments had decreased, the myocardium was considered viable. In the acute phase, the number of dysfunctional segments was slightly higher in patients with viable myocardium than in those without: 5.7 ± 2.1 vs. 4.4 ± 2.4 ($p = 0.017$). After MI healing, the number of dysfunctional segments was 1.9 ± 1.7 vs. 6.5 ± 2.6, and EF was 60 ± 8% vs. 49 ± 9% in the viable vs. the non-viable group (both $p > 0.001$).

Acute-phase BSPM variables best in predicting recovery of LV function differed for all three culprit-artery-defined ischemic regions, as did the best recording location with the highest predictive accuracy. The best recording location differed between depolarization and repolarization variables (Table 8). For most BSPM variables, we found also a reciprocal recording location, with good predictive accuracy for the inverse values of the BSPM variables at the best recording locations.

Table 8. *Best-performing BSPM variables and their accuracy in predicting left ventricular recovery.*

BSPM Variable	Cut-off	Sens, %	Spes, %	PPV, %	NPV, %	Recording site	AUC	P-Value
LAD group								
1st QRS quartile	-0.15	85	79	85	79	around V4–V6	0.821	0.002
STT integral	-9.03	80	71	80	71	left upper back and neck	0.786	0.005
RCA group								
1st QRS quartile	2.22	91	80	91	80	upper sternum	0.891	0.015
ST integral	1.3	100	80	92	83	upper sternum	0.982	0.003
LCX group								
STT area	8.98	100	83	86	100	around V6–V7	0.972	0.006

The unit for BSPM variables is mVms. "Median" indicates median value of the average integrals calculated in each patient from the best recording site; "cutoff," the average integral value yielding the highest sum of sensitivity and specificity. For definition of BSPM variables, see Table 3. AUC = area under the curve, LAD = left anterior descending coronary artery, LCX = left circumflex coronary artery, NPV = negative predictive value, PPV = positive predictive value, Sens = sensitivity, Spes = specificity, RCA = right coronary artery, V4 – V7 = standard ECG chest leads.

Optimal recording locations

Figure 11 shows the best recording locations for predicting recovery of the LV territories by culprit artery.

The best recording location for predicting recovery of LAD–defined dysfunction was on the left side around standard leads V4 to V6. Here, of all BSPM variables, the 1st QRSint performed the best. Repolarization variables predicted LAD-defined dysfunction best on the left upper back and neck, and the upper sternum performed rather well, as did the best reciprocal recording site on the lower chest centrally.

The best recording location for predicting recovery of RCA-defined LV dysfunction was on the upper sternum and in the region below the right clavicle. Here, STint and other repolarization variables performed best. The right upper back and neck were also equally good recording sites. The best reciprocal recording site was on the left side, at or below standard lead V5.

For predicting recovery from LCX-defined dysfunction, the best recording location was on the posterior left side, around standard leads V6 and V7.

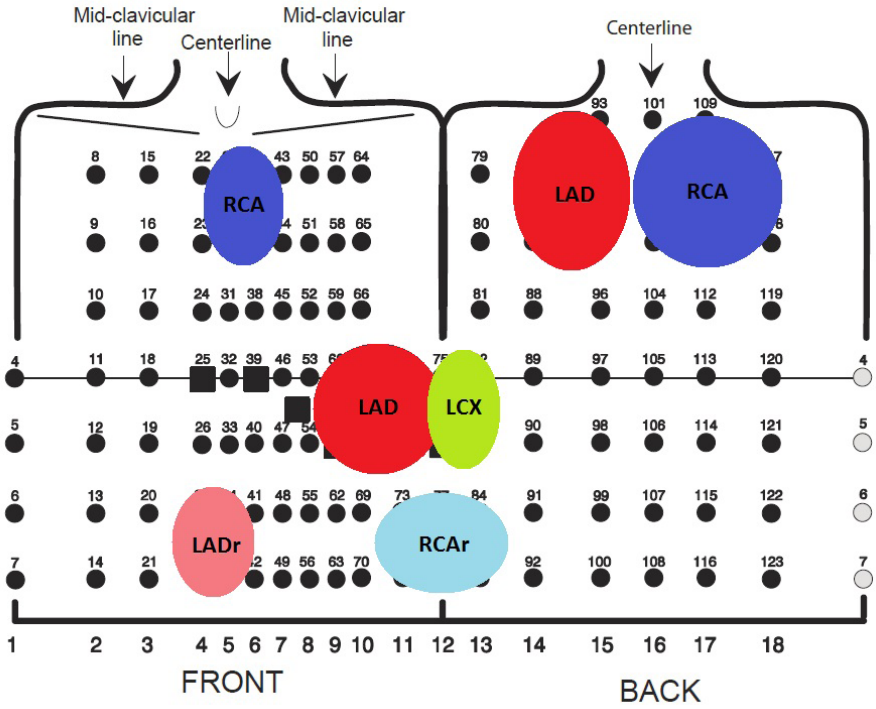

Figure 11. *Best recording locations for predicting recovery of various culprit-artery defined ischemic territories. Best reciprocal recording locations indicated with an r. LAD = left anterior descending coronary artery, LCX = left circumflex coronary artery, RCA = right coronary artery.*

Best depolarization variables

In the LAD group, the 1st QRSint was the very best variable at predicting functional recovery, with its optimal recording site being on the left side (AUC 0.82, p = 0.002). Here, the group medians were 1.01 mVms in patients recovering vs. -1.33 mVms in those not recovering (Table 8). At the best reciprocal recording site on the right back, the group median 1st QRSint in patients recovering, was negative, and in those not recovering, positive (Figure 12). The torso map of the 1st QRSint in the recovery group resembled that of the healthy controls very closely.

In the RCA group also, the 1st QRSint was the best of the depolarization variables for predicting functional recovery, with its optimal recording site being on the upper sternum (AUC 0.89, p = 0.015). Here, the group medians were 1.72 mVms in patients recovering vs. 2.66 mVms in those not recovering (Table 8). Recovery of the RCA territory could also be accurately predicted reciprocally from the left side, where the group median 1st QRSint was less negative in patients recovering than in those not recovering (Figure 12).

In the LCX group, the 4th QRSint, recorded on the left side of the back, was less positive in patients recovering than in those not recovering. Reciprocally on the right

shoulder, the 4th QRSint was positive in patients recovering, and negative in those not recovering. However, its discriminatory accuracy was not strong (Figure 12).

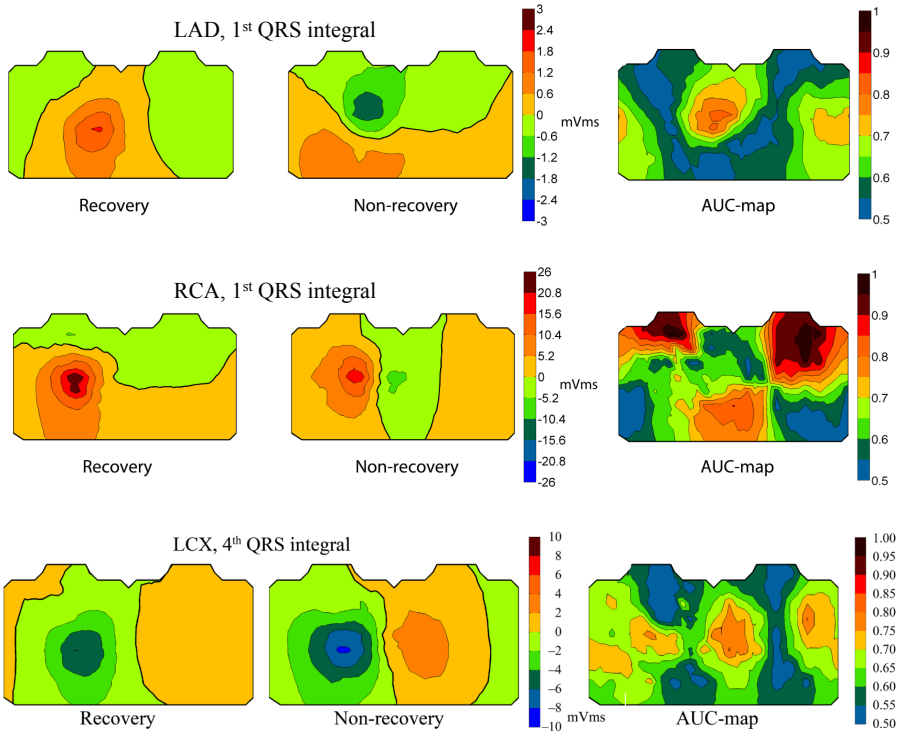

Figure 12. *Best depolarization variables in patients with and without recovery according to culprit artery, and the corresponding AUC values showing the best recording locations with the highest predictive accuracy.*

Best repolarization variables

The STint, STTint, and STT area performed well at predicting recovery of both LAD- and RCA-defined LV dysfunction. At the best recording site, the STint and STTint were less negative and the STT area smaller in patients recovering than in those not recovering from LAD-related LV dysfunction. Relationships between these variables and recovery of RCA-related dysfunction were the opposite.

In the LAD group, STTint was the best of the repolarization variables, with its optimal recording site being on the left upper back and neck (AUC 0.79, p = 0.005). Here, the group medians were -5.52 mVms in patients recovering vs. -10.65 mVms in those not recovering from LV dysfunction (Table 8). STTint performed in a similar fashion also on the upper sternum. The best reciprocal recording site was centrally on the upper abdomen, where the STTint was less positive in patients recovering than in those not recovering. STint had a discriminatory pattern similar to that of STTint. The STT area was smaller in patients recovering than in those not recovering at all these aforementioned recording sites (Figure 13).

In the RCA group, STint was the best variable of all, with its optimal recording site including the region below the right clavicle and the upper sternum (AUC 0.98, p = 0.003). Here, the group medians were –3.90 mVms in patients recovering vs. 2.37 mVms in those not recovering from LV dysfunction (Table 8). The region that included the right upper back and neck, was an equally good discrimination site. The best reciprocal recording site was on the left side, where STint was positive in patients recovering, and negative in those not recovering. STTint, as well as STamp, had a similar discriminatory pattern as STint. STT area was larger in patients recovering than in those not recovering at all these sites (Figure 13).

In the LCX group, STT area was the best variable at predicting recovery, with the optimal recording site being on the left side (AUC 0.97, p = 0.006). Here, the group medians were 15.19 mVms in patients recovering vs. 7.77 mVms in those not recovering (Table 8). No variables other than STT area could reliably predict recovery of LCX-related LV dysfunction (Figure 13).

T-end integral and T-wave integral could predict recovery of the LAD territory in a manner similar to that of the STint and the STTint. At the best recording locations on the left shoulder and the upper sternum, these variables were less negative in patients recovering than in those not recovering. The T-end integral predicted recovery of the RCA territory also. As for STint, STTint, and STamp, the best recording locations were on the upper sternum, below the right clavicle, and on the right shoulder, at which sites the T-end integral was more negative in patients recovering than in those not recovering (Figure 13).

The torso maps of all repolarization variables in the RCA- and LCX- recovery groups resembled those of the healthy controls. In the LAD group, both patient groups had torso maps similar to those of healthy controls (Publication III, supplementary Figure S4).

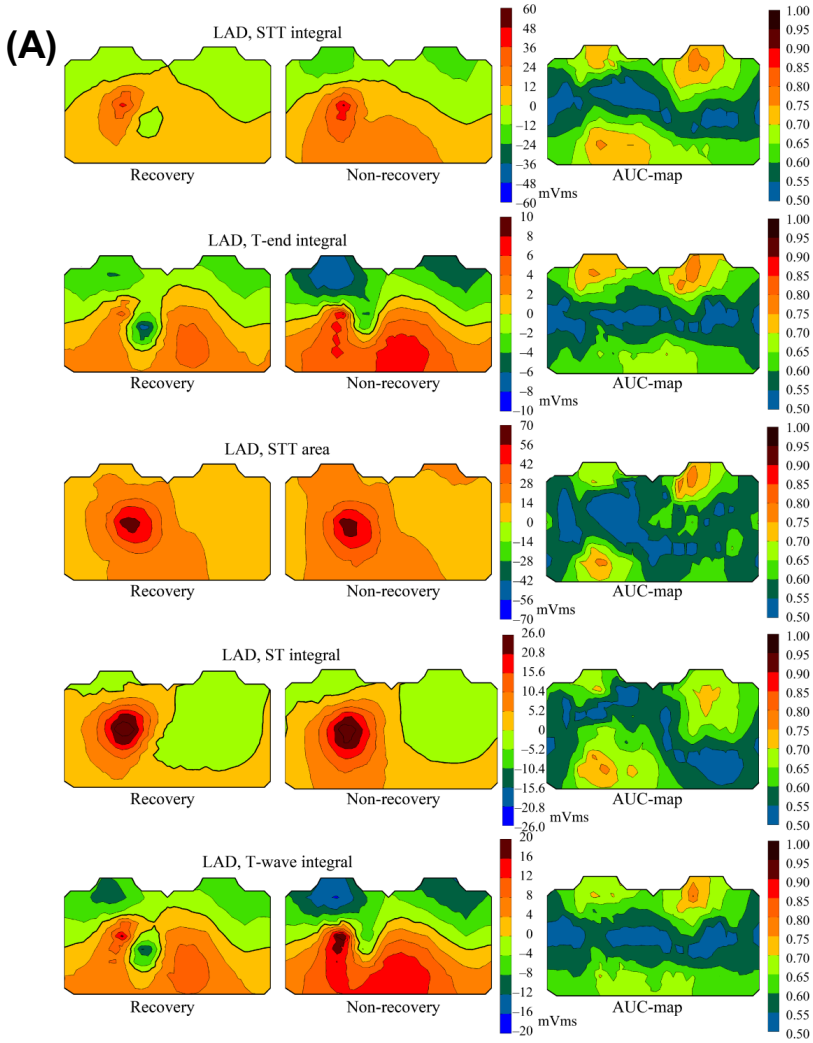

Figure 13. A) *to* **C)** *Best repolarization variables in patients with and without recovery according to culprit artery, and corresponding AUC-values showing the best recording locations with the highest predictive accuracy.* **A)** *LAD, left anterior descending artery;* **B)** *RCA, right coronary artery;* **C)** *LCX, left circumflex coronary artery.*

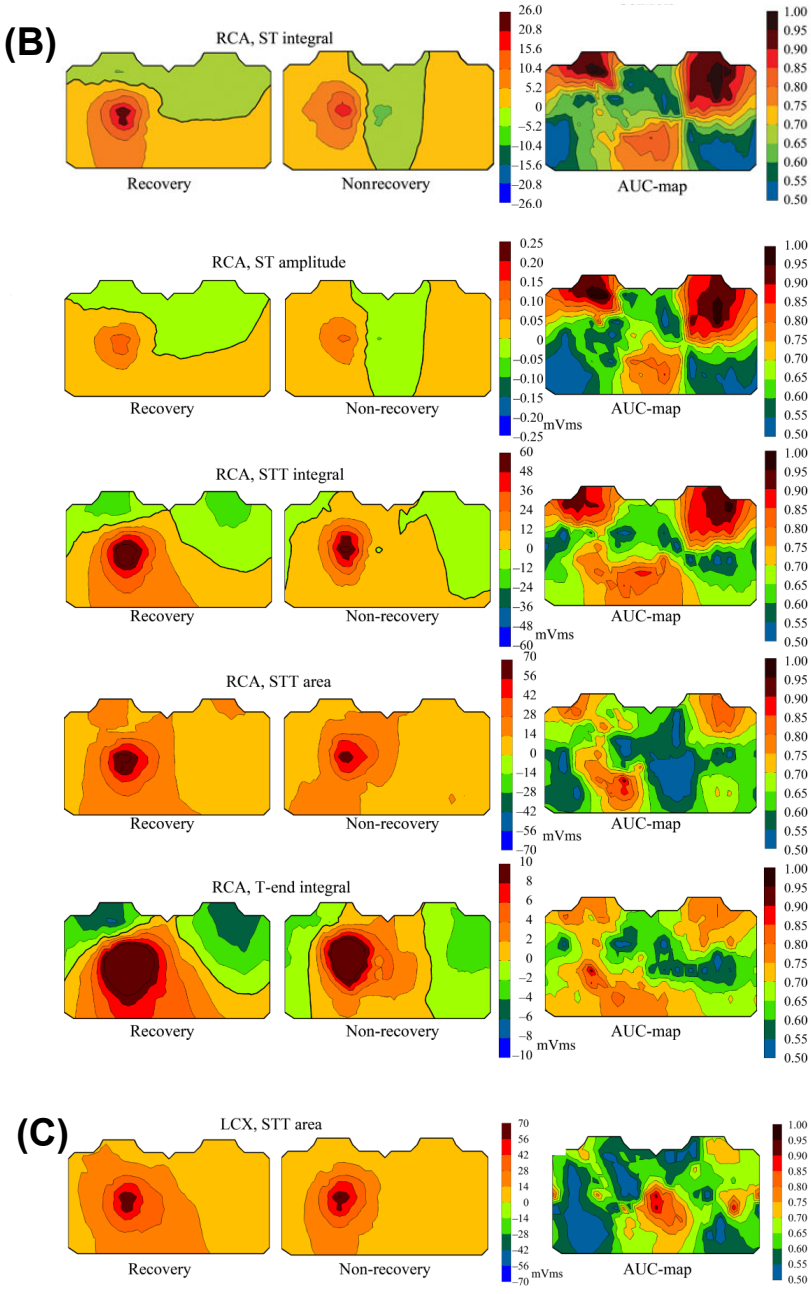
(B)
RCA, ST integral
Recovery
Nonrecovery
AUC-map
RCA, ST amplitude
Recovery
Non-recovery
AUC-map
mVms
RCA, STT integral
Recovery
Non-recovery
AUC-map
mVms
RCA, STT area
Recovery
Non-recovery
AUC-map
mVms
RCA, T-end integral
Recovery
Non-recovery
AUC-map
mVms
(C)
LCX, STT area
Recovery
Non-recovery
AUC-map
mVms

6 DISCUSSION

6.1 Main findings

The aim of this thesis was to learn whether echocardiographic strain rate imaging and electrocardiographic BSPM can estimate myocardial viability and infarct size in patients with acute and chronic MI. DE-CMR performed after healing of the infarction served as the gold standard for determining segmental as well as global LV infarct size.

In patients with chronic MI, tissue Doppler strain-mapping was validated for assessing regional systolic strain and extent of infarct, to our best knowledge, for the first time. Systolic strain, measured quantitatively as well as by strain mapping, could differentiate between segments with transmural infarct and those with non-transmural, or no infarct. Global systolic strain and BSPM variables correlated with MI size in chronic MI.

In patients with acute MI, strain- and strain-rate variables could assess myocardial viability, and predict recovery of contraction of akinetic segments. Acutely measured global strain- and strain-rate variables reflected LV function after healing of the infarction, and correlated with final MI size. Moreover, acute-phase BSPM variables correlated with final MI size and could predict recovery of LV function.

6.1.1 Validation of strain mapping in chronic MI

Systolic strain is a measure of myocardial contraction possible to quantify by tissue Doppler echocardiography. In modern ultrasound machines, tissue Doppler strain can be color-coded and displayed in real-time on top of the two-dimensional image. Systolic strain values can then be semi-quantitatively assessed from these strain maps, a method that we call strain mapping. In Study I, strain mapping was, for the first time, validated for assessing regional systolic strain and extent of chronic MI.

Systolic strain was scored by strain mapping: Score 1 for normal contraction; scores 2, 3, and 4 for increasing degrees of contraction abnormality. Strain mapping showed itself to be feasible and repeatable, with substantial inter-observer agreement for strain-mapping scores (SMS). Segmental and global SMS of the LV showed excellent agreement with corresponding quantitative systolic strain values.

SMS reflected the segmental extent of chronic MI; the higher the score, the larger the transmural extent of infarct. SMS could separate segments with transmural infarct (extent of MI > 50% of the segmental thickness) from those with non-transmural or no infarct, performing equally well as quantitative strain values.

Strain mapping as well as quantitative strain analysis failed, however, to separate segments with non-transmural infarct from those with no infarct. Global SMS, as well as global strain by quantitative analysis, showed a strong correlation with global LV infarction percentage by DE-CMR (r = 0.76 and r = 0.74, respectively).

In comparison to visual wall-motion scoring (WMS) of segmental contraction, strain mapping was as good at ruling out transmural infarction in patients with chronic MI, at a specificity of 95%. SMS 1 or 2, indicating normal or moderately reduced contraction, excluded transmural MI with an excellent negative predictive value of 96%. SMS 3 or 4, indicating severely reduced or absent contraction, signified in most cases that the segment had an infarct, one which probably was transmural. In segments with SMS 1 and 2 respectively, WMS was closer to 1, which could signify that strain mapping is more sensitive than WMS at identifying segments with a mild contraction abnormality. WMS was around 2.5 in segments with SMS 3 and 4, indicating that strain mapping is more sensitive than is the eye at detecting dyskinesia. Supporting this finding, segments with a transmural extent of infarct > 75% were at SMS 4 for dyskinesia in 61%, and WMS 4 for dyskinesia only in 11% of cases.

6.1.2 Strain- and strain rate imaging in assessment of viability and extent of MI

If myocardium contracts, it is viable. Myocardial segments with systolic strain values more negative than -7% have preserved contraction, and therefore are viable. Study II showed that in patients with acute MI, strain- and strain-rate values could assess myocardial viability. Acute-phase segmental strain- and strain-rate values correlated with final end-systolic strain. These variables could predict with good accuracy whether segments with severely reduced or absent contraction (end-systolic strain > -7%) would recover: These variables were significantly better in viable segments with functional recovery than in non-viable segments not recovering. The most accurate variable in assessment of viability (AUC = 0.78), was post-systolic strain, followed by end-systolic strain; systolic and diastolic strain rates were also good at predicting recovery of non-contractile segments, but performed no better than strain did. Global values of acute systolic strain and strain rate, as well as early diastolic strain rate, correlated with final global systolic strain values, and thus predicted final LV systolic function.

Myocardial viability and contraction are connected with the transmural extent of MI. In both acute and chronic MI, segmental systolic strain values became less negative with increasing transmurality of the infarct. In acute MI, systolic strain, post-systolic strain, and systolic strain rate showed significant correlations with segmental infarct transmurality. In viable non-contractile segments with functional recovery after the acute event, median infarction percentage was 19%, as compared

with non-viable segments with a median infarction percentage of 60%. In both acute and chronic MI, global systolic strain—and acutely also global systolic strain rate—showed good correlations with LV infarction percentage, reflecting the global extent of MI. The less negative the values, the larger the MI size.

6.1.3 BSPM in assessment of viability and MI size

BSPM records cardiac electric potentials by leads covering the entire thorax, and thus yields ECG data from a much larger thoracic area than the conventional 12-lead ECG. From the BSPM recordings, a multitude of different variables related to the QRSSTT complex can be automatically calculated. Studies III and IV show that at all stages of the infarction, BSPM variables can determine final MI size. In acute MI, BSPM variables can predict recovery of dysfunctional myocardium. Thus, BSPM can assess myocardial viability as well as LV infarct size.

At all stages of the infarction, depolarization variables were better than repolarization variables at estimating MI size, the computed Q- and R waves performing best. At all time-points, the best recording sites were on the left side, in the vicinity of V3 to V5, and reciprocally on the right upper back. Interestingly, the computed Q wave performed the best reciprocally, where the QRS values are the inverse to those on the left side, a reciprocal Q wave being a positive deflection. Leads at a distance may see the heart in more of a panorama view than do leads overlying the LV, which could explain why the right upper back was a good recording site, especially in a patient group including multiple MI locations. In comparison with the Q- and R-wave variables, the QRS variables from the second half of the QRS showed only modest correlations with MI size. The T-wave variables had moderate correlations with MI size in the acute phase, correlations that grew stronger during recovery; in the chronic phase, the T-wave variables performed nearly as good as the R-wave variables. The ST-segment variables had only weak correlations with MI size, regardless of infarction stage.

BSPM variables could predict recovery of dysfunctional myocardium in patients with acute MI, irrespective of clinician-assessed Q-wave status in the 12-lead ECG, EF, or peak CK-MBm. The best variables and best recording sites differed depending on MI location. The best variable at predicting LAD-related LV dysfunction was the 1st QRSint on the left side at, or above V3 to V6. The 1st QRSint performed well also at predicting recovery from RCA-related LV dysfunction, with the best recording site on the upper sternum. No other QRS integrals were useful, except for the 4th QRSint that seemed to predict recovery from LCX-related LV dysfunction on the posterior left side. Regarding repolarization, variables containing the ST segment performed best, the STT area being the only variable capable of assessing viability irrespective of MI location. Repolarization variables predicted recovery of RCA- and LCX-related LV dysfunction better than did QRS variables. The best recording

site for predicting RCA-related LV dysfunction was the right upper back and the region including the upper sternum and the right clavicle; the best recording site for predicting recovery from LCX-related dysfunction was on the left side around V6 and V7. At these optimal recording locations, the best repolarization variables in patients recovering resembled those in healthy controls more than did the variables in patients not recovering. The repolarization variables were also good predictors of LAD-related LV dysfunction, although not as strong as was the 1st QRSint, with their best recording site on the left upper back and neck.

Of all BSPM variables, only the 1st QRSint was a good estimator of both final infarct percentage and viability in acute MI: Patients with a computed Q wave had a larger infarct and less viable myocardium. The ST-segment variables that predicted recovery of LV function showed only weak correlations with infarct percentage in the acute phase. This could indicate that within 48 hours after onset of chest pain, in patients reperfused for acute MI, the ST changes reflect the size of stunned myocardium more than of final MI size. In the acute phase, ST-segment variables correlated fairly well with peak CK-MBm, but poorly with final infarction percentage by DE-CMR—another indication that the ST segment reflects the size of viable, but dysfunctional myocardium early after reperfusion.

6.2 Findings in the context of previous studies

6.2.1 Evaluation of myocardial ischemic injury

Established imaging techniques for direct quantification of MI size and assessment of myocardial viability are DE-CMR, SPECT, and PET. These techniques have served as a reference in validation studies of indirect methods of estimating MI size such as echocardiography, electrocardiography, and biomarkers. In the studies for this thesis, DE-CMR was the golden standard for determining segmental infarct transmurality and global MI size. DE-CMR has proved very sensitive and specific in quantifying infarct scar, capable of detecting even very small infarct lesions of 1 gram (Wu et al. 2001a). Transmural extent of infarct correlates with myocardial contraction, and predicts recovery of ischemic, dysfunctional myocardium with revascularization: Contraction in segments with infarct transmurality > 75% does not recover, whereas the probability of recovery is possible with less severe infarct damage, and most probable if the infarct transmurality is < 25% (Choi et al. 2001, Gerber et al. 2002).

In Study IV, infarction injury was also assessed by peak CK-MBm release. CK-MBm reflects the size of the ischemic region at risk. After timely reperfusion, CK-MBm release is higher and more rapid, and it reflects the amount of myocardium salvaged in addition to the amount of myocardium lost (Ong et al. 1983, Tamaki et al. 1983, Hedstrom et al. 2007). In Study IV, the timing of CK-BMm measurements

was not strictly prespecified with regards to the onset of chest pain or reperfusion; even so, the routine measurements yielded a good correlation between peak CK-MBm and final infarction percentage, r = 0.65, which falls within the range seen in other studies.

6.2.2 Echocardiographic assessment of infarct size and myocardial viability

Myocardial contraction has been assessed by echocardiography since the 1970's. Experimental, as well as clinical autopsy- and DE-CMR studies have shown that the extent and severity of contraction abnormality by two-dimensional echocardiography strongly correlates with segmental and global LV infarct size during and after infarction healing (Weiss et al. 1981, Shen et al. 1991, Gjesdal et al. 2008, Sjoli et al. 2009). In the acute phase of infarction, infarct-related contraction abnormalities appear alongside contraction abnormalities that are due to potentially reversible causes, such as acute ischemia, stunning, and hibernation. Thus, contraction abnormalities in the early acute phase may overestimate MI size (Wyatt et al. 1981, Nieminen et al. 1982). Recovery of segmental contraction abnormalities after acute MI is determined by transmural extent of MI. Segments with a transmural extent < 50% most probably recover. In patients with prior MI, all segments with visible contraction within the weeks before death had subendocardial, or no infarction at autopsy (Weiss et al. 1981, Shen et al. 1991). In chronic MI, such non-transmural infarcts may go unnoticed, as the segments may be normokinetic (Mahrholdt et al. 2003). Early after thrombolysis, and later, visual WMS was able to differentiate between transmural and non-transmural infarctions. In chronic MI, the WMS index and EF could separate large infarctions from medium-sized ones, but not medium from small infarctions (Gjesdal et al. 2008, Sjoli et al. 2009, Thorstensen et al. 2012).

MI size and extent by strain rate imaging

Strain- and strain rate imaging has previously been validated mostly for detection of acute ischemia and presence of an infarct. Studies I and II showed that estimates of transmural extent of MI, as well as global MI size, are also possible by strain rate imaging. In acute MI, the correlation with final MI size was less close than in chronic MI, a finding which could be expected. The correlation between global strain and infarct percentage in chronic MI (r = 0.74) was equal to that in one study (Sachdev et al. 2006), but lower in acute MI (r = 0.54) than also reported (Vartdal et al. 2007). In chronic MI, segmental systolic strain values decreased with increasing extent of infarct transmurality. These findings are concordant with experimental and clinical studies showing a similar association between systolic strain- and strain-rate values and transmurality (Derumeaux et al. 2001, Weidemann et al. 2003, Zhang et al. 2005, Weidemann et al. 2006b, Vartdal et al. 2007). In accordance with these studies, systolic strain values could differentiate between segments with

transmural infarct and those with non-transmural or no infarct, but systolic strain values could not differ segments without infarct from those with non-transmural infarct. This was in contrast to findings further suggesting strain rate imaging to be more sensitive than WMS in this regard (Zhang et al. 2005, Weidemann et al. 2006b, Vartdal et al. 2007).

Viability by strain rate imaging in acute MI

In acute MI, recovery of contraction in acutely non-contractile segments was predictable by strain- and strain-rate values (Study II). Interestingly, post-systolic strain had the highest predictive accuracy. In experimental studies, post-systolic strain has been a marker of viability and active contraction, present in myocardial segments with < 70% infarct transmurality. The absence of post-systolic strain is due to decreased tissue compliance in transmurally infarcted myocardium (Pislaru et al. 2004a, Lyseggen et al. 2005, Skulstad et al. 2006b). Viability has not been earlier assessed in a way similar to that in our Study II, but our results receive support from clinical studies showing that soon after reperfusion for acute MI, systolic strain- and strain-rate variables can distinguish segments without transmural infarct, these being presumably viable (Zhang et al. 2005, Weidemann et al. 2006b, Vartdal et al. 2007). Our Study II results were recently reproduced in a study using two-dimensional speckle-tracking echocardiography[1]; in patients with acute MI, systolic strain, systolic strain rate, and post-systolic strain each predicted recovery of severely dysfunctional segments (Park et al. 2013). Other recent speckle-tracking studies, as well, have shown an association between strain variables and viability (Lipiec et al. 2011, Cimino et al. 2013, Altiok et al. 2014, Rost et al. 2014).

6.2.3 Electrocardiographic assessment of MI size and viability

Recommendations for diagnosis of MI based on QRS-, ST-, and T-wave changes in the conventional 12-lead ECG appeared in the first WHO report on the definition of MI in 1959 (Groen et al.). BSPM studies in the 1970's and later have found that recording ECG outside the standard 12 leads improves the diagnostic accuracy for MI (Menown et al. 2001, Vesterinen 2007). The extent and magnitude of ST elevation and of Q-, and R waves on the thoracic surface have correlated with MI location and MI size. Especially departure maps, displaying the location and extent of pathologic values exceeding normal values by 2 SD, have shown strong correlations with MI size. In those studies, the computed QRS- and QRST integrals performed even better than did the Q wave (Tonooka et al. 1983b, Kubota et al. 1985, Hayashi

1 Speckle-tracking echocardiography measures myocardial strain and strain rate by tracking acoustic markers in the myocardium.

et al. 1993). Recent studies have found computed BSPM variables to outperform the Q wave in diagnosis of prior MI, irrespective of MI location (Vesterinen et al. 2008a, 2008b). Studies III and IV were, to our knowledge, the first to report on the performance of a variety of computed single-lead BSPM variables in assessment of MI size at different stages of infarction, and in prediction of recovery of LV function in patients with acute MI.

Depolarization variables

The classical Q wave (width ≥ 20–30 ms and depth ≥ 1 mm) in standard 12-lead ECG is clinically the most important marker of infarct scar, and interestingly, the computed Q wave showed itself to be the best BSPM variable of all in assessment of MI size and viability. The computed Q wave was already strongly correlated with MI size within 48 hours of the acute event; these correlations grew even stronger during the healing phase, and were strongest after complete infarction healing. The slightly stronger correlations noted after the acute phase may have been connected with Q waves appearing later in some patients (Kleiger et al. 1990). Acute Q waves can also result from electrocardiographic stunning, and may not always reflect irreversible damage (Birnbaum & Ware 2005, Isobe et al. 2006).

In patients with acute MI, the 1st QRSint predicted recovery from LAD- and RCA-related dysfunction with good accuracy, although the proportion of patients with clinical QMI in the recovery and the non-recovery groups did not differ. Other studies also have indicated that Q waves do not necessarily exclude viability, as Q waves are more closely related to total MI size and extent of subendocardial MI than they are to the segmental transmurality of MI (Moon et al. 2004, Kaandorp et al. 2005, Engblom et al. 2007). Recovery of LV dysfunction after thrombolysis was, however, greater in the absence of Q waves (Isselbacher et al. 1996, Lancellotti et al. 2001). That the 1st QRSint would perform better than the clinical Q wave may be due to the computed Q wave's being more sensitive, and also be because the best recording site for assessing viability in RCA territory was on the upper sternum, clearly outside the standard ECG leads. The 4th QRSint was better than the 1st QRSint at predicting recovery from LCX-related LV dysfunction. This is in accordance with the finding that posterolateral MIs cause changes in the terminal part of the QRS (Pahlm et al. 1998).

In addition to the computed Q wave, the computed R wave and the QRSint also showed strong correlations with final MI size at all stages of the infarction, from acute to chronic. Correlations of the computed QRS variables were of a magnitude similar to magnitudes observed for the Selvester QRS score, the best-validated ECG score for assessing MI size. The computed QRS variables already performed well in the acute phase, while the Selvester QRS score has been validated mainly in the subacute phase and later (Engblom et al. 2005a, Geerse et al. 2009, Welinder et al. 2009, Knippenberg et al. 2010, Carlsen et al. 2012). Correlation of Selvester QRS score with MI size varied with MI location, being highest in anterior MI, and lowest

in multiple MI (Pahlm et al. 1998, De Sutter et al. 1999, Engblom et al. 2005a). In contrast, computed QRS variables reflected MI size in an unselected group of patients with differing MI locations, the best recording sites being on the left side around standard leads V3 to V6, and on the right upper back. This may indicate that computed QRS variables can assess MI size irrespective of MI location from these two sites. However, on the basis of these results, it is impossible to say how the computed QRS variables perform with regards to individual MI locations.

Repolarization variables

In acute MI, the repolarization variables predicted recovery of LV dysfunction with good accuracy, irrespective of MI location. Studies have found that the greater the maximal residual ST deviation (elevation or depression) 1 to 24 hours after reperfusion for STEMI, the larger the MI size, the smaller the EF, and the worse the prognosis (McLaughlin et al. 2004, Brodie et al. 2005, De Luca et al. 2008, Hallen et al. 2010). Residual ST elevation indicates severe microvascular damage, associated with adverse LV remodeling (Nijveldt et al. 2009, Weaver et al. 2011). In NSTEMI, deeper ST depression implies worse prognosis (Schechtman et al. 1989, Cannon et al. 1997, Kaul et al. 2001, Savonitto et al. 2005, Yan et al. 2010). After reperfusion for STEMI, negative T waves indicate successful reperfusion and smaller MI size; positive T waves remaining high are associated with larger MI size and smaller EF (Matetzky et al. 1994, Corbalan et al. 1999, Sorensen et al. 2009). In accordance with those observations, in our Study III, the ST segment was lower and the T wave smaller in patients with recovery from LAD-related LV dysfunction than in patients without. However, the best recording site was on the left upper back, showing negative STT values in both patient groups, equal to those in healthy controls.

Despite their good performance in assessing viability, the acute-phase repolarization variables showed only weak or moderate correlations with final MI size. Correlations with T-wave variables improved with time, whereas correlations with ST-segment variables remained weak. Others' studies have shown that after the acute event, patients with a larger MI have T waves remaining low or negative, whereas in patients with a small MI, during recovery, negative T waves turn positive, and positive T waves increase in amplitude. In chronic MI, a negative T wave indicates transmural infarct (Maeda et al. 1996, Bosimini et al. 2000, Sakata et al. 2001, Lancellotti et al. 2002). However, in most patients, the ST segment gradually returns to normal. In Study IV, the poor correlation of repolarization variables with MI size acutely may be due to pooling patients with multiple MI locations. An additional explanation is the dynamic nature of repolarization variables in the early acute phase, because the timing of measurement could differ by 24 hours. QRS variables are more stable throughout the infarction process, and probably therefore performed better than the repolarization variables.

6.3 Clinical implications

In patients with acute and chronic MI, infarct scar size correlates with LV function, and is an important prognostic marker. Patients with a large MI are at risk for developing severe arrhythmias and heart failure, and need to be closely followed up to optimize therapy. In patients with dysfunctional myocardium after infarction, viability assessment may help in deciding upon the need for revascularization.

This thesis shows that in acute as well as chronic MI, strain rate imaging and BSPM can be helpful in assessing MI size and myocardial viability. These echocardiographic and electrocardiographic techniques are easily available and possible to perform at bedside at any time. Validated imaging methods for defining the extent of infarct scar, ones such as DE-CMR, are not widely available and in general, in acute cases cannot be performed.

Strain rate imaging measures regional myocardial contraction. In comparison with traditional wall-motion assessment by echocardiography, strain rate imaging is objective, quantitative, and more sensitive. Contraction abnormalities are not always easy to discern by eye, but strain rate imaging can help determine the degree of abnormal contraction. Strain rate imaging was feasible and reproducible also in the studies for this thesis. Here, strain mapping was validated as a semi-quantitative method for estimating myocardial systolic strain. Strain mapping can quickly scan for contraction abnormalities. In patients with chronic MI, severely reduced systolic strain found by strain mapping can identify segments with transmural infarct, similar to quantitative strain. Segments with normal, or only slightly impaired strain, are viable, and most probably have no infarct, or a non-transmural one. In acute MI, strain rate imaging can discern viable myocardium and predict functional recovery of non-contracting segments. In both acute and chronic MI, global systolic strain correlates with global MI size. This study shows that strain rate imaging is possible in most of the segments (80%), even though poor visibility is a problem, as it is for echocardiography in general.

The BSPM studies for this thesis show that automatically computed ECG variables can estimate MI size at all stages of MI: in acute MI after reperfusion, as well as during and after healing of the infarction. In patients with acute MI, computed ECG variables can predict functional recovery of the LV. The BSPM studies found that MI size is best assessed from the region around standard ECG leads V3 to V5, and the right upper back. The optimal site for assessing myocardial viability depends on the region of LV dysfunction: Recovery from LAD- and LCX-related LV dysfunction is best assessed from the region around standard leads V4 to V6, whereas recovery from RCA-related LV dysfunction should be assessed from the upper sternum or the right upper back. Thus, assessment of MI size and viability is possible by placing only a few supplementary ECG leads outside the standard chest leads, and would be feasible even in clinical practice.

Both strain rate imaging and computed analysis of electrocardiography seem to be promising tools to aid the clinician in assessing the degree of permanent infarction damage in patients with MI.

7 CONCLUSIONS

1. Regional myocardial systolic strain can be estimated in a semi-quantitative manner from color-coded two-dimensional images by tissue Doppler imaging, a method we call strain mapping.

2. Systolic strain can assess segmental and global infarct size. Systolic strain values obtained quantitatively, or by strain mapping, reflect the transmural extent of segmental infarct scar in chronic MI, and can differentiate transmural from non-transmural MI. Global systolic strain shows good correlation with global MI size in chronic as well as in acute MI.

3. Strain rate imaging can predict recovery of segmental and global LV dysfunction in acute MI. Acutely measured strain- and strain-rate values correlate with final segmental and global strain after healing of the infarction, and can differentiate between viable and non-viable non-contractile segments. Systolic and post-systolic strain, and systolic strain rate perform the best.

4. Computed ECG variables by BSPM in acute MI can predict recovery of LV dysfunction. Repolarization variables perform well irrespective of MI location. Only in LAD-related MI is the 1st QRSint the best variable of all. The best recording location for predicting LAD- and LCX-associated LV dysfunction was around standard ECG leads V4 to V6. For predicting RCA-associated LV dysfunction, the best recording location was on the upper sternum and the right upper back, outside the standard chest leads.

5. BSPM can estimate MI size at all stages of the infarction. Depolarization- as well as repolarization variables computed by BSPM show good correlations with MI size in chronic MI. Depolarization variables perform well even in the acute phase of MI; repolarization variables do not. Both depolarization- and repolarization variables show good correlations with final MI size in the healing phase of infarction. At all time-points, Q- and R-wave variables, and QRSint, perform best of all. Q-wave variables showed their highest correlations with MI size on the right upper back; the R-wave variables and the QRSint performed the best around standard ECG leads V3 to V5.

ACKNOWLEDGEMENTS

These studies were carried out from 2005 to 2014 in the Division of Cardiology and the BioMag Laboratory of Helsinki University Central Hospital, as part of the ISKE project in collaboration with the Department of Biomedical Engineering and Computational Science at the Helsinki University of Technology (now Aalto University).

My warmest gratitude goes to Professor Markku Nieminen, head of the Heart and Lung Center, for his encouraging attitude toward and interest in this thesis. I highly esteem his pioneering research in echocardiography and feel proud to have continued with the same theme. I extend my gratitude to Professor Markku Kupari, head of the Division of Cardiology, whom I greatly admire for his clinical excellence; his opinion was decisive for my choice of subject.

I am greatly indebted to Professor Jyrki Mäkelä and Docent Juha Montonen for placing the top modern research facilities at the BioMag laboratory at my disposal and for their warm support; and Professor Risto Ilmoniemi, Head of the Department of Biomedical Engineering and Computational Science, Aalto University, for supporting the ISKE project.

My deepest appreciation goes to Professor Lauri Toivonen, who took me under his wing and provided me with a thesis project. I have had the privilege of enjoying his brilliance during our many scientific discussions. His expertise in electrocardiology and his friendly support have been crucial.

I extend my deepest gratitude to Docent Mika Laine, my other supervisor, whose know-how and inspiring guidance were vital. I thank Mika for his company on our exciting trip to London to learn about strain rate imaging, then an unknown method in Finland. His outstanding ideas and clear views were central for presenting the advantages of this new method.

Heartfelt thanks go to Professor Sutherland for his breathtaking lecture providing me with my subject, and for inviting me to his echocardiography department in London to learn the essence of strain rate imaging. I'm very honoured that he accepted to be my opponent.

My sincere appreciation and admiration go to Docents Marja Hedman and Kjell Nikus for their amazingly rapid review of this thesis, their smart criticism, and expert advice; and to Carolyn Norris for professional language editing, truly linguistic virtuosity; I thank her also for her excellent and inspiring courses, and for being a sincere friend.

I warmly thank all my co-authors for their invaluable contribution to this thesis: my colleagues Helena Hänninen and Paula Vesterinen for sharing their expertise of the BSPM method, Helena for introducing me to my supervisor and for her expert

advice and commitment throughout the project, Paula for the great effort she made to get the ISKE project started and for recruitment and investigation of the patients as my predecessor in the project; my collaborators at the Helsinki University of Technology, Teijo Konttila for his meticulous calculations of BSPM data and his fantastic illustrations, Mats Lindholm for operating the BSPM recording device and software and his thorough pre-processing of BSPM data, Heikki Väänänen for the ingenious software he developed for BSPM analysis and which he helped us use, Matti Stenroos for his intelligent statistical and illustrating tools for BSPM data; my radiologist colleagues Margareta Antila, Sari Kivistö, and Kirsi Lauerma for extremely well-performed cardiac magnetic resonance imaging and skilled interpretation. I immensely appreciate the many inspiring scientific discussions with all my co-authors and their valuable comments.

I thank Docents Markku Mäkijärvi, Lasse Oikarinen, and Petri Korhonen, as well as Ilkka Tierala for their valuable pathfinding work preceding the ISKE project. I am also grateful to Ilkka and his staff at the Coronary Care Unit of Meilahti Hospital for essential help during patient recruitment. All study patients and volunteers earn my greatest thanks for their engagement, which was crucial for the entire project.

My sincere gratitude goes to study nurses Suvi Heikkilä and Hanna Ranne for their indispensable assistance with patients' BSPM recordings; physicist Markku Ventilä for sharing his valuable know-how on ultrasound technology, Leena Missonen for excellent library services, Tiina Heino, Eeva-Liisa Aatola, and Katri Larmo at Terkko, for valuable help with informatics; photographer Juhani Lassander for help with image- and abstract preparation ; Pirjo Kari, Lea Enjala, Anneli Keskinen, and Anna-Maija Rosnell, all very friendly and helpful secretaries.

I am immensely grateful to the many colleagues who helped me gather a solid base of knowledge and to mature as a clinician during my route towards a speciality in internal medicine and cardiology: Kristofer von Alfthan for inviting me to start my career at the health-care center in Kristiinankaupunki and for sharing with me his vast experience. Kristofer and his wife Sole, to whom I have close family ties, cared for me and made me feel very welcome during my precious time in Kristiinankaupunki; Vilho Tuunanen, then chief physician at the adjacent Selkämeri Hospital, for teaching me echocardiography and for being a role model as a great clinician; Docent Jouko Karjalainen at Tilkka Hospital for my short but unforgettable experience as a military doctor; Docent Risto Kala for employing me as a resident at Maria hospital, the special and positive atmosphere of which he was much to thank for; Docent Matti Mänttäri for his valuable teaching of clinical cardiology at Maria and Jorvi Hospitals; Professors Kimmo Kontula and Reijo Tilvis, and Docent Juhani Kahri, my superiors guiding my fellowship in internal medicine at Meilahti Hospital; Janne Rapola, a talented cardiologist, for tutoring me in echocardiography; Docent Jyri Lommi for arranging my research leave when needed; Docent Matti Viitasalo, chief of the Cardiac Outpatient Clinic at Meilahti Hospital where I felt most comfortable making an endless amount of echocardiographies. May he represent all

senior cardiologists who have been so willing to instruct a novice, regardless of their many other responsibilities; Professor Tom Pettersson for his support throughout the years starting in medical school, and for the possibility to teach medical students in cardiology; and Professor Herman Adlercreutz for introducing me to research work at his internationally recognized biochemistry lab when writing my pro gradu.

My warmest thanks to my good friends and colleagues Alla, Hanna, Iina, Markareetta, and Pirjo, the Maria gang, for their cheerful company on our fine dinners and relaxing trips, helping me revive my brain, for which the Lady Cardiologists' Club and the Cardiologist Golfers also deserve thanks; all my colleagues to whom I owe my enjoyment in going to work; my colleague Mika Lehto together with my other research fellows at BioMag (Pantelis et al.) for the welcoming ambiance.

My deepest gratitude to late Professor Börje Kuhlbäck who shared my passion for classical music and accompanied my singing on the piano; my late grandmother Margareta for eternal love, my devoted parents, Karin and Jouko, for encouraging my creativeness and faith in myself; and Mikko, my loving fiancé, for bringing joy to my life.

This work was supported by grants from Helsinki University Central Hospital Research Funds (EVO grant), the Finnish Foundation for Cardiovascular Research, the Finnish Funding Agency for Technology and Innovation (TEKES), the Finnish Medical Society Duodecim, Finska Läkaresällskapet, the Waldemar von Frenckell Foundation, the Instrumentarium Foundation, the Aarne Koskelo Foundation, the Medicine Fund of Helsinki University, the Wilhelm and Else Stockmann Foundation, and the Aarne and Aili Turunen Foundation to all of whom I am sincerely grateful.

Helsinki, June 2014

Minna Kylmälä

REFERENCES

Adler, Y., Zafrir, N., Ben-Gal, T., Lulu, O.B., Maynard, C., Sclarovsky, S., Balicer, R., Mager, A., Strasberg, B., Solodky, A., Wagner, G.S. & Birnbaum, Y. 2000, "Relation between evolutionary ST segment and T-wave direction and electrocardiographic prediction of mycardial infarct size and left ventricular function among patients with anterior wall Q-wave acute myocardial infarction who received reperfusion therapy.", *American Journal of Cardiology,* vol. 85, no. 8, pp. 927-933.

Aguirre, F.V., Younis, L.T., Chaitman, B.R., Ross, A.M., McMahon, R.P., Kern, M.J., Berger, P.B., Sopko, G., Rogers, W.J. & Shaw, L. 1995, "Early and 1-year clinical outcome of patients' evolving non-Q-wave versus Q-wave myocardial infarction after thrombolysis. Results from The TIMI II Study.", *Circulation,* vol. 91, no. 10, pp. 2541-2548.

Alexander, J.H., Harrington, R.A., Bhapkar, M., Mahaffey, K.W., Lincoff, A.M., Ohman, E.M., Klootwijk, P., Pahlm, O., Henden, B., Deckers, J.W., Simoons, M.L., Califf, R.M. & Wagner, G.S. 2003, "Prognostic importance of new small Q waves following non-ST-elevation acute coronary syndromes.", *American Journal of Medicine,* vol. 115, no. 8, pp. 613-619.

Allman, K.C. 2013, "Noninvasive assessment myocardial viability: current status and future directions", *Journal of Nuclear Cardiology,* vol. 20, no. 4, pp. 618-637.

Allman, K.C., Shaw, L.J., Hachamovitch, R. & Udelson, J.E. 2002a, "Myocardial viability testing and impact of revascularization on prognosis in patients with coronary artery disease and left ventricular dysfunction: a meta-analysis.", *Journal of the American College of Cardiology,* vol. 39, no. 7, pp. 1151-1158.

Allman, K.C., Shaw, L.J., Hachamovitch, R. & Udelson, J.E. 2002b, "Myocardial viability testing and impact of revascularization on prognosis in patients with coronary artery disease and left ventricular dysfunction: a meta-analysis.", *Journal of the American College of Cardiology,* vol. 39, no. 7, pp. 1151-1158.

Alpert, J.S., Thygesen, K., Antman, E. & Bassand, J.P. 2000, "Myocardial infarction redefined--a consensus document of The Joint European Society of Cardiology/American College of Cardiology Committee for the redefinition of myocardial infarction", *Journal of the American College of Cardiology,* vol. 36, no. 3, pp. 959-969.

Altiok, E., Tiemann, S., Becker, M., Koos, R., Zwicker, C., Schroeder, J., Kraemer, N., Schoth, F., Adam, D., Friedman, Z., Marx, N. & Hoffmann, R. 2014, "Myocardial deformation imaging by two-dimensional speckle-tracking echocardiography for prediction of global and segmental functional changes after acute myocardial infarction: a comparison with late gadolinium enhancement cardiac magnetic resonance.", *Journal of the American Society of Echocardiography,* vol. 27, no. 3, pp. 249-257.

Armstrong, P.W., Fu, Y., Westerhout, C.M., Hudson, M.P., Mahaffey, K.W., White, H.D., Todaro, T.G., Adams, P.X., Aylward, P.E. & Granger, C.B. 2009, "Baseline Q-wave surpasses time from symptom onset as a prognostic marker in ST-segment elevation myocardial infarction patients treated with primary percutaneous coronary intervention.", *Journal of the American College of Cardiology,* vol. 53, no. 17, pp. 1503-1509.

Awan, N.A., Miller, R.R., Vera, Z., Janzen, D.A., Amsterdam, E.A. & Mason, D.T. 1977, "Noninvasive assessment of cardiac function and ventricular dyssynergy by precordial Q wave mapping in anterior myocardial infarction.", *Circulation,* vol. 55, no. 6, pp. 833-838.

Baks, T., van Geuns, R.J., Biagini, E., Wielopolski, P., Mollet, N.R., Cademartiri, F., van der Giessen, W.J., Krestin, G.P., Serruys, P.W., Duncker, D.J. & de Feyter, P.J. 2006, "Effects of primary angioplasty for acute myocardial infarction on early and late infarct size and left ventricular wall characteristics.", *Journal of the American College of Cardiology,* vol. 47, no. 1, pp. 40-44.

Bang, L.E., Ripa, R.S., Grande, P., Kastrup, J., Clemmensen, P.M. & Wagner, G.S. 2008, "Comparison of infarct size changes with delayed contrast-enhanced magnetic resonance imaging and electrocardiogram QRS scoring during the 6 months after acutely reperfused myocardial infarction.", *Journal of electrocardiology,* vol. 41, no. 6, pp. 609-613.

Bar, F.W., Vermeer, F., de Zwaan, C., Ramentol, M., Braat, S., Simoons, M.L., Hermens, W.T., van der Laarse, A., Verheugt, F.W. & Krauss, X.H. 1987, "Value of admission electrocardiogram in predicting outcome of thrombolytic therapy in acute myocardial infarction. A randomized trial conducted by The Netherlands Interuniversity Cardiology Institute.", *American Journal of Cardiology,* vol. 59, no. 1, pp. 6-13.

Barbagelata, A., Califf, R.M., Sgarbossa, E.B., Knight, D., Mark, D.B., Granger, C.B., Armstrong, P.W., Elizari, M., Birnbaum, Y., Grinfeld, L.R., Ohman, E.M., Wagner, G.S. & GUSTO-1, I. 2004, "Prognostic value of predischarge electrocardiographic measurement of infarct size after thrombolysis: insights from GUSTO I Economics and Quality of Life substudy.", *American Heart Journal,* vol. 148, no. 5, pp. 795-802.

Barbagelata, A., Di Carli, M.F., Califf, R.M., Garg, J., Birnbaum, Y., Grinfeld, L., Gibbons, R.J., Granger, C.B., Goodman, S.G., Wagner, G.S., Mahaffey, K.W. & AMISTAD, I. 2005, "Electrocardiographic infarct size assessment after thrombolysis: insights from the Acute Myocardial Infarction STudy ADenosine (AMISTAD) trial.", *American Heart Journal,* vol. 150, no. 4, pp. 659-665.

Bax, J.J., Poldermans, D., Elhendy, A., Boersma, E. & van der Wall, E.E. 2005, "Assessment of myocardial viability by nuclear imaging techniques.", *Current cardiology reports,* vol. 7, no. 2, pp. 124-129.

Bax, J.J., Visser, F.C., Poldermans, D., Elhendy, A., Cornel, J.H., Boersma, E., Valkema, R., Van Lingen, A., Fioretti, P.M. & Visser, C.A. 2001, "Relationship between preoperative viability and postoperative improvement in LVEF and heart failure symptoms.", *Journal of Nuclear Medicine,* vol. 42, no. 1, pp. 79-86.

Beanlands, R.S., Nichol, G., Huszti, E., Humen, D., Racine, N., Freeman, M., Gulenchyn, K.Y., Garrard, L., deKemp, R., Guo, A., Ruddy, T.D., Benard, F., Lamy, A., Iwanochko, R.M. & PARR-2, I. 2007, "F-18-fluorodeoxyglucose positron emission tomography imaging-assisted management of patients with severe left ventricular dysfunction and suspected coronary disease: a randomized, controlled trial (PARR-2).", *Journal of the American College of Cardiology,* vol. 50, no. 20, pp. 2002-2012.

Beller, G.A. 2000, "Noninvasive assessment of myocardial viability.", *New England Journal of Medicine,* vol. 343, no. 20, pp. 1488-1490.

Beller, G.A. & Heede, R.C. 2011, "SPECT imaging for detecting coronary artery disease and determining prognosis by noninvasive assessment of myocardial perfusion and myocardial viability", *Journal of Cardiovascular Translational Research,* vol. 4, no. 4, pp. 416-424.

Beller, G.A., Hood, W.B.,Jr & Smith, T.W. 1977, "Effects of ischaemia and coronary reperfusion on regional myocardial blood flow and on the epicardial electrogram.", *Cardiovascular research,* vol. 11, no. 6, pp. 489-498.

Bello, D., Einhorn, A., Kaushal, R., Kenchaiah, S., Raney, A., Fieno, D., Narula, J., Goldberger, J., Shivkumar, K., Subacius, H. & Kadish, A. 2011, "Cardiac magnetic resonance imaging: infarct size is an independent predictor of mortality in patients with coronary artery disease.", *Magnetic resonance imaging,* vol. 29, no. 1, pp. 50-56.

Bengel, F.M., Higuchi, T., Javadi, M.S. & Lautamaki, R. 2009, "Cardiac positron emission tomography", *Journal of the American College of Cardiology,* vol. 54, no. 1, pp. 1-15.

Bijnens, B. & Sutherland, G.R. 2008, "Myocardial oedema: a forgotten entity essential to the understanding of regional function after ischaemia or reperfusion injury.", *Heart,* vol. 94, no. 9, pp. 1117-1119.

Birnbaum, Y. & Drew, B.J. 2003, "The electrocardiogram in ST elevation acute myocardial infarction: correlation with coronary anatomy and prognosis", *Postgraduate medical journal,* vol. 79, no. 935, pp. 490-504.

Birnbaum, Y. & Ware, D.L. 2005, "Electrocardiogram of acute ST-elevation myocardial infarction: the significance of the various "scores".", *Journal of electrocardiology,* vol. 38, no. 2, pp. 113-118.

Bodi, V., Sanchis, J., Guillem, M.S., Nunez, J., Lopez-Lereu, M.P., Gomez, C., Moratal, D., Chorro, F.J., Millet, J. & Llacer, A. 2006, "Analysis of the extension of Q-waves after infarction with body surface map: relationship with infarct size.", *International journal of cardiology,* vol. 111, no. 3, pp. 399-404.

Boersma, E., Maas, A.C., Deckers, J.W. & Simoons, M.L. 1996, "Early thrombolytic treatment in acute myocardial infarction: reappraisal of the golden hour.", *Lancet,* vol. 348, no. 9030, pp. 771-775.

Boersma, E., Primary Coronary Angioplasty, v. & Thrombolysis, G. 2006, "Does time matter? A pooled analysis of randomized clinical trials comparing primary percutaneous coronary intervention and in-hospital fibrinolysis in acute myocardial infarction patients.", *European heart journal,* vol. 27, no. 7, pp. 779-788.

Bosimini, E., Giannuzzi, P., Temporelli, P.L., Gentile, F., Lucci, D., Maggioni, A.P., Tavazzi, L., Badano, L., Stoian, I., Piazza, R., Heyman, I., Levantesi, G., Cervesato, E., Geraci, E. & Nicolosi, G.L. 2000, "Electrocardiographic evolutionary changes and left ventricular remodeling after acute myocardial infarction: results of the GISSI-3 Echo substudy.", *Journal of the American College of Cardiology,* vol. 35, no. 1, pp. 127-135.

Bounous, E.P.,Jr, Califf, R.M., Harrell, F.E.,Jr, Hinohara, T., Mark, D.B., Ideker, R.E., Selvester, R.H. & Wagner, G.S. 1988, "Prognostic value of the simplified Selvester QRS score in patients with coronary artery disease.", *Journal of the American College of Cardiology,* vol. 11, no. 1, pp. 35-41.

Bourdillon, P.D., Broderick, T.M., Williams, E.S., Davis, C., Dillon, J.C., Armstrong, W.F., Fineberg, N., Ryan, T. & Feigenbaum, H. 1989, "Early recovery of regional left ventricular function

after reperfusion in acute myocardial infarction assessed by serial two-dimensional echocardiography.", *American Journal of Cardiology,* vol. 63, no. 11, pp. 641-646.

Brodie, B.R., Stuckey, T.D., Hansen, C., VerSteeg, D.S., Muncy, D.B., Moore, S., Gupta, N. & Downey, W.E. 2005, "Relation between electrocardiographic ST-segment resolution and early and late outcomes after primary percutaneous coronary intervention for acute myocardial infarction.", *American Journal of Cardiology,* vol. 95, no. 3, pp. 343-348.

Bush, L.R., Buja, L.M., Samowitz, W., Rude, R.E., Wathen, M., Tilton, G.D. & Willerson, J.T. 1983, "Recovery of left ventricular segmental function after long-term reperfusion following temporary coronary occlusion in conscious dogs. Comparison of 2- and 4-hour occlusions.", *Circulation research,* vol. 53, no. 2, pp. 248-263.

Byrne, R.A., Ndrepepa, G., Braun, S., Tiroch, K., Mehilli, J., Schulz, S., Schomig, A. & Kastrati, A. 2010, "Peak cardiac troponin-T level, scintigraphic myocardial infarct size and one-year prognosis in patients undergoing primary percutaneous coronary intervention for acute myocardial infarction.", *American Journal of Cardiology,* vol. 106, no. 9, pp. 1212-1217.

Cahyadi, Y.H., Murakami, E., Takekoshi, N., Matsui, S., Fujita, S., Tsugawa, H., Miyamoto, M., Maeda, T. & Miyagawa, S. 1989, "Body surface potential mapping in anterior myocardial infarction--a longitudinal study in acute, convalescent and chronic phases.", *Japanese circulation journal,* vol. 53, no. 3, pp. 206-212.

Cannon, C.P., McCabe, C.H., Stone, P.H., Rogers, W.J., Schactman, M., Thompson, B.W., Pearce, D.J., Diver, D.J., Kells, C., Feldman, T., Williams, M., Gibson, R.S., Kronenberg, M.W., Ganz, L.I., Anderson, H.V. & Braunwald, E. 1997, "The electrocardiogram predicts one-year outcome of patients with unstable angina and non-Q wave myocardial infarction: results of the TIMI III Registry ECG Ancillary Study. Thrombolysis in Myocardial Ischemia.", *Journal of the American College of Cardiology,* vol. 30, no. 1, pp. 133-140.

Canty, J.M.,Jr & Fallavollita, J.A. 2005, "Hibernating myocardium", *Journal of Nuclear Cardiology,* vol. 12, no. 1, pp. 104-119.

Carlsen, E.A., Bang, L.E., Ahtarovski, K.A., Engstrom, T., Kober, L., Kelbaek, H., Vejlstrup, N., Jorgensen, E., Helqvist, S., Saunamaki, K., Clemmensen, P., Holmvang, L., Wagner, G.S. & Lonborg, J. 2012, "Comparison of Selvester QRS score with magnetic resonance imaging measured infarct size in patients with ST elevation myocardial infarction.", *Journal of electrocardiology,* vol. 45, no. 4, pp. 414-419.

Cerqueira, M.D., Weissman, N.J., Dilsizian, V., Jacobs, A.K., Kaul, S., Laskey, W.K., Pennell, D.J., Rumberger, J.A., Ryan, T., Verani, M.S. & American Heart Association Writing Group on Myocardial Segmentation and Registration for Cardiac,Imaging 2002, "Standardized myocardial segmentation and nomenclature for tomographic imaging of the heart: a statement for healthcare professionals from the Cardiac Imaging Committee of the Council on Clinical Cardiology of the American Heart Association", *Circulation,* vol. 105, no. 4, pp. 539-542.

Chan, M.Y., Sun, J.L., Newby, L.K., Shaw, L.K., Lin, M., Peterson, E.D., Califf, R.M., Kong, D.F. & Roe, M.T. 2009, "Long-term mortality of patients undergoing cardiac catheterization for ST-elevation and non-ST-elevation myocardial infarction", *Circulation,* vol. 119, no. 24, pp. 3110-3117.

Cheitlin, M.D., Armstrong, W.F., Aurigemma, G.P., Beller, G.A., Bierman, F.Z., Davis, J.L., Douglas, P.S., Faxon, D.P., Gillam, L.D., Kimball, T.R., Kussmaul, W.G., Pearlman, A.S., Philbrick,

J.T., Rakowski, H., Thys, D.M., Antman, E.M., Smith, S.C.,Jr, Alpert, J.S., Gregoratos, G., Anderson, J.L., Hiratzka, L.F., Hunt, S.A., Fuster, V., Jacobs, A.K., Gibbons, R.J., Russell, R.O., American College of, C., American Heart, A. & American Society of, E. 2003, "ACC/AHA/ASE 2003 guideline update for the clinical application of echocardiography: summary article: a report of the American College of Cardiology/American Heart Association Task Force on Practice Guidelines (ACC/AHA/ASE Committee to Update the 1997 Guidelines for the Clinical Application of Echocardiography).", *Circulation,* vol. 108, no. 9, pp. 1146-1162.

Chen, C., Li, L., Chen, L.L., Prada, J.V., Chen, M.H., Fallon, J.T., Weyman, A.E., Waters, D. & Gillam, L. 1995, "Incremental doses of dobutamine induce a biphasic response in dysfunctional left ventricular regions subtending coronary stenoses.", *Circulation,* vol. 92, no. 4, pp. 756-766.

Chia, S., Senatore, F., Raffel, O.C., Lee, H., Wackers, F.J. & Jang, I.K. 2008, "Utility of cardiac biomarkers in predicting infarct size, left ventricular function, and clinical outcome after primary percutaneous coronary intervention for ST-segment elevation myocardial infarction.", *Jacc: Cardiovascular Interventions,* vol. 1, no. 4, pp. 415-423.

Choi, K.M., Kim, R.J., Gubernikoff, G., Vargas, J.D., Parker, M. & Judd, R.M. 2001, "Transmural extent of acute myocardial infarction predicts long-term improvement in contractile function.", *Circulation,* vol. 104, no. 10, pp. 1101-1107.

Christian, T.F., Clements, I.P., Behrenbeck, T., Huber, K.C., Chesebro, J.H., Gersh, B.J. & Gibbons, R.J. 1991, "Limitations of the electrocardiogram in estimating infarction size after acute reperfusion therapy for myocardial infarction.", *Annals of Internal Medicine,* vol. 114, no. 4, pp. 264-270.

Cimino, S., Canali, E., Petronilli, V., Cicogna, F., De Luca, L., Francone, M., Sardella, G., Iacoboni, C. & Agati, L. 2013, "Global and regional longitudinal strain assessed by two-dimensional speckle tracking echocardiography identifies early myocardial dysfunction and transmural extent of myocardial scar in patients with acute ST elevation myocardial infarction and relatively preserved LV function.", *European heart journal cardiovascular Imaging,* vol. 14, no. 8, pp. 805-811.

Cook, R.W., Edwards, J.E. & Pruitt, R.D. 1958a, "Electrocardiographic Changes in Acute Subendocardial Infarction I. Large Subendocardial and Large Nontransmural Infarctions", *Circulation,* vol. 8, pp. 603-612.

Cook, R.W., Edwards, J.E. & Pruitt, R.D. 1958b, "Electrocardiographic Changes in Acute Subendocardial Infarction II Small Subendocardial Infarcts", *Circulation,* vol. 8, pp. 113-122.

Corbalan, R., Prieto, J.C., Chavez, E., Nazzal, C., Cumsille, F. & Krucoff, M. 1999, "Bedside markers of coronary artery patency and short-term prognosis of patients with acute myocardial infarction and thrombolysis.", *American Heart Journal,* vol. 138, no. 3 Pt 1, pp. 533-539.

Cornel, J.H., Bax, J.J., Elhendy, A., Maat, A.P., Kimman, G.J., Geleijnse, M.L., Rambaldi, R., Boersma, E. & Fioretti, P.M. 1998, "Biphasic response to dobutamine predicts improvement of global left ventricular function after surgical revascularization in patients with stable coronary artery disease: implications of time course of recovery on diagnostic accuracy.", *Journal of the American College of Cardiology,* vol. 31, no. 5, pp. 1002-1010.

Cotran, R., Kumar, V. & Robbins, S.L. 2010, "The Heart" in *Robbins and Cotran Pathologic Basis of Disease*, 8th edn, Saunders/ Elsevier, Philadelphia, PA, pp. 550-552.

Cwajg, J.M., Cwajg, E., Nagueh, S.F., He, Z.X., Qureshi, U., Olmos, L.I., Quinones, M.A., Verani, M.S., Winters, W.L. & Zoghbi, W.A. 2000, "End-diastolic wall thickness as a predictor of recovery of function in myocardial hibernation: relation to rest-redistribution T1-201 tomography and dobutamine stress echocardiography.", *Journal of the American College of Cardiology,* vol. 35, no. 5, pp. 1152-1161.

Daly, M., Finlay, D., Guldenring, D., Nugent, C., Tomlin, A., Smith, B., Adgey, A. & Harbinson, M. 2012, "Detection of acute coronary occlusion in patients with acute coronary syndromes presenting with isolated ST-segment depression.", *European Heart Journal Acute Cardiovascular Care,* vol. 1, no. 2, pp. 128-135.

De Ambroggi, L., Landolina, M., Galdangelo, F., Repetto, S., Peloso, A. & Bertoni, T. 1982, "Limits of precordial electrocardiographic mapping in assessing anterior myocardial infarction size.", *Giornale italiano di cardiologia,* vol. 12, no. 5, pp. 317-323.

De Luca, G., Suryapranata, H., Ottervanger, J.P., Hoorntje, J.C., Gosselink, A.T., Dambrink, J.H., de Boer, M.J. & van't Hof, A.W. 2008, "Postprocedural single-lead ST-segment deviation and long-term mortality in patients with ST-segment elevation myocardial infarction treated by primary angioplasty.", *Heart,* vol. 94, no. 1, pp. 44-47.

De Sutter, J., Van de Wiele, C., Gheeraert, P., De Buyzere, M., Gevaert, S., Taeymans, Y., Dierckx, R., De Backer, G. & Clement, D. 1999, "The Selvester 32-point QRS score for evaluation of myocardial infarct size after primary coronary angioplasty.", *American Journal of Cardiology,* vol. 83, no. 2, pp. 255-257.

Derumeaux, G., Loufoua, J., Pontier, G., Cribier, A. & Ovize, M. 2001, "Tissue Doppler imaging differentiates transmural from nontransmural acute myocardial infarction after reperfusion therapy", *Circulation,* vol. 103, no. 4, pp. 589-596.

Derumeaux, G., Ovize, M., Loufoua, J., Pontier, G., Andre-Fouet, X. & Cribier, A. 2000, "Assessment of nonuniformity of transmural myocardial velocities by color-coded tissue Doppler imaging: characterization of normal, ischemic, and stunned myocardium", *Circulation,* vol. 101, no. 12, pp. 1390-1395.

D'hooge, J., Heimdal, A., Jamal, F., Kukulski, T., Bijnens, B., Rademakers, F., Hatle, L., Suetens, P. & Sutherland, G.R. 2000a, "Regional strain and strain rate measurements by cardiac ultrasound: principles, implementation and limitations.[erratum appears in Eur J Echocardiogr 2000 Dec;1(4):295-9]", *European Journal of Echocardiography,* vol. 1, no. 3, pp. 154-170.

D'hooge, J., Heimdal, A., Jamal, F., Kukulski, T., Bijnens, B., Rademakers, F., Hatle, L., Suetens, P. & Sutherland, G.R. 2000b, "Regional strain and strain rate measurements by cardiac ultrasound: principles, implementation and limitations.[erratum appears in Eur J Echocardiogr 2000 Dec;1(4):295-9]", *European Journal of Echocardiography,* vol. 1, no. 3, pp. 154-170.

Di Carli, M.F. & Hachamovitch, R. 2007, "New technology for noninvasive evaluation of coronary artery disease", *Circulation,* vol. 115, no. 11, pp. 1464-1480.

Di Chiara, A., Dall'Armellina, E., Badano, L.P., Meduri, S., Pezzutto, N. & Fioretti, P.M. 2010, "Predictive value of cardiac troponin-I compared to creatine kinase-myocardial band for the assessment of infarct size as measured by cardiac magnetic resonance.", *Journal of Cardiovascular Medicine,* vol. 11, no. 8, pp. 587-592.

Dokainish, H., Rajaram, M., Prabhakaran, D., Afzal, R., Orlandini, A., Staszewsky, L., Franzosi, M.G., Llanos, J., Martinoli, E., Roy, A., Yusuf, S., Mehta, S. & Lonn, E. 2014, "Incremental Value of Left Ventricular Systolic and Diastolic Function to Determine Outcome in Patients with Acute ST-Segment Elevation Myocardial Infarction: The Echocardiographic Substudy of the OASIS-6 Trial", *Echocardiography,* vol. 31, no. 5, pp. 569-578.

Edvardsen, T., Gerber, B.L., Garot, J., Bluemke, D.A., Lima, J.A. & Smiseth, O.A. 2002, "Quantitative assessment of intrinsic regional myocardial deformation by Doppler strain rate echocardiography in humans: validation against three-dimensional tagged magnetic resonance imaging.[see comment]", *Circulation,* vol. 106, no. 1, pp. 50-56.

Edvardsen, T., Skulstad, H., Aakhus, S., Urheim, S. & Ihlen, H. 2001, "Regional myocardial systolic function during acute myocardial ischemia assessed by strain Doppler echocardiography. see comment", *Journal of the American College of Cardiology,* vol. 37, no. 3, pp. 726-730.

Eek, C., Grenne, B., Brunvand, H., Aakhus, S., Endresen, K., Smiseth, O.A., Edvardsen, T. & Skulstad, H. 2010, "Strain echocardiography predicts acute coronary occlusion in patients with non-ST-segment elevation acute coronary syndrome", *European journal of echocardiography : the journal of the Working Group on Echocardiography of the European Society of Cardiology,* .

Ellis, S.G., Henschke, C.I., Sandor, T., Wynne, J., Braunwald, E. & Kloner, R.A. 1983, "Time course of functional and biochemical recovery of myocardium salvaged by reperfusion.", *Journal of the American College of Cardiology,* vol. 1, no. 4, pp. 1047-1055.

Engblom, H., Carlsson, M.B., Hedstrom, E., Heiberg, E., Ugander, M., Wagner, G.S. & Arheden, H. 2007, "The endocardial extent of reperfused first-time myocardial infarction is more predictive of pathologic Q waves than is infarct transmurality: a magnetic resonance imaging study.", *Clinical Physiology & Functional Imaging,* vol. 27, no. 2, pp. 101-108.

Engblom, H., Hedstrom, E., Heiberg, E., Wagner, G.S., Pahlm, O. & Arheden, H. 2005a, "Size and transmural extent of first-time reperfused myocardial infarction assessed by cardiac magnetic resonance can be estimated by 12-lead electrocardiogram.", *American Heart Journal,* vol. 150, no. 5, pp. 920.

Engblom, H., Hedstrom, E., Heiberg, E., Wagner, G.S., Pahlm, O. & Arheden, H. 2005b, "Size and transmural extent of first-time reperfused myocardial infarction assessed by cardiac magnetic resonance can be estimated by 12-lead electrocardiogram.", *American Heart Journal,* vol. 150, no. 5, pp. 920.

Fieno, D.S., Kim, R.J., Chen, E.L., Lomasney, J.W., Klocke, F.J. & Judd, R.M. 2000, "Contrast-enhanced magnetic resonance imaging of myocardium at risk: distinction between reversible and irreversible injury throughout infarct healing.", *Journal of the American College of Cardiology,* vol. 36, no. 6, pp. 1985-1991.

Fieno, D.S., Thomson, L.E., Slomka, P., Abidov, A., Friedman, J.D., Germano, G. & Berman, D.S. 2007, "Quantitation of infarct size in patients with chronic coronary artery disease using rest-redistribution Tl-201 myocardial perfusion SPECT: correlation with contrast-enhanced cardiac magnetic resonance.", *Journal of Nuclear Cardiology,* vol. 14, no. 1, pp. 59-67.

Fleming, A.D., Xia, X., McDicken, W.N., Sutherland, G.R. & Fenn, L. 1994, "Myocardial velocity gradients detected by Doppler imaging.", *British Journal of Radiology,* vol. 67, no. 799, pp. 679-688.

Geerse, D.A., Wu, K.C., Gorgels, A.P., Zimmet, J., Wagner, G.S. & Miller, J.M. 2009, "Comparison between contrast-enhanced magnetic resonance imaging and Selvester QRS scoring system in estimating changes in infarct size between the acute and chronic phases of myocardial infarction.", *Annals of Noninvasive Electrocardiology,* vol. 14, no. 4, pp. 360-365.

Gerber, B.L., Garot, J., Bluemke, D.A., Wu, K.C. & Lima, J.A. 2002, "Accuracy of contrast-enhanced magnetic resonance imaging in predicting improvement of regional myocardial function in patients after acute myocardial infarction.", *Circulation,* vol. 106, no. 9, pp. 1083-1089.

Ghosh, N., Rimoldi, O.E., Beanlands, R.S. & Camici, P.G. 2010, "Assessment of myocardial ischaemia and viability: role of positron emission tomography", *European heart journal,* vol. 31, no. 24, pp. 2984-2995.

Gibbons, R.J. 2011, "Tc-99m SPECT sestamibi for the measurement of infarct size", *Journal of Cardiovascular Pharmacology & Therapeutics,* vol. 16, no. 3-4, pp. 321-331.

Gjesdal, O., Helle-Valle, T., Hopp, E., Lunde, K., Vartdal, T., Aakhus, S., Smith, H.J., Ihlen, H. & Edvardsen, T. 2008, "Noninvasive separation of large, medium, and small myocardial infarcts in survivors of reperfused ST-elevation myocardial infarction: a comprehensive tissue Doppler and speckle-tracking echocardiography study", *Circulation.Cardiovascular imaging,* vol. 1, no. 3, pp. 189-96, 2 p following 196.

Goldman, M.R., Brady, T.J., Pykett, I.L., Burt, C.T., Buonanno, F.S., Kistler, J.P., Newhouse, J.H., Hinshaw, W.S. & Pohost, G.M. 1982, "Quantification of experimental myocardial infarction using nuclear magnetic resonance imaging and paramagnetic ion contrast enhancement in excised canine hearts", *Circulation,* vol. 66, no. 5, pp. 1012-1016.

Groen, J.J. Expert Committee on Cardiovascular Diseases and Hypertension 1959, "Hypertension and coronary heart disease: Classification and criteria for epidemiological studies.", World Health Organization Technical Report Series No. 168.

Grande, P., Hindman, N.B., Saunamaki, K., Prather, J.D., Hinohara, T. & Wagner, G.S. 1987, "A comprehensive estimation of acute myocardial infarct size using enzymatic, electrocardiographic and mechanical methods.", *American Journal of Cardiology,* vol. 59, no. 15, pp. 1239-1244.

Hackel, D.B., Reimer, K.A., Ideker, R.E., Mikat, E.M., Hartwell, T.D., Parker, C.B., Braunwald, E.B., Buja, M., Gold, H.K. & Jaffe, A.S. 1984, "Comparison of enzymatic and anatomic estimates of myocardial infarct size in man.", *Circulation,* vol. 70, no. 5, pp. 824-835.

Hallen, J., Sejersten, M., Johanson, P., Atar, D. & Clemmensen, P.M. 2010, "Influence of ST-segment recovery on infarct size and ejection fraction in patients with ST-segment elevation myocardial infarction receiving primary percutaneous coronary intervention.", *American Journal of Cardiology,* vol. 105, no. 9, pp. 1223-1228.

Hayashi, H., Hirai, M., Suzuki, A., Ichihara, Y., Adachi, M., Kondo, K., Takatsu, F. & Saito, H. 1993, "Correlation between various parameters derived from body surface maps and ejection fraction in patients with anterior myocardial infarction.", *Journal of electrocardiology,* vol. 26, no. 1, pp. 17-24.

Hayashi, H., Watanabe, Y., Ishikawa, T., Wada, M., Uematsu, H. & Inagaki, H. 1980, "Diagnostic value of body surface map in myocardial infarction: assessment of location, size and ejection fraction as compared with coronary cineangiography and 201Tl myocardial scintigraphy.", *Japanese circulation journal,* vol. 44, no. 3, pp. 197-208.

Hedstrom, E., Astrom-Olsson, K., Ohlin, H., Frogner, F., Carlsson, M., Billgren, T., Jovinge, S., Cain, P., Wagner, G.S. & Arheden, H. 2007, "Peak CKMB and cTnT accurately estimates myocardial infarct size after reperfusion.", *Scandinavian Cardiovascular Journal,* vol. 41, no. 1, pp. 44-50.

Heikkilä, J. & Nieminen, M. 1975, "Echoventriculographic detection, localization, and quantification of left ventricular asynergy in acute myocardial infarction. A correlative echo- and electrocardiographic study.", *British heart journal,* vol. 37, no. 1, pp. 46-59.

Heimdal, A., Stoylen, A., Torp, H. & Skjaerpe, T. 1998, "Real-time strain rate imaging of the left ventricle by ultrasound", *Journal of the American Society of Echocardiography,* vol. 11, no. 11, pp. 1013-1019.

Herbots, L. 2006, "Description of deformation values in healthy volunteers and the influence of BMI, age and gender." in *Quantification of Regional Myocardial Deformation: Normal Characteristics and Clinical Use in Ischaemic Heart Disease.* Leuven University Press, , pp. 45-72.

Herlitz, J., Hjalmarson, A. & Waldenstrom, J. 1984, "Relationship between electrocardiographically and enzymatically estimated size in anterior myocardial infarction.", *Journal of electrocardiology,* vol. 17, no. 4, pp. 361-370.

Heusch, G., Schulz, R. & Rahimtoola, S.H. 2005, "Myocardial hibernation: a delicate balance", *American Journal of Physiology - Heart & Circulatory Physiology,* vol. 288, no. 3, pp. H984-99.

Heyndrickx, G.R., Millard, R.W., McRitchie, R.J., Maroko, P.R. & Vatner, S.F. 1975, "Regional myocardial functional and electrophysiological alterations after brief coronary artery occlusion in conscious dogs.", *Journal of Clinical Investigation,* vol. 56, no. 4, pp. 978-985.

Hillis, L.D., Askenazi, J., Braunwald, E., Radvany, P., Muller, J.E., Fishbein, M.C. & Maroko, P.R. 1976, "Use of changes in the epicardial QRS complex to assess interventions which modify the extent of myocardial necrosis following coronary artery occlusion.", *Circulation,* vol. 54, no. 4, pp. 591-598.

Hindman, N., Grande, P., Harrell, F.E.,Jr, Anderson, C., Harrison, D., Ideker, R.E., Selvester, R.H. & Wagner, G.S. 1986, "Relation between electrocardiographic and enzymatic methods of estimating acute myocardial infarct size.", *American Journal of Cardiology,* vol. 58, no. 1, pp. 31-35.

Hindman, N.B., Schocken, D.D., Widmann, M., Anderson, W.D., White, R.D., Leggett, S., Ideker, R.E., Hinohara, T., Selvester, R.H. & Wagner, G.S. 1985, "Evaluation of a QRS scoring system for estimating myocardial infarct size. V. Specificity and method of application of the complete system.", *American Journal of Cardiology,* vol. 55, no. 13 Pt 1, pp. 1485-1490.

Hochrein, J., Sun, F., Pieper, K.S., Lee, K.L., Gates, K.B., Armstrong, P.W., Weaver, W.D., Goodman, S.G., Topol, E.J., Califf, R.M., Granger, C.B. & Wagner, G.S. 1998, "Higher T-wave amplitude associated with better prognosis in patients receiving thrombolytic therapy for acute myocardial infarction (a GUSTO-I substudy). Global Utilization of Streptokinase and Tissue plasminogen Activator for Occluded Coronary Arteries.", *American Journal of Cardiology,* vol. 81, no. 9, pp. 1078-1084.

Holly, T.A., Abbott, B.G., Al-Mallah, M., Calnon, D.A., Cohen, M.C., DiFilippo, F.P., Ficaro, E.P., Freeman, M.R., Hendel, R.C., Jain, D., Leonard, S.M., Nichols, K.J., Polk, D.M., Soman, P.

& American Society of Nuclear, C. 2010, "Single photon-emission computed tomography.", *Journal of Nuclear Cardiology,* vol. 17, no. 5, pp. 941-973.

Hombach, V., Grebe, O., Merkle, N., Waldenmaier, S., Hoher, M., Kochs, M., Wohrle, J. & Kestler, H.A. 2005, "Sequelae of acute myocardial infarction regarding cardiac structure and function and their prognostic significance as assessed by magnetic resonance imaging.", *European heart journal,* vol. 26, no. 6, pp. 549-557.

Horacek, B.M. & Wagner, G.S. 2002, "Electrocardiographic ST-segment changes during acute myocardial ischemia", *Cardiac Electrophysiology Review,* vol. 6, no. 3, pp. 196-203.

Huang, H.D., Birnbaum, I. & Birnbaum, Y. 2013, "The double edged T wave.", *Journal of electrocardiology,* vol. 46, no. 1, pp. 8-10.

Huey, B.L., Gheorghiade, M., Crampton, R.S., Beller, G.A., Kaiser, D.L., Watson, D.D., Nygaard, T.W., Craddock, G.B., Sayre, S.L. & Gibson, R.S. 1987, "Acute non-Q wave myocardial infarction associated with early ST segment elevation: evidence for spontaneous coronary reperfusion and implications for thrombolytic trials.", *Journal of the American College of Cardiology,* vol. 9, no. 1, pp. 18-25.

Ideker, R.E., Wagner, G.S., Ruth, W.K., Alonso, D.R., Bishop, S.P., Bloor, C.M., Fallon, J.T., Gottlieb, G.J., Hackel, D.B., Phillips, H.R., Reimer, K.A., Roark, S.F., Rogers, W.J., Savage, R.M., White, R.D. & Selvester, R.H. 1982, "Evaluation of a QRS scoring system for estimating myocardial infarct size. II. Correlation with quantitative anatomic findings for anterior infarcts.", *American Journal of Cardiology,* vol. 49, no. 7, pp. 1604-1614.

Isobe, S., Takada, Y., Ando, A., Ohshima, S., Yamada, K., Nanasato, M., Unno, K., Ogawa, T., Kondo, T., Izawa, H., Inden, Y., Hirai, M. & Murohara, T. 2006, "Increase in electrocardiographic R-waves after revascularization in patients with acute myocardial infarction.", *Circulation Journal,* vol. 70, no. 11, pp. 1385-1391.

Isselbacher, E.M., Siu, S.C., Weyman, A.E. & Picard, M.H. 1996, "Absence of Q waves after thrombolysis predicts more rapid improvement of regional left ventricular dysfunction.", *American Heart Journal,* vol. 131, no. 4, pp. 649-654.

Jamal, F., Kukulski, T., Strotmann, J., Szilard, M., D'hooge, J., Bijnens, B., Rademakers, F., Hatle, L., De Scheerder, I. & Sutherland, G.R. 2001, "Quantification of the spectrum of changes in regional myocardial function during acute ischemia in closed chest pigs: an ultrasonic strain rate and strain study", *Journal of the American Society of Echocardiography,* vol. 14, no. 9, pp. 874-884.

Jamal, F., Kukulski, T., Sutherland, G.R., Weidemann, F., D'hooge, J., Bijnens, B. & Derumeaux, G. 2002, "Can changes in systolic longitudinal deformation quantify regional myocardial function after an acute infarction? An ultrasonic strain rate and strain study", *Journal of the American Society of Echocardiography,* vol. 15, no. 7, pp. 723-730.

Jamal, F., Strotmann, J., Weidemann, F., Kukulski, T., D'hooge, J., Bijnens, B., Van de Werf, F., De Scheerder, I. & Sutherland, G.R. 2001a, "Noninvasive quantification of the contractile reserve of stunned myocardium by ultrasonic strain rate and strain", *Circulation,* vol. 104, no. 9, pp. 1059-1065.

Jamal, F., Strotmann, J., Weidemann, F., Kukulski, T., D'hooge, J., Bijnens, B., Van de Werf, F., De Scheerder, I. & Sutherland, G.R. 2001b, "Noninvasive quantification of the contractile

reserve of stunned myocardium by ultrasonic strain rate and strain.", *Circulation,* vol. 104, no. 9, pp. 1059-1065.

Jennings, R.B. & Reimer, K.A. 1983, "Factors involved in salvaging ischemic myocardium: effect of reperfusion of arterial blood.", *Circulation,* vol. 68, no. 2 Pt 2, pp. 25-36.

Johanson, P., Fu, Y., Goodman, S.G., Dellborg, M., Armstrong, P.W., Krucoff, M.W., Wallentin, L. & Wagner, G.S. 2005, "A dynamic model forecasting myocardial infarct size before, during, and after reperfusion therapy: an ASSENT-2 ECG/VCG substudy.", *European heart journal,* vol. 26, no. 17, pp. 1726-1733.

Johanson, P., Fu, Y., Wagner, G.S., Goodman, S.G., Granger, C.B., Wallentin, L., Van de Werf, F., Armstrong, P.W. & ASSENT, 3.I. 2009, "ST resolution 1 hour after fibrinolysis for prediction of myocardial infarct size: insights from ASSENT 3.", *American Journal of Cardiology,* vol. 103, no. 2, pp. 154-158.

Juergens, C.P., Fernandes, C., Hasche, E.T., Meikle, S., Bautovich, G., Currie, C.A., Freedman, S.B. & Jeremy, R.W. 1996, "Electrocardiographic measurement of infarct size after thrombolytic therapy.", *Journal of the American College of Cardiology,* vol. 27, no. 3, pp. 617-624.

Kaandorp, T.A., Bax, J.J., Lamb, H.J., Viergever, E.P., Boersma, E., Poldermans, D., van der Wall, E.E. & de Roos, A. 2005, "Which parameters on magnetic resonance imaging determine Q waves on the electrocardiogram?.", *American Journal of Cardiology,* vol. 95, no. 8, pp. 925-929.

Kaul P. Fu Y. Chang WC. Harrington RA. Wagner GS. Goodman SG. Granger CB. Moliterno DJ. Van de Werf F. Califf RM. Topol EJ. Armstrong PW. PARAGON-A and GUSTO IIb Investigators. Platelet IIb/IIIa Antagonism for the Reduction of Acute Global Organization Network 2001, "Prognostic value of ST segment depression in acute coronary syndromes: insights from PARAGON-A applied to GUSTO-IIb. PARAGON-A and GUSTO IIb Investigators. Platelet IIb/IIIa Antagonism for the Reduction of Acute Global Organization Network.", *Journal of the American College of Cardiology,* vol. 38, no. 1, pp. 64-71.

Kerber, R.E., Marcus, M.L., Ehrhardt, J., Wilson, R. & Abboud, F.M. 1975, "Correlation between echocardiographically demonstrated segmental dyskinesis and regional myocardial perfusion.", *Circulation,* vol. 52, no. 6, pp. 1097-1104.

Kim, H.W., Farzaneh-Far, A. & Kim, R.J. 2009a, "Cardiovascular magnetic resonance in patients with myocardial infarction: current and emerging applications", *Journal of the American College of Cardiology,* vol. 55, no. 1, pp. 1-16.

Kim, H.W., Farzaneh-Far, A. & Kim, R.J. 2009b, "Cardiovascular magnetic resonance in patients with myocardial infarction: current and emerging applications", *Journal of the American College of Cardiology,* vol. 55, no. 1, pp. 1-16.

Kim, R.J., Albert, T.S., Wible, J.H., Elliott, M.D., Allen, J.C., Lee, J.C., Parker, M., Napoli, A., Judd, R.M. & Gadoversetamide Myocardial Infarction Imaging, I. 2008, "Performance of delayed-enhancement magnetic resonance imaging with gadoversetamide contrast for the detection and assessment of myocardial infarction: an international, multicenter, double-blinded, randomized trial.", *Circulation,* vol. 117, no. 5, pp. 629-637.

Kim, R.J., Wu, E., Rafael, A., Chen, E.L., Parker, M.A., Simonetti, O., Klocke, F.J., Bonow, R.O. & Judd, R.M. 2000, "The use of contrast-enhanced magnetic resonance imaging to identify

reversible myocardial dysfunction.", *New England Journal of Medicine,* vol. 343, no. 20, pp. 1445-1453.

Kleiger, R.E., Boden, W.E., Schechtman, K.B., Gibson, R.S., Schwartz, D.J., Geiger, B.J., Capone, R.J. & Roberts, R. 1990, "Frequency and significance of late evolution of Q waves in patients with initial non-Q-wave acute myocardial infarction. Diltiazem Reinfarction Study Group.", *American Journal of Cardiology,* vol. 65, no. 1, pp. 23-27.

Klein, C., Nekolla, S.G., Bengel, F.M., Momose, M., Sammer, A., Haas, F., Schnackenburg, B., Delius, W., Mudra, H., Wolfram, D. & Schwaiger, M. 2002, "Assessment of myocardial viability with contrast-enhanced magnetic resonance imaging: comparison with positron emission tomography.", *Circulation,* vol. 105, no. 2, pp. 162-167.

Kloner, R.A. & Jennings, R.B. 2001, "Consequences of brief ischemia: stunning, preconditioning, and their clinical implications: part 1", *Circulation,* vol. 104, no. 24, pp. 2981-2989.

Knippenberg, S.A., Wagner, G.S., Ubachs, J.F., Gorgels, A., Hedstrom, E., Arheden, H. & Engblom, H. 2010, "Consideration of the impact of reperfusion therapy on the quantitative relationship between the Selvester QRS score and infarct size by cardiac MRI.", *Annals of Noninvasive Electrocardiology,* vol. 15, no. 3, pp. 238-244.

Kontos, M.C., Kurdziel, K.A., Ornato, J.P., Schmidt, K.L., Jesse, R.L. & Tatum, J.L. 2001, "A nonischemic electrocardiogram does not always predict a small myocardial infarction: results with acute myocardial perfusion imaging.", *American Heart Journal,* vol. 141, no. 3, pp. 360-366.

Kornreich, F. 1998, "Identification of best electrocardiographic leads for diagnosing acute myocardial ischemia.", *Journal of electrocardiology,* vol. 31, no. Suppl, pp. 157-163.

Kornreich, F., Montague, T.J. & Rautaharju, P.M. 1993, "Body surface potential mapping of ST segment changes in acute myocardial infarction. Implications for ECG enrollment criteria for thrombolytic therapy.", *Circulation,* vol. 87, no. 3, pp. 773-782.

Kowalski, M., Kukulski, T., Jamal, F., D'hooge, J., Weidemann, F., Rademakers, F., Bijnens, B., Hatle, L. & Sutherland, G.R. 2001, "Can natural strain and strain rate quantify regional myocardial deformation? A study in healthy subjects", *Ultrasound in medicine & biology,* vol. 27, no. 8, pp. 1087-1097.

Kubota, I., Ikeda, K., Kanaya, T., Yamaki, M., Tonooka, I., Watanabe, Y., Tsuiki, K. & Yasui, S. 1985, "Noninvasive assessment of left ventricular wall motion abnormalities by QRS isointegral maps in previous anterior infarction.", *American Heart Journal,* vol. 109, no. 3 Pt 1, pp. 464-471.

Kudej, R.K., Ghaleb, B., Sato, N., Shen, Y.T., Bishop, S.P. & Vatner, S.F. 1998, "Ineffective perfusion-contraction matching in conscious, chronically instrumented pigs with an extended period of coronary stenosis.", *Circulation research,* vol. 82, no. 11, pp. 1199-1205.

Kuhl, H.P., Beek, A.M., van der Weerdt, A.P., Hofman, M.B., Visser, C.A., Lammertsma, A.A., Heussen, N., Visser, F.C. & van Rossum, A.C. 2003, "Myocardial viability in chronic ischemic heart disease: comparison of contrast-enhanced magnetic resonance imaging with (18)F-fluorodeoxyglucose positron emission tomography", *Journal of the American College of Cardiology,* vol. 41, no. 8, pp. 1341-1348.

Kuhl, H.P., Lipke, C.S., Krombach, G.A., Katoh, M., Battenberg, T.F., Nowak, B., Heussen, N., Buecker, A. & Schaefer, W.M. 2006, "Assessment of reversible myocardial dysfunction

in chronic ischaemic heart disease: comparison of contrast-enhanced cardiovascular magnetic resonance and a combined positron emission tomography-single photon emission computed tomography imaging protocol.", *European heart journal,* vol. 27, no. 7, pp. 846-853.

Kukulski, T., Jamal, F., Herbots, L., D'hooge, J., Bijnens, B., Hatle, L., De Scheerder, I. & Sutherland, G.R. 2003, "Identification of acutely ischemic myocardium using ultrasonic strain measurements. A clinical study in patients undergoing coronary angioplasty", *Journal of the American College of Cardiology,* vol. 41, no. 5, pp. 810-819.

Kwon, D.H., Halley, C.M., Carrigan, T.P., Zysek, V., Popovic, Z.B., Setser, R., Schoenhagen, P., Starling, R.C., Flamm, S.D. & Desai, M.Y. 2009, "Extent of left ventricular scar predicts outcomes in ischemic cardiomyopathy patients with significantly reduced systolic function: a delayed hyperenhancement cardiac magnetic resonance study.", *Jacc: Cardiovascular Imaging,* vol. 2, no. 1, pp. 34-44.

La Canna, G., Rahimtoola, S.H., Visioli, O., Giubbini, R., Alfieri, O., Zognio, M., Milan, E., Ceconi, C., Gargano, M., Lo Russo, R. & Ferrari, R. 2000, "Sensitivity, specificity, and predictive accuracies of non-invasive tests, singly and in combination, for diagnosis of hibernating myocardium.", *European heart journal,* vol. 21, no. 16, pp. 1358-1367.

Lancellotti, P., Albert, A., Berthe, C. & Pierard, L.A. 2001, "Full recovery of contraction late after acute myocardial infarction: determinants and early predictors.", *Heart,* vol. 85, no. 5, pp. 521-526.

Lancellotti, P., Gerard, P.L., Kulbertus, H.E. & Pierard, L.A. 2002, "Persistent negative T waves in the infarct-related leads as an independent predictor of poor long-term prognosis after acute myocardial infarction.", *American Journal of Cardiology,* vol. 90, no. 8, pp. 833-837.

Lang RM. Bierig M. Devereux RB. Flachskampf FA. Foster E. Pellikka PA. Picard MH. Roman MJ. Seward J. Shanewise J. Solomon S. Spencer KT. St John Sutton M. Stewart W. American Society of Echocardiography's Nomenclature and Standards Committee. Task Force on Chamber Quantification. American College of Cardiology Echocardiography Committee. American Heart Association. European Association of Echocardiography,European Society of Cardiology 2006, "Recommendations for chamber quantification", *European Journal of Echocardiography,* vol. 7, no. 2, pp. 79-108.

Larose, E., Rodes-Cabau, J., Pibarot, P., Rinfret, S., Proulx, G., Nguyen, C.M., Dery, J.P., Gleeton, O., Roy, L., Noel, B., Barbeau, G., Rouleau, J., Boudreault, J.R., Amyot, M., De Larochelliere, R. & Bertrand, O.F. 2010, "Predicting Late Myocardial Recovery and Outcomes in the Early Hours of ST-Segment Elevation Myocardial Infarction Traditional Measures Compared With Microvascular Obstruction, Salvaged Myocardium, and Necrosis Characteristics by Cardiovascular Magnetic Resonance", *Journal of the American College of Cardiology,* vol. 55, no. 22, pp. 2459-2469.

Lieberman, A.N., Weiss, J.L., Jugdutt, B.I., Becker, L.C., Bulkley, B.H., Garrison, J.G., Hutchins, G.M., Kallman, C.A. & Weisfeldt, M.L. 1981, "Two-dimensional echocardiography and infarct size: relationship of regional wall motion and thickening to the extent of myocardial infarction in the dog", *Circulation,* vol. 63, no. 4, pp. 739-746.

Lipiec, P., Szymczyk, E., Michalski, B., Stefanczyk, L., Wozniakowski, B., Rotkiewicz, A., Szymczyk, K. & Kasprzak, J.D. 2011, "Echocardiographic quantitative analysis of resting myocardial

function for the assessment of viability after myocardial infarction--comparison with magnetic resonance imaging.", *Kardiologia polska,* vol. 69, no. 9, pp. 915-922.

Lux, R.L. 2011, "Body Surface Potential Mapping Techniques." in *Comprehensive Electrocardiology*., eds. P.W. Macfarelane, A. van Oosterom, O. Pahlm, P. Kligfield, M. Janse & J. Camm, 2nd edn, Springer, London, pp. 1361-1374.

Lyseggen, E., Skulstad, H., Helle-Valle, T., Vartdal, T., Urheim, S., Rabben, S.I., Opdahl, A., Ihlen, H. & Smiseth, O.A. 2005, "Myocardial strain analysis in acute coronary occlusion: a tool to assess myocardial viability and reperfusion.[see comment]", *Circulation,* vol. 112, no. 25, pp. 3901-3910.

Maeda, S., Imai, T., Kuboki, K., Chida, K., Watanabe, C. & Ohkawa, S. 1996, "Pathologic implications of restored positive T waves and persistent negative T waves after Q wave myocardial infarction.", *Journal of the American College of Cardiology,* vol. 28, no. 6, pp. 1514-1518.

Mahrholdt, H., Wagner, A., Holly, T.A., Elliott, M.D., Bonow, R.O., Kim, R.J. & Judd, R.M. 2002, "Reproducibility of chronic infarct size measurement by contrast-enhanced magnetic resonance imaging", *Circulation,* vol. 106, no. 18, pp. 2322-2327.

Mahrholdt, H., Wagner, A., Parker, M., Regenfus, M., Fieno, D.S., Bonow, R.O., Kim, R.J. & Judd, R.M. 2003, "Relationship of contractile function to transmural extent of infarction in patients with chronic coronary artery disease.", *Journal of the American College of Cardiology,* vol. 42, no. 3, pp. 505-512.

Marcassa, C., Galli, M., Paino, A., Campini, R., Giubbini, R. & Giannuzzi, P. 2001, "Electrocardiographic evolution after Q-wave anterior myocardial infarction: correlations between QRS score and changes in left ventricular perfusion and function.", *Journal of Nuclear Cardiology,* vol. 8, no. 5, pp. 561-567.

Marwick, T.H. 2006, "Measurement of strain and strain rate by echocardiography: ready for prime time?", *Journal of the American College of Cardiology,* vol. 47, no. 7, pp. 1313-1327.

Matetzky, S., Barabash, G.I., Shahar, A., Rabinowitz, B., Rath, S., Zahav, Y.H., Agranat, O., Kaplinsky, E. & Hod, H. 1994, "Early T wave inversion after thrombolytic therapy predicts better coronary perfusion: clinical and angiographic study", *Journal of the American College of Cardiology,* vol. 24, no. 2, pp. 378-383.

Matsuzaki, M., Gallagher, K.P., Kemper, W.S., White, F. & Ross, J.,Jr 1983, "Sustained regional dysfunction produced by prolonged coronary stenosis: gradual recovery after reperfusion.", *Circulation,* vol. 68, no. 1, pp. 170-182.

Mauri, F., Franzosi, M.G., Maggioni, A.P., Santoro, E. & Santoro, L. 2002, "Clinical value of 12-lead electrocardiography to predict the long-term prognosis of GISSI-1 patients.", *Journal of the American College of Cardiology,* vol. 39, no. 10, pp. 1594-1600.

McCallister, B.D.,Jr, Christian, T.F., Gersh, B.J. & Gibbons, R.J. 1993, "Prognosis of myocardial infarctions involving more than 40% of the left ventricle after acute reperfusion therapy.", *Circulation,* vol. 88, no. 4 Pt 1, pp. 1470-1475.

McDicken, W.N., Sutherland, G.R., Moran, C.M. & Gordon, L.N. 1992, "Colour Doppler velocity imaging of the myocardium.", *Ultrasound in medicine & biology,* vol. 18, no. 6-7, pp. 651-654.

McLaughlin, M.G., Stone, G.W., Aymong, E., Gardner, G., Mehran, R., Lansky, A.J., Grines, C.L., Tcheng, J.E., Cox, D.A., Stuckey, T., Garcia, E., Guagliumi, G., Turco, M., Josephson, M.E., Zimetbaum, P. & Controlled Abciximab and Device Investigation to Lower Late Angioplasty Complications,trial 2004, "Prognostic utility of comparative methods for assessment of ST-segment resolution after primary angioplasty for acute myocardial infarction: the Controlled Abciximab and Device Investigation to Lower Late Angioplasty Complications (CADILLAC) trial.", *Journal of the American College of Cardiology,* vol. 44, no. 6, pp. 1215-1223.

Meijs, L.P., Gorgels, A.P., Bekkers, S.C., Maynard, C.C., Lemmert, M.E. & Wagner, G.S. 2011, "The relationship between serial postinfarction T wave changes and infarct size and ventricular function as determined by cardiac magnetic resonance imaging.", *Journal of electrocardiology,* vol. 44, no. 5, pp. 555-560.

Menown, I.B., Allen, J., Anderson, J.M. & Adgey, A.A. 2001, "ST depression only on the initial 12-lead ECG: early diagnosis of acute myocardial infarction", *European heart journal,* vol. 22, no. 3, pp. 218-227.

Mercier, J.C., Lando, U., Kanmatsuse, K., Ninomiya, K., Meerbaum, S., Fishbein, M.C., Swan, H.J. & Ganz, W. 1982, "Divergent effects of inotropic stimulation on the ischemic and severely depressed reperfused myocardium.", *Circulation,* vol. 66, no. 2, pp. 397-400.

Merli, E., Sutherland, G.R., Bijnens, B., Fischer, A., Chaparro, M., Karu, T., Sutcliffe, S., Marciniak, A., Baltabaeva, A., Bunce, N. & Brecker, S. 2008, "Usefulness of changes in left ventricular wall thickness to predict full or partial pressure reperfusion in ST-elevation acute myocardial infarction.", *American Journal of Cardiology,* vol. 102, no. 3, pp. 249-256.

Mills, R.M.,Jr, Young, E., Gorlin, R. & Lesch, M. 1975, "Natural history of S-T segment elevation after acute myocardial infarction.", *American Journal of Cardiology,* vol. 35, no. 5, pp. 609-614.

Mirvis, D.M. 1987, "Current status of body surface electrocardiographic mapping", *Circulation,* vol. 75, no. 4, pp. 684-688.

Miyatake, K., Yamagishi, M., Tanaka, N., Uematsu, M., Yamazaki, N., Mine, Y., Sano, A. & Hirama, M. 1995, "New method for evaluating left ventricular wall motion by color-coded tissue Doppler imaging: in vitro and in vivo studies.", *Journal of the American College of Cardiology,* vol. 25, no. 3, pp. 717-724.

Moon, J.C., De Arenaza, D.P., Elkington, A.G., Taneja, A.K., John, A.S., Wang, D., Janardhanan, R., Senior, R., Lahiri, A., Poole-Wilson, P.A. & Pennell, D.J. 2004, "The pathologic basis of Q-wave and non-Q-wave myocardial infarction: a cardiovascular magnetic resonance study.[see comment]", *Journal of the American College of Cardiology,* vol. 44, no. 3, pp. 554-560.

Muller, J.E., Maroko, P.R. & Braunwald, E. 1975, "Evaluation of precordial electrocardiographic mapping as a means of assessing changes in myocardial ischemic injury.", *Circulation,* vol. 52, no. 1, pp. 16-27.

Murray, C. & Alpert, J.S. 1994, "Diagnosis of acute myocardial infarction", *Current opinion in cardiology,* vol. 9, no. 4, pp. 465-470.

Murray, R.G., Peshock, R.M., Parkey, R.W., Bonte, F.J., Willerson, J.T. & Blomqvist, C.G. 1979, "ST isopotential precordial surface maps in patients with acute myocardial infarction.", *Journal of electrocardiology,* vol. 12, no. 1, pp. 55-64.

Nieminen, M., Parisi, A.F., O'Boyle, J.E., Folland, E.D., Khuri, S. & Kloner, R.A. 1982, "Serial evaluation of myocardial thickening and thinning in acute experimental infarction: identification and quantification using two-dimensional echocardiography.", *Circulation,* vol. 66, no. 1, pp. 174-180.

Nijveldt, R., van der Vleuten, P.A., Hirsch, A., Beek, A.M., Tio, R.A., Tijssen, J.G., Piek, J.J., van Rossum, A.C. & Zijlstra, F. 2009, "Early electrocardiographic findings and MR imaging-verified microvascular injury and myocardial infarct size.", *Jacc: Cardiovascular Imaging,* vol. 2, no. 10, pp. 1187-1194.

Nishimura, R.A., Tajik, A.J., Shub, C., Miller, F.A.,Jr, Ilstrup, D.M. & Harrison, C.E. 1984, "Role of two-dimensional echocardiography in the prediction of in-hospital complications after acute myocardial infarction.", *Journal of the American College of Cardiology,* vol. 4, no. 6, pp. 1080-1087.

Nixon, J.V., Narahara, K.A. & Smitherman, T.C. 1980, "Estimation of myocardial involvement in patients with acute myocardial infarction by two-dimensional echocardiography.", *Circulation,* vol. 62, no. 6, pp. 1248-1255.

Ohta, T., Kinoshita, A., Ohsugi, J., Isomura, S., Takatsu, F., Ishikawa, H., Toyama, J., Nagaya, T. & Yamada, K. 1982, "Correlation between body surface isopotential maps and left ventriculograms in patients with old inferoposterior myocardial infarction.", *American Heart Journal,* vol. 104, no. 6, pp. 1262-1270.

Ohta, T., Toyama, J., Ohsugi, J., Kinoshita, A., Isomura, S., Takatsu, F., Ishikawa, H., Nagaya, T. & Yamada, K. 1981, "Correlation between body surface isopotential maps and left ventriculograms in patients with old anterior myocardial infarction.", *Japanese heart journal,* vol. 22, no. 5, pp. 747-761.

Oikarinen, L., Paavola, M., Montonen, J., Viitasalo, M., Makijarvi, M., Toivonen, L. & Katila, T. 1998, "Magnetocardiographic QT interval dispersion in postmyocardial infarction patients with sustained ventricular tachycardia: validation of automated QT measurements.", *Pacing & Clinical Electrophysiology,* vol. 21, no. 10, pp. 1934-1942.

Ong, L., Reiser, P., Coromilas, J., Scherr, L. & Morrison, J. 1983, "Left ventricular function and rapid release of creatine kinase MB in acute myocardial infarction. Evidence for spontaneous reperfusion.", *New England Journal of Medicine,* vol. 309, no. 1, pp. 1-6.

Oostendorp, T.F., van Oosterom, A. & Huiskamp, G. 1989, "Interpolation on a triangulated 3D surface", *Journal of Computational Physics,* vol. 80, no. 2, pp. 331-343.

Ornato, J.P., Menown, I.B., Peberdy, M.A., Kontos, M.C., Riddell, J.W., Higgins, G.L.,3rd, Maynard, S.J. & Adgey, J. 2009, "Body surface mapping vs 12-lead electrocardiography to detect ST-elevation myocardial infarction.", *American Journal of Emergency Medicine,* vol. 27, no. 7, pp. 779-784.

Otto, C.M. 2004, "Principles of Echocardiographic Image Acquisition and Doppler Analysis" in *Textbook of Clinical Echocardiography*, eds. A. Lenehan & V. Ginsburgs, 3rd edn, Elsevier/ Saunders, Philadelphi, PA, pp. 1-27.

Pahlm, U.S., Chaitman, B.R., Rautaharju, P.M., Selvester, R.H. & Wagner, G.S. 1998, "Comparison of the various electrocardiographic scoring codes for estimating anatomically documented sizes of single and multiple infarcts of the left ventricle.", *American Journal of Cardiology,* vol. 81, no. 7, pp. 809-815.

Perazzolo Marra, M., Lima, J.A. & Iliceto, S. 2011, "MRI in acute myocardial infarction", *European heart journal,* vol. 32, no. 3, pp. 284-293.

Pfisterer, M., Zuber, M., Wenzel, R. & Burkart, F. 1991, "Prolonged myocardial stunning after thrombolysis: can left ventricular function be assessed definitely at hospital discharge?.", *European heart journal,* vol. 12, no. 2, pp. 214-217.

Pislaru, C., Bruce, C.J., Anagnostopoulos, P.C., Allen, J.L., Seward, J.B., Pellikka, P.A., Ritman, E.L. & Greenleaf, J.F. 2004a, "Ultrasound strain imaging of altered myocardial stiffness: stunned versus infarcted reperfused myocardium", *Circulation,* vol. 109, no. 23, pp. 2905-2910.

Pislaru, C., Bruce, C.J., Seward, J.B. & Greenleaf, J.F. 2004b, "Distinctive changes in end-diastolic wall thickness and postsystolic thickening in viable and infarcted myocardium.", *Journal of the American Society of Echocardiography,* vol. 17, no. 8, pp. 855-862.

Prigent, F., Maddahi, J., Garcia, E.V., Satoh, Y., Van Train, K. & Berman, D.S. 1986, "Quantification of myocardial infarct size by thallium-201 single-photon emission computed tomography: experimental validation in the dog.", *Circulation,* vol. 74, no. 4, pp. 852-861.

Raunio, H., Rissanen, V., Romppanen, T., Jokinen, Y., Rehnberg, S., Helin, M. & Pyorala, K. 1979, "Changes in the QRS complex and ST segment in transmural and subendocardial myocardial infarctions. A clinicopathologic study.", *American Heart Journal,* vol. 98, no. 2, pp. 176-184.

Reimer, K.A., Lowe, J.E., Rasmussen, M.M. & Jennings, R.B. 1977, "The wavefront phenomenon of ischemic cell death. 1. Myocardial infarct size vs duration of coronary occlusion in dogs.", *Circulation,* vol. 56, no. 5, pp. 786-794.

Roark, S.F., Ideker, R.E., Wagner, G.S., Alonso, D.R., Bishop, S.P., Bloor, C.M., Bramlet, D.A., Edwards, J.E., Fallon, J.T., Gottlieb, G.J., Hackel, D.B., Phillips, H.R., Reimer, K.A., Rogers, W.J., Ruth, W.K., Savage, R.M., White, R.D. & Selvester, R.H. 1983, "Evaluation of a QRS scoring system for estimating myocardial infarct size. III. Correlation with quantitative anatomic findings for inferior infarcts.", *American Journal of Cardiology,* vol. 51, no. 3, pp. 382-389.

Roes, S.D., Kelle, S., Kaandorp, T.A., Kokocinski, T., Poldermans, D., Lamb, H.J., Boersma, E., van der Wall, E.E., Fleck, E., de Roos, A., Nagel, E. & Bax, J.J. 2007, "Comparison of myocardial infarct size assessed with contrast-enhanced magnetic resonance imaging and left ventricular function and volumes to predict mortality in patients with healed myocardial infarction.", *American Journal of Cardiology,* vol. 100, no. 6, pp. 930-936.

Ross, J.„Jr 1991, "Myocardial perfusion-contraction matching. Implications for coronary heart disease and hibernation.", *Circulation,* vol. 83, no. 3, pp. 1076-1083.

Rost, C., Rost, M.C., Breithardt, O., Schmid, M., Klinghammer, L., Stumpf, C., Daniel, W.G., Flachskampf, F.A. In press. *Journal of the American Society of Echocardiography,* http://dx.doi.org/10.1016/j.echo.2014.02.004.

Sachdev, V., Aletras, A.H., Padmanabhan, S., Sidenko, S., Rao, Y.N., Brenneman, C.L., Shizukuda, Y., Lie, G.R., Vincent, P.S., Waclawiw, M.A. & Arai, A.E. 2006, "Myocardial strain decreases with increasing transmurality of infarction: a Doppler echocardiographic and magnetic resonance correlation study", *Journal of the American Society of Echocardiography,* vol. 19, no. 1, pp. 34-39.

Sadanandan, S., Hochman, J.S., Kolodziej, A., Criger, D.A., Ross, A., Selvester, R. & Wagner, G.S. 2003, "Clinical and angiographic characteristics of patients with combined anterior and inferior ST-segment elevation on the initial electrocardiogram during acute myocardial infarction.", *American Heart Journal,* vol. 146, no. 4, pp. 653-661.

Sakata, K., Yoshino, H., Houshaku, H., Koide, Y., Yotsukura, M. & Ishikawa, K. 2001, "Myocardial damage and left ventricular dysfunction in patients with and without persistent negative T waves after Q-wave anterior myocardial infarction.", *American Journal of Cardiology,* vol. 87, no. 5, pp. 510-515.

Savage, R.M., Wagner, G.S., Ideker, R.E., Podolsky, S.A. & Hackel, D.B. 1977, "Correlation of postmortem anatomic findings with electrocardiographic changes in patients with myocardial infarction: retrospective study of patients with typical anterior and posterior infarcts.", *Circulation,* vol. 55, no. 2, pp. 279-285.

Savonitto, S., Ardissino, D., Granger, C.B., Morando, G., Prando, M.D., Mafrici, A., Cavallini, C., Melandri, G., Thompson, T.D., Vahanian, A., Ohman, E.M., Califf, R.M., Van de Werf, F. & Topol, E.J. 1999, "Prognostic value of the admission electrocardiogram in acute coronary syndromes.", *JAMA,* vol. 281, no. 8, pp. 707-713.

Savonitto, S., Cohen, M.G., Politi, A., Hudson, M.P., Kong, D.F., Huang, Y., Pieper, K.S., Mauri, F., Wagner, G.S., Califf, R.M., Topol, E.J. & Granger, C.B. 2005, "Extent of ST-segment depression and cardiac events in non-ST-segment elevation acute coronary syndromes.", *European heart journal,* vol. 26, no. 20, pp. 2106-2113.

Schechtman, K.B., Capone, R.J., Kleiger, R.E., Gibson, R.S., Schwartz, D.J., Roberts, R., Young, P.M. & Boden, W.E. 1989, "Risk stratification of patients with non-Q wave myocardial infarction. The critical role of ST segment depression. The Diltiazem Reinfarction Study Research Group.", *Circulation,* vol. 80, no. 5, pp. 1148-1158.

Schiller, N.B., Shah, P.M., Crawford, M., DeMaria, A., Devereux, R., Feigenbaum, H., Gutgesell, H., Reichek, N., Sahn, D. & Schnittger, I. 1989a, "Recommendations for quantitation of the left ventricle by two-dimensional echocardiography. American Society of Echocardiography Committee on Standards, Subcommittee on Quantitation of Two-Dimensional Echocardiograms", *Journal of the American Society of Echocardiography,* vol. 2, no. 5, pp. 358-367.

Schiller, N.B., Shah, P.M., Crawford, M., DeMaria, A., Devereux, R., Feigenbaum, H., Gutgesell, H., Reichek, N., Sahn, D. & Schnittger, I. 1989b, "Recommendations for quantitation of the left ventricle by two-dimensional echocardiography. American Society of Echocardiography Committee on Standards, Subcommittee on Quantitation of Two-Dimensional Echocardiograms", *Journal of the American Society of Echocardiography,* vol. 2, no. 5, pp. 358-367.

Schinkel, A.F., Bax, J.J., Elhendy, A., Boersma, E., Vourvouri, E.C., Sozzi, F.B., Valkema, R., Roelandt, J.R. & Poldermans, D. 2002, "Assessment of viable tissue in Q-wave regions

by metabolic imaging using single-photon emission computed tomography in ischemic cardiomyopathy.", *American Journal of Cardiology,* vol. 89, no. 10, pp. 1171-1175.

Schinkel, A.F., Bax, J.J., Poldermans, D., Elhendy, A., Ferrari, R. & Rahimtoola, S.H. 2007, "Hibernating myocardium: diagnosis and patient outcomes", *Current problems in cardiology,* vol. 32, no. 7, pp. 375-410.

Schmitt, C., Lehmann, G., Schmieder, S., Karch, M., Neumann, F.J. & Schomig, A. 2001, "Diagnosis of acute myocardial infarction in angiographically documented occluded infarct vessel : limitations of ST-segment elevation in standard and extended ECG leads.", *Chest,* vol. 120, no. 5, pp. 1540-1546.

Schroder, R., Wegscheider, K., Schroder, K., Dissmann, R. & Meyer-Sabellek, W. 1995, "Extent of early ST segment elevation resolution: a strong predictor of outcome in patients with acute myocardial infarction and a sensitive measure to compare thrombolytic regimens. A substudy of the International Joint Efficacy Comparison of Thrombolytics (INJECT) trial.", *Journal of the American College of Cardiology,* vol. 26, no. 7, pp. 1657-1664.

Seino, Y., Staniloff, H.M., Shell, W.E., Mickle, D., Shah, P.K. & Vyden, J.K. 1983, "Evaluation of a QRS scoring system in acute myocardial infarction: relation to infarct size, early stage left ventricular ejection fraction, and exercise performance.", *American Journal of Cardiology,* vol. 52, no. 1, pp. 37-42.

Selvanayagam, J.B., Kardos, A., Francis, J.M., Wiesmann, F., Petersen, S.E., Taggart, D.P. & Neubauer, S. 2004, "Value of delayed-enhancement cardiovascular magnetic resonance imaging in predicting myocardial viability after surgical revascularization.", *Circulation,* vol. 110, no. 12, pp. 1535-1541.

Selvester, R.H., Strauss, D.G. & Wagner, G.S. 2011a, "Myocardial Infarction" in *Comprehensive Electrocardiology*, eds. P.W. Macfarelane, A. van Oosterom, O. Pahlm, P. Kligfield, M. Janse & J. Camm, 2nd edn, Springer, , pp. 664-665.

Selvester, R.H., Strauss, D.G. & Wagner, G.S. 2011b, "Myocardial Infarction" in *Comprehensive Electrocardiology*, eds. P.W. Macfarelane, A. van Oosterom, O. Pahlm, P. Kligfield, M. Janse & J. Camm, 2nd edn, Springer, London, pp. 683-686.

Selvester, R.H., Wagner, G.S. & Hindman, N.B. 1985a, "The Selvester QRS scoring system for estimating myocardial infarct size. The development and application of the system.", *Archives of Internal Medicine,* vol. 145, no. 10, pp. 1877-1881.

Selvester, R.H., Wagner, G.S. & Hindman, N.B. 1985b, "The Selvester QRS scoring system for estimating myocardial infarct size. The development and application of the system.", *Archives of Internal Medicine,* vol. 145, no. 10, pp. 1877-1881.

Sevilla, D.C., Wagner, N.B., White, R.D., Peck, S.L., Ideker, R.E., Hackel, D.B., Reimer, K.A., Selvester, R.H. & Wagner, G.S. 1990, "Anatomic validation of electrocardiographic estimation of the size of acute or healed myocardial infarcts.", *American Journal of Cardiology,* vol. 65, no. 20, pp. 1301-1307.

Sgarbossa, E.B., Meyer, P.M., Pinski, S.L., Pavlovic-Surjancev, B., Barbagelata, A., Goodman, S.G., Lum, A.S., Underwood, D.A., Gates, K.B., Califf, R.M., Topol, E.J. & Wagner, G.S. 2000, "Negative T waves shortly after ST-elevation acute myocardial infarction are a powerful marker for improved survival rate.", *American Heart Journal,* vol. 140, no. 3, pp. 385-394.

Shen, W.K., Khandheria, B.K., Edwards, W.D., Oh, J.K., Miller, F.A.,Jr, Naessens, J.M. & Tajik, A.J. 1991, "Value and limitations of two-dimensional echocardiography in predicting myocardial infarct size", *American Journal of Cardiology,* vol. 68, no. 11, pp. 1143-1149.

Shenasa, M., Hamel, D., Nasmith, J., Nadeau, R., Dutoy, J.L., Derome, D. & Savard, P. 1993, "Body surface potential mapping of ST-segment shift in patients undergoing percutaneous transluminal coronary angioplasty. Correlations with the ECG and vectorcardiogram.", *Journal of electrocardiology,* vol. 26, no. 1, pp. 43-51.

Sicari, R., Nihoyannopoulos, P., Evangelista, A., Kasprzak, J., Lancellotti, P., Poldermans, D., Voigt, J.U., Zamorano, J.L. & European Association of, E. 2008, "Stress echocardiography expert consensus statement: European Association of Echocardiography (EAE) (a registered branch of the ESC)", *European Journal of Echocardiography,* vol. 9, no. 4, pp. 415-437.

Simson, M.B. 1981, "Use of signals in the terminal QRS complex to identify patients with ventricular tachycardia after myocardial infarction.", *Circulation,* vol. 64, no. 2, pp. 235-242.

Sjoli, B., Orn, S., Grenne, B., Vartdal, T., Smiseth, O.A., Edvardsen, T. & Brunvand, H. 2009, "Comparison of left ventricular ejection fraction and left ventricular global strain as determinants of infarct size in patients with acute myocardial infarction.", *Journal of the American Society of Echocardiography,* vol. 22, no. 11, pp. 1232-1238.

Skulstad, H., Urheim, S., Edvardsen, T., Andersen, K., Lyseggen, E., Vartdal, T., Ihlen, H. & Smiseth, O.A. 2006a, "Grading of myocardial dysfunction by tissue Doppler echocardiography: a comparison between velocity, displacement, and strain imaging in acute ischemia", *Journal of the American College of Cardiology,* vol. 47, no. 8, pp. 1672-1682.

Skulstad, H., Urheim, S., Edvardsen, T., Andersen, K., Lyseggen, E., Vartdal, T., Ihlen, H. & Smiseth, O.A. 2006b, "Grading of myocardial dysfunction by tissue Doppler echocardiography: a comparison between velocity, displacement, and strain imaging in acute ischemia", *Journal of the American College of Cardiology,* vol. 47, no. 8, pp. 1672-1682.

Smith, G.T., Soeter, J.R., Haston, H.H. & McNamara, J.J. 1974, "Coronary reperfusion in primates. Serial electrocardiographic and histologic assessment.", *Journal of Clinical Investigation,* vol. 54, no. 6, pp. 1420-1427.

Sorensen, J.T., Murinson, M.A., Kaltoft, A.K., Nikus, K.C., Wagner, G.S. & Terkelsen, C.J. 2009, "Significance of T-wave amplitude and dynamics at the time of reperfusion in patients with acute ST-segment elevation myocardial infarction treated with primary percutaneous coronary intervention.", *Journal of electrocardiology,* vol. 42, no. 6, pp. 677-683.

Spekhorst, H., SippensGroenewegen, A., David, G.K., Janse, M.J. & Dunning, A.J. 1990, "Body surface mapping during percutaneous transluminal coronary angioplasty. QRS changes indicating regional myocardial conduction delay.", *Circulation,* vol. 81, no. 3, pp. 840-849.

Sun, J.P., Chinchoy, E., Donal, E., Popovi, Z.B., Perlic, G., Asher, C.R., Greenberg, N.L., Grimm, R.A., Wilkoff, B.L. & Thomas, J.D. 2004, "Evaluation of ventricular synchrony using novel Doppler echocardiographic indices in patients with heart failure receiving cardiac resynchronization therapy", *Journal of the American Society of Echocardiography,* vol. 17, no. 8, pp. 845-850.

Tamaki, S., Murakami, T., Kadota, K., Kambara, H., Yui, Y., Nakajima, H., Suzuki, Y., Nohara, R., Takatsu, Y. & Kawai, C. 1983, "Effects of coronary artery reperfusion on relation between creatine kinase-MB release and infarct size estimated by myocardial emission tomography

with thallium-201 in man.", *Journal of the American College of Cardiology,* vol. 2, no. 6, pp. 1031-1038.

Task Force for Diagnosis and Treatment of Non-ST-Segment Elevation Acute Coronary Syndromes of European Society of,Cardiology, Bassand, J.P., Hamm, C.W., Ardissino, D., Boersma, E., Budaj, A., Fernandez-Aviles, F., Fox, K.A., Hasdai, D., Ohman, E.M., Wallentin, L. & Wijns, W. 2007, "Guidelines for the diagnosis and treatment of non-ST-segment elevation acute coronary syndromes", *European heart journal,* vol. 28, no. 13, pp. 1598-1660.

Tateishi, S., Abe, S., Yamashita, T., Okino, H., Lee, S., Toda, H., Saigo, M., Arima, S., Atsuchi, Y., Nakao, S. & Tanaka, H. 1997, "Use of the QRS scoring system in the early estimation of myocardial infarct size following reperfusion.", *Journal of electrocardiology,* vol. 30, no. 4, pp. 315-322.

Theroux, P., Franklin, D., Ross, J.,Jr & Kemper, W.S. 1974, "Regional myocardial function during acute coronary artery occlusion and its modification by pharmacologic agents in the dog.", *Circulation research,* vol. 35, no. 6, pp. 896-908.

Thorstensen, A., Amundsen, B.H., Dalen, H., Hala, P., Kiss, G., Aase, S.A., Torp, H. & Stoylen, A. 2012, "Strain rate imaging combined with wall motion analysis gives incremental value in direct quantification of myocardial infarct size.", *European heart journal cardiovascular Imaging,* vol. 13, no. 11, pp. 914-921.

Thygesen K. Alpert JS. Jaffe AS. Simoons ML. Chaitman BR. White HD. Writing Group on the Joint ESC/ACCF/AHA/WHF Task Force for the Universal Definition of Myocardial Infarction. Thygesen K. Alpert JS. White HD. Jaffe AS. Katus HA. Apple FS. Lindahl B. Morrow DA. Chaitman BA. Clemmensen PM. Johanson P. Hod H. Underwood R. Bax JJ. Bonow RO. Pinto F. Gibbons RJ. Fox KA. Atar D. Newby LK. Galvani M. Hamm CW. Uretsky BF. Steg PG. Wijns W. Bassand JP. Menasche P. Ravkilde J. Ohman EM. Antman EM. Wallentin LC. Armstrong PW. Simoons ML. Januzzi JL. Nieminen MS. Gheorghiade M. Filippatos G. Luepker RV. Fortmann SP. Rosamond WD. Levy D. Wood D. Smith SC. Hu D. Lopez-Sendon JL. Robertson RM. Weaver D. Tendera M. Bove AA. Parkhomenko AN. Vasilieva EJ. Mendis S. ESC Committee for Practice Guidelines (CPG) 2012, "Third universal definition of myocardial infarction.", *European heart journal,* vol. 33, no. 20, pp. 2551-2567.

Tibrewala, A.V., Asch, F., Shah, S., Fuisz, A. & Lindsay, J.,Jr 2007, "Association of size of myocardial scar and persistence of ST-segment elevation after healing of anterior wall myocardial infarction.", *American Journal of Cardiology,* vol. 99, no. 8, pp. 1106-1108.

Timmis, G.C. 1987, "Electrocardiographic effects of reperfusion", *Cardiology clinics,* vol. 5, no. 3, pp. 427-445.

Tjandrawidjaja, M.C., Fu, Y., Westerhout, C.M., Wagner, G.S., Granger, C.B., Armstrong, P.W. & APEX-AMI, I. 2010, "Usefulness of the QRS score as a strong prognostic marker in patients discharged after undergoing primary percutaneous coronary intervention for ST-segment elevation myocardial infarction.", *American Journal of Cardiology,* vol. 106, no. 5, pp. 630-634.

Tonooka, I., Kubota, I., Watanabe, Y., Tsuiki, K. & Yasui, S. 1983a, "Isointegral analysis of body surface maps for the assessment of location and size of myocardial infarction.", *American Journal of Cardiology,* vol. 52, no. 10, pp. 1174-1180.

Tonooka, I., Kubota, I., Watanabe, Y., Tsuiki, K. & Yasui, S. 1983b, "Isointegral analysis of body surface maps for the assessment of location and size of myocardial infarction.", *American Journal of Cardiology,* vol. 52, no. 10, pp. 1174-1180.

Toyama, S., Suzuki, K., Koyama, M., Yoshino, K. & Fujimoto, K. 1982, "The body surface isopotential mapping of the QRS wave in myocardial infarction. a comparative study of the scintigram with thallium-201.", *Journal of electrocardiology,* vol. 15, no. 3, pp. 241-248.

Urheim, S., Edvardsen, T., Torp, H., Angelsen, B. & Smiseth, O.A. 2000, "Myocardial strain by Doppler echocardiography. Validation of a new method to quantify regional myocardial function", *Circulation,* vol. 102, no. 10, pp. 1158-1164.

Vaananen, H., Korhonen, P., Montonen, J., Makijarvi, M., Nenonen, J., Oikarinen, L., Simelius, K., Toivonen, L. & Katila, T. 2000, "Non-invasive arrhythmia risk evaluation in clinical environment", *Herzschrittmachertherapie und Elektrophysiologie,* vol. 11, no. 4, pp. 229-234.

Vachova, J., Eglis, M., Fidler, V., Stanek, V., Malek, I., Pavlovic, J., Gebauerova, M. & Bergmann, K. 1979, "Assessment of myocardial infarct size in clinical practice.", *Cor et vasa,* vol. 21, no. 6, pp. 387-397.

van der Vleuten, P.A., Vogelzang, M., Svilaas, T., van der Horst, I.C., Tio, R.A. & Zijlstra, F. 2009, "Predictive value of Q waves on the 12-lead electrocardiogram after reperfusion therapy for ST elevation myocardial infarction.", *Journal of electrocardiology,* vol. 42, no. 4, pp. 310-318.

van 't Hof, A.W., Liem, A., de Boer, M.J. & Zijlstra, F. 1997, "Clinical value of 12-lead electrocardiogram after successful reperfusion therapy for acute myocardial infarction. Zwolle Myocardial infarction Study Group.", *Lancet,* vol. 350, no. 9078, pp. 615-619.

Vargas, S.O., Sampson, B.A. & Schoen, F.J. 1999, "Pathologic detection of early myocardial infarction: a critical review of the evolution and usefulness of modern techniques", *Modern Pathology,* vol. 12, no. 6, pp. 635-645.

Vartdal, T., Brunvand, H., Pettersen, E., Smith, H.J., Lyseggen, E., Helle-Valle, T., Skulstad, H., Ihlen, H. & Edvardsen, T. 2007, "Early prediction of infarct size by strain Doppler echocardiography after coronary reperfusion", *Journal of the American College of Cardiology,* vol. 49, no. 16, pp. 1715-1721.

Vatner, S.F. 1980, "Correlation between acute reductions in myocardial blood flow and function in conscious dogs.", *Circulation research,* vol. 47, no. 2, pp. 201-207.

Vesterinen, P. 2007, *Electrocardiographic repolarization variables in detecting myocardial infarction and ischemic injury*. Paula Vesterinen, Helsinki, Finland.

Vesterinen, P., Vaananen, H., Hanninen, H., Korhonen, P., Tierala, I., Husa, T., Makijarvi, M. & Toivonen, L. 2008a, "Single-lead electrocardiographic variables in the detection of prior myocardial infarction with respect to Q-wave status and infarct age.", *Cardiology,* vol. 109, no. 4, pp. 222-229.

Vesterinen, P., Vaananen, H., Stenroos, M., Hanninen, H., Korhonen, P., Tierala, I., Husa, T., Makijarvi, M. & Toivonen, L. 2008b, "Localization of prior myocardial infarction by repolarization variables.", *International journal of cardiology,* vol. 124, no. 1, pp. 100-106.

Voigt, J.U., Arnold, M.F., Karlsson, M., Hubbert, L., Kukulski, T., Hatle, L. & Sutherland, G.R. 2000, "Assessment of regional longitudinal myocardial strain rate derived from doppler myocardial imaging indexes in normal and infarcted myocardium", *Journal of the American Society of Echocardiography,* vol. 13, no. 6, pp. 588-598.

Volpi, A., De Vita, C., Franzosi, M.G., Geraci, E., Maggioni, A.P., Mauri, F., Negri, E., Santoro, E., Tavazzi, L. & Tognoni, G. 1993, "Determinants of 6-month mortality in survivors of myocardial infarction after thrombolysis. Results of the GISSI-2 data base. The Ad hoc Working Group of the Gruppo Italiano per lo Studio della Sopravvivenza nell'Infarto Miocardico (GISSI)-2 Data Base.", *Circulation,* vol. 88, no. 2, pp. 416-429.

Wagner, A., Mahrholdt, H., Holly, T.A., Elliott, M.D., Regenfus, M., Parker, M., Klocke, F.J., Bonow, R.O., Kim, R.J. & Judd, R.M. 2003, "Contrast-enhanced MRI and routine single photon emission computed tomography (SPECT) perfusion imaging for detection of subendocardial myocardial infarcts: an imaging study.see comment", *Lancet,* vol. 361, no. 9355, pp. 374-379.

Wagner, G.S., Freye, C.J., Palmeri, S.T., Roark, S.F., Stack, N.C., Ideker, R.E., Harrell, F.E.,Jr & Selvester, R.H. 1982, "Evaluation of a QRS scoring system for estimating myocardial infarct size. I. Specificity and observer agreement.", *Circulation,* vol. 65, no. 2, pp. 342-347.

Ward, R.M., White, R.D., Ideker, R.E., Hindman, N.B., Alonso, D.R., Bishop, S.P., Bloor, C.M., Fallon, J.T., Gottlieb, G.J. & Hackel, D.B. 1984a, "Evaluation of a QRS scoring system for estimating myocardial infarct size. IV. Correlation with quantitative anatomic findings for posterolateral infarcts.", *American Journal of Cardiology,* vol. 53, no. 6, pp. 706-714.

Ward, R.M., White, R.D., Ideker, R.E., Hindman, N.B., Alonso, D.R., Bishop, S.P., Bloor, C.M., Fallon, J.T., Gottlieb, G.J. & Hackel, D.B. 1984b, "Evaluation of a QRS scoring system for estimating myocardial infarct size. IV. Correlation with quantitative anatomic findings for posterolateral infarcts.", *American Journal of Cardiology,* vol. 53, no. 6, pp. 706-714.

Weaver, J.C., Ramsay, D.D., Rees, D., Binnekamp, M.F., Prasan, A.M. & McCrohon, J.A. 2011, "Dynamic Changes in ST Segment Resolution After Myocardial Infarction and the Association with Microvascular Injury on Cardiac Magnetic Resonance Imaging.", *Heart, Lung & Circulation,* vol. 20, no. 2, pp. 111-118.

Weidemann, F., Dommke, C., Bijnens, B., Claus, P., D'hooge, J., Mertens, P., Verbeken, E., Maes, A., Van de Werf, F., De Scheerder, I. & Sutherland, G.R. 2003, "Defining the transmurality of a chronic myocardial infarction by ultrasonic strain-rate imaging: implications for identifying intramural viability: an experimental study", *Circulation,* vol. 107, no. 6, pp. 883-888.

Weidemann, F., Eyskens, B., Jamal, F., Mertens, L., Kowalski, M., D'Hooge, J., Bijnens, B., Gewillig, M., Rademakers, F., Hatle, L. & Sutherland, G.R. 2002a, "Quantification of regional left and right ventricular radial and longitudinal function in healthy children using ultrasound-based strain rate and strain imaging.", *Journal of the American Society of Echocardiography,* vol. 15, no. 1, pp. 20-28.

Weidemann, F., Jamal, F., Sutherland, G.R., Claus, P., Kowalski, M., Hatle, L., De Scheerder, I., Bijnens, B. & Rademakers, F.E. 2002b, "Myocardial function defined by strain rate and strain during alterations in inotropic states and heart rate.", *American Journal of Physiology - Heart & Circulatory Physiology,* vol. 283, no. 2, pp. H792-9.

Weidemann, F., Wacker, C., Rauch, A., Bauer, W.R., Bijnens, B., Sutherland, G.R., Ertl, G., Voelker, W., Fidler, F. & Strotmann, J.M. 2006a, "Sequential changes of myocardial

function during acute myocardial infarction, in the early and chronic phase after coronary intervention described by ultrasonic strain rate imaging", *Journal of the American Society of Echocardiography,* vol. 19, no. 7, pp. 839-847.

Weidemann, F., Wacker, C., Rauch, A., Bauer, W.R., Bijnens, B., Sutherland, G.R., Ertl, G., Voelker, W., Fidler, F. & Strotmann, J.M. 2006b, "Sequential changes of myocardial function during acute myocardial infarction, in the early and chronic phase after coronary intervention described by ultrasonic strain rate imaging", *Journal of the American Society of Echocardiography : official publication of the American Society of Echocardiography,* vol. 19, no. 7, pp. 839-847.

Weir, R.A., Martin, T.N., Murphy, C.A., Petrie, C.J., Clements, S., Steedman, T., Dargie, H.J. & Wagner, G.S. 2010, "Comparison of serial measurements of infarct size and left ventricular ejection fraction by contrast-enhanced cardiac magnetic resonance imaging and electrocardiographic QRS scoring in reperfused anterior ST-elevation myocardial infarction.", *Journal of electrocardiology,* vol. 43, no. 3, pp. 230-236.

Weir, R.A. & McMurray, J.J. 2006, "Epidemiology of heart failure and left ventricular dysfunction after acute myocardial infarction", *Current Heart Failure Reports,* vol. 3, no. 4, pp. 175-180.

Weiss, J.L., Bulkley, B.H., Hutchins, G.M. & Mason, S.J. 1981, "Two-dimensional echocardiographic recognition of myocardial injury in man: comparison with postmortem studies.", *Circulation,* vol. 63, no. 2, pp. 401-408.

Welinder, A.E., Wagner, G.S., Horacek, B.M., Martin, T.N., Maynard, C. & Pahlm, O. 2009, "EASI-Derived vs standard 12-lead electrocardiogram for Selvester QRS score estimations of chronic myocardial infarct size, using cardiac magnetic resonance imaging as gold standard.", *Journal of electrocardiology,* vol. 42, no. 2, pp. 145-151.

White, H.D., Norris, R.M., Brown, M.A., Brandt, P.W., Whitlock, R.M. & Wild, C.J. 1987, "Left ventricular end-systolic volume as the major determinant of survival after recovery from myocardial infarction.", *Circulation,* vol. 76, no. 1, pp. 44-51.

Wilkenshoff, U.M., Sovany, A., Wigstrom, L., Olstad, B., Lindstrom, L., Engvall, J., Janerot-Sjoberg, B., Wranne, B., Hatle, L. & Sutherland, G.R. 1998, "Regional mean systolic myocardial velocity estimation by real-time color Doppler myocardial imaging: a new technique for quantifying regional systolic function.", *Journal of the American Society of Echocardiography,* vol. 11, no. 7, pp. 683-692.

Willems, J.L., Willems, R.J., Willems, G.M., Arnold, A.E., Van de Werf, F. & Verstraete, M. 1990, "Significance of initial ST segment elevation and depression for the management of thrombolytic therapy in acute myocardial infarction. European Cooperative Study Group for Recombinant Tissue-Type Plasminogen Activator.", *Circulation,* vol. 82, no. 4, pp. 1147-1158.

Wong, C.K., Gao, W., Raffel, O.C., French, J.K., Stewart, R.A., White, H.D. & HERO-2, I. 2006, "Initial Q waves accompanying ST-segment elevation at presentation of acute myocardial infarction and 30-day mortality in patients given streptokinase therapy: an analysis from HERO-2.", *Lancet,* vol. 367, no. 9528, pp. 2061-2067.

Wu, E., Judd, R.M., Vargas, J.D., Klocke, F.J., Bonow, R.O. & Kim, R.J. 2001a, "Visualisation of presence, location, and transmural extent of healed Q-wave and non-Q-wave myocardial infarction", *Lancet,* vol. 357, no. 9249, pp. 21-28.

Wu, E., Judd, R.M., Vargas, J.D., Klocke, F.J., Bonow, R.O. & Kim, R.J. 2001b, "Visualisation of presence, location, and transmural extent of healed Q-wave and non-Q-wave myocardial infarction.", *Lancet,* vol. 357, no. 9249, pp. 21-28.

Wu, E., Ortiz, J.T., Tejedor, P., Lee, D.C., Bucciarelli-Ducci, C., Kansal, P., Carr, J.C., Holly, T.A., Lloyd-Jones, D., Klocke, F.J. & Bonow, R.O. 2008, "Infarct size by contrast enhanced cardiac magnetic resonance is a stronger predictor of outcomes than left ventricular ejection fraction or end-systolic volume index: prospective cohort study.", *Heart,* vol. 94, no. 6, pp. 730-736.

Wyatt, H.L., Meerbaum, S., Heng, M.K., Rit, J., Gueret, P. & Corday, E. 1981, "Experimental evaluation of the extent of myocardial dyssynergy and infarct size by two-dimensional echocardiography", *Circulation,* vol. 63, no. 3, pp. 607-614.

Yan, R.T., Yan, A.T., Mahaffey, K.W., White, H.D., Pieper, K., Sun, J.L., Pepine, C.J., Biasucci, L.M., Gulba, D.C., Lopez-Sendon, J., Goodman, S.G. & SYNERGY Trial, I. 2010, "Prognostic utility of quantifying evolutionary ST-segment depression on early follow-up electrocardiogram in patients with non-ST-segment elevation acute coronary syndromes.", *European heart journal,* vol. 31, no. 8, pp. 958-966.

Yang, H., Pu, M., Rodriguez, D., Underwood, D., Griffin, B.P., Kalahasti, V., Thomas, J.D. & Brunken, R.C. 2004, "Ischemic and viable myocardium in patients with non-Q-wave or Q-wave myocardial infarction and left ventricular dysfunction: a clinical study using positron emission tomography, echocardiography, and electrocardiography.", *Journal of the American College of Cardiology,* vol. 43, no. 4, pp. 592-598.

Zhang, Y., Chan, A.K., Yu, C.M., Yip, G.W., Fung, J.W., Lam, W.W., So, N.M., Wang, M., Wu, E.B., Wong, J.T. & Sanderson, J.E. 2005, "Strain rate imaging differentiates transmural from non-transmural myocardial infarction: a validation study using delayed-enhancement magnetic resonance imaging", *Journal of the American College of Cardiology,* vol. 46, no. 5, pp. 864-871.